DOCKETED	
Docket Number:	25-OPT-02
Project Title:	Prairie Song Reliability Project
TN #:	268944
Document Title:	Save Our Rural Town Comments - Scoping Comment letter and Attachments 1-5 submitted by Save Our Rural Town
Description:	N/A
Filer:	System
Organization:	Save Our Rural Town
Submitter Role:	Public
Submission Date:	3/4/2026 4:35:54 PM
Docketed Date:	3/4/2026

Comment Received From: Save Our Rural Town
Submitted On: 3/4/2026
Docket Number: 25-OPT-02

Scoping Comment letter and Attachments 1-5 submitted by Save Our Rural Town

Additional submitted attachment is included below.

SAVE OUR RURAL TOWN

March 4, 2026

Lisa Worrall
Project Manager
California Energy Commission
715 P Street, MS-40
Sacramento, CA 95814
Submittal of a 46 page letter and 12 attachments

Subject: Scoping Comments by Save Our Rural Town (SORT) pertaining to the AB-205 Application Submitted for a Proposed Battery Energy Storage Project in Acton, CA.

Reference: California Energy Commission Docket Number 25-OPT-02.

Dear Ms. Worrall;

Save Our Rural Town (SORT) respectfully offers the following Scoping Comments in response to the Notice of Preparation (NOP) of a Draft Environmental Impact Report (DEIR) issued by the California Energy Commission (Commission) pursuant to the referenced licensing Application filed by "Prairie Song Reliability Project LLC", a Delaware limited liability company (referred to hereafter as "developer"). The developer seeks to construct a 9,200 MWh Battery Energy Storage System (BESS) that will stretch more than a mile in length within the rural community of Acton in unincorporated Los Angeles County.

Consistent with Guidelines established for the California Environmental Quality Act (CEQA), the Scoping Comments offered below identify potentially significant environmental impacts of the BESS project, feasible alternatives to the BESS project, and mitigation measures that will substantially reduce significant impacts [14 CCR § 15083]. These comments were prepared by Jacqueline Ayer, the Director of SORT. Ms. Ayer has decades of engineering experience in air quality (air toxic and criteria pollutant emissions assessments, toxic risk determinations, pollution control, etc.), environmental compliance, land use, and energy/transmission system assessments. Accordingly, the comments offered below constitute "substantial evidence" as that term is defined by CEQA. In the interest of brevity, the comments are arranged by topic area; within each topic area, significant impacts are identified and, when practicable, alternatives and mitigation measures are offered.

WATER RESOURCES.

The NOP does not identify any potentially significant water resource impacts associated with BESS project operations; this is consistent with the developer's opinion that BESS project operations will not require significant quantities of water. In fact, the developer asserts that BESS operations will require less than 1.5 acre feet of water per year[1] and that all water needed for onsite operations will be supplied by an existing domestic well on the project site that is currently being used for residential purposes[2]. However, both the NOP and the developer fail to properly consider the water resources needed for firefighting purposes because the BESS system will utilize a lithium iron phosphate ($LiFPO_4$ or "LFP") battery chemistry which renders each BESS container susceptible to spontaneous and lengthy deflagration. Equally important, lithium BESS fires cannot be extinguished, they take days to burn themselves out, and when they burn, they release significant toxic emissions (including hydrogen fluoride and hydrogen chloride). Adequate water resources are essential to BESS operations because copious quantities of water must be applied during a BESS fire to cool surrounding BESS containers and thereby prevent additional BESS deflagrations. Additionally, because lithium BESS fires result in toxic emissions, BESS deflagration events require firefighters to remain a safe distance from the burning BESS while applying water to the surrounding area; the International Association of Fire Chiefs (IAFC) recommends a 300 foot separation (Attachment 1).

In recognition of the substantial fire risk posed by lithium BESS, new standards and certification procedures have been developed over the last decade. A key certification protocol is UL 9540A. Developed by Underwriters Laboratories, it establishes that a BESS design is "acceptable" if a fire that engulfs one BESS container does not spread to an adjacent container (as shown in Attachment 2). However, the UL 9540A certification is only valid when ambient windspeeds are 12 miles per hour or less; BESS container fires can (and do) spread at higher windspeeds. For example, the Victoria BESS fire in Australia involved UL9540A certified BESS facilities, and because the ambient windspeed exceeded 12 mph, the fire that engulfed one BESS container spread to the adjacent BESS container[3]. This resulted in even more toxic emissions.

Another test that was recently developed in Canada[4] is the "Large Scale Burn Test"; insofar as SORT is aware, only a handful of BESS systems have been subject to the LSBT. The Sungrow PowerTitan 2.0 was tested sometime in 2024; SORT has not found the LSBT test report among the documents that the developer has submitted in the

[1] Data Request Response 2 Part 4 at 3.15-13.
[2] Data Request Response 3 Part 2 at 2-8.
[3] *Report Of Technical Findings*: Victorian Big Battery Fire: July 30, 2021 at 5. See Attachment 3.
[4] The Canadian Standards Association developed test method CSA TS-800.

docket. However, the developer does explain that the test was conducted at windspeeds below 2.7 meters per second (6 miles per hour) and that, at this low windspeed, the fire was restricted to a single BESS container.

SORT is particularly concerned that UL 9540A and LSBT tests on the Sungrow PowerTitan 2.0 system were conducted under circumstances that do not reflect "real world" conditions in Acton. For example, the "windrose" data that the developer provided in response to data request #5[5] indicates that winds exceed 12 mph nearly 40% of the time. Notably, the developer's windrose data represents conditions at the Palmdale Meteorological Station which is approximately 10 miles from the project site and located in the heart of the flat Antelope Valley which is approximately 60 miles wide and 40 miles long. In other words, it substantially understates wind conditions in Acton (which is in a narrow river valley between two mountain ranges). For instance, the developer's windrose shows that windspeeds in Palmdale rarely exceed 21.58 knots (24.8 miles per hour); however, 25 mile per hour winds are common in Acton (which is why SCE constantly shuts off power in our community during dry "Santa Ana Wind" conditions). These facts demonstrate that the assurances provided by a UL9540A certification (namely, that BESS deflagration events will be limited to a single container) are not a certainty in Acton where windspeeds frequently exceed the conditions under such assurances are valid.

The reason that SORT is so concerned about the circumstances under which BESS systems are tested is that BESS fires can be very violent and result in significantly large flames; these flames will "flatten" under windy conditions and can actually contact adjacent containers. These are certainly the circumstances that occurred during the Victoria BESS fire. Figure 1 illustrates the ferocity of a BESS fire in Peoria Arizona that occurred on October 1, 2025; the fire erupted four years after the system was commissioned. The BESS deflagration event here clearly occurred when winds were calm because the flames (which are estimated to be at least 15 feet high) were generally vertical and thus did not threaten adjacent BESS containers. Such a BESS fire occurring in Acton will look quite different.

Because the developer is choosing to place the BESS project in a very a windy area, additional protections must be provided to ensure adequate public safety. For instance, the BESS project must be configured to provide both adequate access and water resources that are sufficient to ensure water can be applied to all BESS surrounding the deflagrating container for at least 3 days. Unfortunately, and as explained below, the BESS project is not configured in a manner that delivers these protections.

[5] The windrose is provided in Figure 2. The response to data request #5 is here: https://efiling.energy.ca.gov/GetDocument.aspx?tn=268721&DocumentContentId=105876

Figure 1. BESS Fire on October 1, 2025 in Glendale, Arizona.

Source: https://www.azfamily.com/2025/10/02/multiple-agencies-fighting-fire-battery-storage-facility-glendale/

The BESS Project Does Not Provide Sufficient Water Resources.

The developer has submitted a "Firefighting Water Supply Analysis" (Analysis) that was prepared by a consulting group identified as the "Fire & Risk Alliance"[6]. According to the Analysis, the BESS project is configured with two 40,000 gallon water tanks that will be filled with water which is extracted onsite using an existing residential well. The Analysis concludes that this 80,000 gallon water volume is sufficient because only 15,000 gallons is needed to extinguish a vehicle fire, only 15,000 gallons is needed to extinguish a transformer fire, only 5,497 gallons is needed to extinguish a fire in the "Control House Enclosure" building, and no water is needed to respond to a BESS fire (see Table 1). According to Fire & Risk Alliance, water is not needed during a BESS deflagration event because the BESS containers will comply with UL 9540A; therefore, every BESS container which becomes engulfed in fire will not cause adjacent containers to ignite[7]. SORT respectfully disagrees. As explained above, a UL9540A certification and its concomitant assurance that all BESS fires will be limited to a single container is meaningless during windy conditions. We further contend that configuring the BESS project without any water resources to respond to a BESS deflagration event is irresponsible and poses a significant public safety risk to the residents of Acton because a burning BESS *will* ignite an adjacent BESS, and the second BESS *will* ignite a third BESS in an infernal chain reaction. And, as the number of burning BESS containers increase, so does the release of toxic emissions.

The BESS Project Configuration does not Permit Effective Firefighting.

"Fire & Risk Alliance" does offer that, in the event of a BESS deflagration, fire crews can "maintain a safe distance, outside of the site perimeter fence" and use a "single 1 3/4-inch handline intermittently flowing at 125 gpm" to "cool nearby exposures" and "control the path of smoke"[8]; "Fire & Risk Alliance" also recommends a "fog pattern from a single one-and-three-quarter inch handline, typically flowing at 125 gpm, to protect neighboring exposures[9]". The BESS project configuration and other factors render this strategy completely impracticable:

- Fire crews staged "outside of the perimeter fence" will not have access to the onsite fire hydrants because (according to the site plan), the hydrants are located *inside* the BESS yard and approximately 50 feet from the 12 foot high perimeter wall. Therefore, the developer's fire hydrants will not be useful in responding to a BESS

[6] Revised Firefighting Water Supply Analysis provided as Attachment 31 to Data Request Response 2 part 6 at 7-8. [https://efiling.energy.ca.gov/GetDocument.aspx?tn=266609&DocumentContentId=103666].
[7] Fire & Risk Alliance states "Based on the results of the UL 9540A unit level fire test, a fixed fire suppression system (such as a sprinkler system or water spray system) or offensive fire department efforts are not required". Id at 5.
[8] Id at 7.
[9] Ibid.

fire, and fire crews will have to bring their own water to the project site. However, Los Angeles County Fire Department (LACoFD) trucks do not carry more than 500 gallons, and LACoFD water tenders do not carry more than 5,000 gallons; this means the 125 gpm handline recommended by "Fire & Risk Alliance" will quickly deplete the water resources provided by LACoFD in minutes. And, if two handlines are used, the water will be gone twice as fast, and in less than half an hour, no fire response will be possible, and additional BESS containers will ignite and cause additional toxic emissions that endanger the public.

- The reach of a typical firefighter handline with a straight stream nozzle is less than 100 feet[10] and fog nozzles have an even shorter reach[11]. This means that, to implement the recommendation made by Fire & Risk Alliance that firefighters use handlines at 125 gpm, firefighters would have to be within 100 feet of the burning BESS. This does not comport with IAFC recommendations. Equally important, the project site plan[12] indicates that the BESS yard is 600 feet wide in some areas and is configured such that most of the BESS containers are more than 100 feet from the perimeter wall; therefore, they cannot be reached by a handline operated at 125 gpm from outside the perimeter wall. Accordingly, the recommendation made by "Fire & Risk Alliance" that firefighters remain outside the perimeter to combat a BESS fire with 125 gpm handlines is intrinsically unworkable.

- If the firefighters were to disregard IAFC's recommendation and enter the BESS yard to access the fire hydrants and get within 100 feet of a burning BESS so they can utilize the 125 gpm handline and lay down a "fog pattern" as recommended by "Fire & Risk Alliance", they would have to get very close to the burning BESS in order to reach the surfaces of the surrounding BESS containers that must be cooled. This is because the project is configured with the BESS containers packed so tightly that ground access to specific BESS surfaces is difficult. And, even if firefighters successfully access these BESS surfaces from the ground and use the handlines recommended by Fire & Risk Alliance, the 80,000 gallons of water stored in the onsite tanks would run out within a few hours[13]. After that, no further fire response will be possible, and the BESS deflagration event will cause surrounding BESS to ignite and release additional toxic emissions that will endanger the public.

As professional firefighters explained during the recent Scoping Meeting, the only effective way for firefighters to safely respond to a BESS fire is to utilize a standard

---

[10] https://www.fireengineering.com/firefighting-equipment/fireground-hydraulics-straight-stream-reach/
[11] https://www.firefighternation.com/training/nozzle-knowledge-is-more-than-just-smooth-bore-or-fog/
[12] "Updated DR Response 2 Attachment 28 - Appendix 2A Site Plan Package - Part 1A" [https://efiling.energy.ca.gov/GetDocument.aspx?tn=266806&DocumentContentId=103897].
[13] If just two handlines are deployed at 125 gpm, the 80,000 gallons of water stored onsite will be depleted in 329 minutes (approximately 5 hours).

engine with a “monitor” (or “deck gun”) that operates at 1,000 gallons per minute and/or a ladder truck operating a 2½ inch line operating at 500 gallons per minute. Both of these are capable of pushing water hundreds of feet, but they require access to a fire hydrant. Figure 2 illustrates how this equipment is effectively deployed by firefighters to cool the surfaces surrounding a BESS fire; it depicts two standard engines and one ladder truck. The firefighters all appear to be at least 100 feet from the fire, and the deck guns and the large hose on the ladder truck are effective in reaching the targeted surfaces surrounding the burning BESS. Notably, the firefighters operating on the standard engines are not hampered by a 12 foot high block wall that is topped with razor sharp concertina wire; firefighters responding to a BESS fire at the BESS project site will not be so fortunate.

Figure 2. Firefighters Responding to the Peoria BESS Fire on October 1, 2025.

Source: Channel 12 news [https://www.youtube.com/watch?v=dcUGgKxUP5s].

Insofar as SORT is aware, the local fire department (Station#80) does not have a ladder truck. Additionally, the 12 foot block wall around the BESS site will present a challenge for standard firetruck operations, particularly if the fire is on the outer edges of the densely packed BESS yard because under such circumstances, LACoFD will have to remain well outside the BESS yard to maintain adequate separation. This would probably require the closure of Soledad Canyon Road (which is a major highway running through the BESS project[14]). However, at this location, the fire trucks will not

[14] Soledad Canyon Road is a designated “Major Highway”; see Figure 7.3 of the Los Angeles County General Plan [https://planning.lacounty.gov/wp-content/uploads/2022/11/7.1_Chapter7_Figures.pdf].

be able to access the onsite fire hydrants so they will be unable to operate their deck guns. Thus, the BESS project configuration will compel firetrucks to enter the BESS yard and reduce their separation distance to respond to BESS fires at the project site. The firefighters will probably be able to effectively operate their deck guns from within the BESS yard; however, a deck gun on just one engine will drain the two 40,000 gallon water tanks in less than two hours (because a deck gun flows at 1,000 gallon per minute). Two trucks with deck guns and a ladder truck operating as depicted in Figure 2 will draw 2,500 gallons per minute and drain both tanks in approximately 30 minutes. After that, there can be no further firefighter response, and during windy conditions, nothing will prevent the deflagration of surrounding BESS containers and the subsequent release of more toxic compounds that will endanger the public.

Fire & Risk Alliance suggests that, when onsite water supplies are depleted, LACoFD can set up a "shuttle service" to bring in more water[15]. This plan is unwise: prudence demands that onsite water resources at industrial facilities be sufficient to properly combat any fire scenario. This plan is also completely unworkable. As explained above, LACoFD firetrucks only carry 500 gallons of water and water tenders only carry 5,000 gallons; thus, a 2,500 gpm fire flow will deplete each truck in less than 20 seconds and deplete each tender in two minutes. Accordingly, this plan will require a veritable "conga line" of LACoFD trucks and water tenders that must be sustained for hours to effectively respond to BESS fires at the project site. SORT does not believe that this constitutes a safe and responsible fire response plan and it certainly does not provide adequate public safety margins. In any event, all of these concerns must be factored into the Commission's consideration of both water supply impacts and public safety impacts.

LACoFD and WWD #37 Must be Consulted Before the Draft EIR is Issued.

During the scoping meeting on February 24, members of the public spoke with LACoFD staff regarding the BESS project. As SORT understands it, LACoFD has the impression that the BESS project is served with a municipal water supply. This troubling news is indicative of a conspicuous lack of communication between the developer, the Fire Department, and the Commission. SORT is very concerned that, as a result of this disconnect, the Commission's assessment of public safety and water resource impacts will be based on developer input and not on substantive input from LACoFD *even though LACoFD bears all the responsibility for delivering on whatever public safety promises the developer makes*. As shown above, the developer's fire response plan is fraught with material deficiencies and cannot be relied upon to draw conclusions regarding water resource or public safety impacts. Accordingly, measures developed by the Commission to mitigate these impacts must be informed by LACoFD input.

[15] Fire & Risk Alliance says a "shuttle service can be set up by the fire service" to bring water. Page 8.

SORT is also not convinced that local municipal water supplies are sufficient to serve the BESS project's emergency response needs. There is a WWD#37 water main west of the project site; it terminates on Tortuga Street just east of Listie Avenue and is approximately one half mile from the northwestern portion of the BESS project. However, it is only an 8 inch water main, and the water it supplies is already largely subscribed by existing WWD #37 customers; accordingly, a new 12 inch water main from the WWD #37 "North Tank" (which is the municipal water tank nearest to the project site that serves the small population of northeast Acton) must be installed because the existing 8 inch line does not have sufficient capacity for the BESS project even if it were extended to the project site. Moreover, WWD #37 only has a limited quantity of water storage at the "North Tank"[16], and it is not sufficient to sustain a 2,500 gpm fire flow for many hours. In fact, a 2,500 gallon per minute fire flow will completely drain the North tank in less than 7 hours[17]. These facts demonstrate that local WWD #37 water resources are not sufficient to serve the BESS project *even if the developer constructed a 12 inch water main from the North tank to the project site*.

The lack of municipal water resources in Acton renders the BESS project intrinsically unsafe because it prevents firefighters from properly "cooling down" the BESS devices that are adjacent to a burning BESS. At the very least, the Commission should confirm whether the North Tank can sustain a lengthy 2,500 gpm fireflow and whether a new 12 inch water line will suffice to deliver these flow rates. This would require substantive discussions with LACoFD and WWD#37; it would also require the preparation of clearly delineated fire response protocols and water resource plans *all of which must be transparently shared with the public*. Without such protocols and plans, the Commission will not have the substantial evidence needed to support any findings that water resource impacts and public safety impacts are "less than significant".

PUBLIC SAFETY.

SORT has consistently maintained that, because the Sungrow PowerTitan 2.0 BESS devices that will be installed for the BESS project utilize a lithium battery chemistry and are will be near residences, they pose a significant public safety risk due to their propensity to deflagrate and release toxic air contaminants (TACs). SORT understands that the Commission is sensitive to these public safety concerns, and we appreciate that the Commission directed the developer to prepare a hazard assessment with Data Request #5. In response, the BESS developer prepared the requested assessment using an EPA Regulatory Model known as AERMOD, and based thereon, concluded the BESS

[16] It was announced at the Acton Town Council meeting on March 2, 2026 that the "North Tank" operated by WWD#37 has a capacity of approximately 1,000,000 gallons.
[17] 1,000,000 gallons ÷ (2.500 gallons per minute x 60 minutes per hour) = 6.67 hours.

project does not pose a public safety risk even if an entire BESS container becomes engulfed in flames. SORT has carefully analyzed the developer's hazard assessment, and found it to be substantially deficient because the projected air toxic emission rates are not supported by substantial evidence (and in fact, they are actually controverted by substantial evidence). We have also found that the information provided by the developer does not comport with Commission directives established in Data Request #5. These deficiencies are discussed in detail below, along with an explanation of why the BESS project poses such a significant public safety risk.

Significant HF Emissions Will be Released From a Deflagrating Sungrow PowerTitan 2.0 BESS Device Because of the Electrolyte and Lithium Battery Chemistry it Uses.

The Sungrow PowerTitan 2.0 devices proposed for the BESS project utilize a "Lithium Iron Phosphate" (LFP) chemistry which energy developers claim is "safe" and not susceptible to ignition even though LFP BESS use the same lithium ion transfer mechanism and flammable electrolyte and carbon anode system as all other lithium BESS. One reason why LFP BESS are claimed to be "safe" is because they have a higher "onset temperature" for thermal runaway under normal charge conditions. A recent study shows the onset temperature for NMC batteries range from 96°C to 111°C, whereas the onset temperature for LFP batteries range from 162°C to 168°C[18]; however, this same source reports that, unlike NMC batteries, LFP batteries quickly begin outgassing flammable and hazardous materials when their onset temperatures are reached.

Another reason why LFP batteries are alleged to be "safe" is because the strong phosphate-oxygen bond in the cathode material breaks down at slightly higher temperatures; thus, the cathode can withstand slightly higher temperatures before releasing oxygen (which then reacts violently with the electrolyte and escalates into a battery fire). However, multiple studies show that, in an overcharged state, the onset temperature of LFP batteries drops to 112°C[19] (because in an overcharged state, there is excess oxygen in the vicinity of the anode which reacts violently with the electrolyte). Furthermore, studies involving fully charged (but not overcharged) LFP batteries show that the Solid Electrolyte Interphase layer (SEI) which separates the anode from the electrolyte begins to degrade at only 80°C[20]; such degradation leads to contact between

[18] Schöberl, J., Ohneseit, S., Schaeffler, S., Förstermann, D., Grahl, L., Jossen, A., Ziebert, C., Lienkamp, M. *Thermal runaway characterization of cylindrical lithium-ion and sodium-ion batteries with various sizes and energy contents*. Journal of Power Sources, Volume 648, 2025. https://www.sciencedirect.com/science/article/pii/S0378775325010766. Table 2.

[19] Dai, Y., Panahi, A. *Thermal runaway process in lithium-ion batteries: A review*. Next Energy, Volume 6, 2025. https://www.sciencedirect.com/science/article/pii/S2949821X24000917 . Fei Gao *et al. Study on Temperature Change of $LiFePO_4$/C Battery Thermal Runaway under Overcharge Conditions*. 2021. Earth Environ. Sci. **631**. https://iopscience.iop.org/article/10.1088/1755-1315/631/1/012114/pdf

[20] Li, T., Jiao, Y. *Revealing the Thermal Runaway Behavior of Lithium Iron Phosphate Power Batteries at Different States of Charge and Operating Environment*. International Journal of Electrochemical Science, Vol. 17. 2022. https://www.sciencedirect.com/science/article/pii/S1452398123027499.

the electrolyte and the anode, then dendrites form and pierce the separation barrier, at which point a short circuit occurs and thermal runaway is immediately triggered. Additionally, LFP batteries are just as susceptible to shrinkage of the separator barrier between the anode and cathode as other batteries; this causes a short circuit and immediately triggers thermal runaway. Finally, aging stressors that occur across all battery types (including LFP)[21] increase the possibility of thermal runaway over time.

All of this demonstrates how and why the Sungrow PowerTitan 2.0 is susceptible to deflagration; this susceptibility is driven by the battery cell characteristics which, according to Safety Data Sheets provided by the developer[22], contain:

- 33.5% by weight of highly flammable electrolyte solution comprised of diethyl carbonate (DEC at 10%), ethyl methyl carbonate (EMC at 5%), ethylene carbonate (EC at 5%), and Lithium hexafluorophosphate ($LiPF_6$ at 13.5%). The $LiPF_6$ is a lithium salt that is dissolved in the DEC, EMC, and EC; 75% of $LiPF_6$ is fluorine[23].
- 37% by weight of lithium iron phosphate ($LiFePO_4$) which forms the cathode.
- 3% by weight aluminum which serves as the current collector for the cathode.
- 19% by weight graphite which forms the anode.
- 6.5% by weight copper which serves as the current collector for the anode.

The highly flammable electrolyte, coupled with its anode and cathode chemistries, are why the Sungrow PowerTitan 2.0 poses a significant risk to Acton residents. Specifically, during thermal runaway, the flammable electrolyte combusts and the ensuing high temperature causes the $LiPF_6$ to break down and release significant quantities of hydrogen fluoride (and other toxics). Once the system hits the key temperature, nothing can stop the ensuing electrolyte combustion or the release of toxic HF vapors. And, because BESS systems are designed to vent gases to the outside when thermal runaway is detected, the toxic HF vapors are intentionally entrained in the air where they endanger surrounding areas.

As SORT has previously pointed out, a 2017 study by Larsson et al (which analyzes LFP and NMC batteries as well as cylindrical and pouch battery formats) reports that HF emissions vary with battery capacity and range from 20-200 mg/Wh[24] (see Attachment

---

[21] Collath, N., Tepe, B., Englberger, S., Jossen, A., Hesse, H. *Aging aware operation of lithium-ion battery energy storage systems: A review*. Journal of Energy Storage. Volume 55. 2022. https://www.sciencedirect.com/science/article/pii/S2352152X2201622X

[22] The SDS is included in the developer's response to Data Request 2 - Part 6 found here: [https://efiling.energy.ca.gov/GetDocument.aspx?tn=266609&DocumentContentId=103666].

[23] The molecular weight of $LiPF_6$ is 152 g/mole, and the molecular weight of F_2 is 38.

[24] Larsson, F., Andersson, P., Blomqvist, P., Mellander, B., *Toxic Fluoride Gas Emissions From Lithium-Ion Battery Fires*. Scientific Reports. Volume 7. 2017. See in Attachment 4.

4). A more recent study of LFP cell emissions published in 2024 by Claassen et al[25] reveals that vapor phase HF emissions vary based on the state of charge as well as battery capacity, and range from 40 mg/Wh to 80 mg/Wh (as shown in Table 8 in Attachment 5). A compilation study by Bugryniec et al published in 2024 concludes that HF emissions increase with battery capacity and that LFP batteries release much more HF than NMC batteries. Bugryniec et al concluded that HF emission rates based on battery capacity for LFP batteries range from 50 g/kWh to 100 g/kWh[26]. This study is provided in Attachment 6 and the relevant portions are highlighted.

Notably, the lithium salt in the electrolyte used in the Sungrow PowerTitan 2.0 system ($LiPF_6$) is particularly rich in fluorine and has *substantially more fluorine than other lithium salts utilized by other BESS manufacturers*[27]. This means that HF emissions from the Sungrow PowerTitan 2.0 system are on the "high end" compared to other BESS systems. This is because the heat generated during electrolyte combustion breaks down the lithium salt: in fact, one molecule of $LiPF_6$ produces ***six*** molecules of HF. This breakdown occurs in a multistep process that involves an intermediary compound (POF_3) which is highly reactive and further breaks down into HF[28]. Other BESS manufacturers use electrolytes with lithium salts that produce far less HF. For example, lithium tetrafluoroborate (LiBF4) produces 4 molecules of HF per molecule of $LiBF_4$ and lithium difluoride sulfonimide (LiFSI) produces one molecule of HF per molecule of LiFSI. In other words, it appears that the Sungrow PowerTitan 2.0 system is configured to maximize HF emissions.

Based on the studies cited above, and given that the PowerTitan 2.0 system utilizes an electrolyte with the highest possible fluorine content, it is reasonable to conclude that each deflagration of a PowerTitan unit will release *at least* 60 kg/MWh of HF (which represents an average of the HF emissions reported by Claassen et al[29] and is on the low end of the emissions reported by Bugryniec et al[30]). SORT contends that a more

---

[25] Claassen, M., Bingham, B., Chow, J. C., Watson, J. G., Chu, P., Wang, Y., & Wang, X. (2024). *Characterization of Lithium-Ion Battery Fire Emissions—Part 2*. Batteries. Vol. 10. Desert Research Institute. https://doi.org/10.3390/batteries10100366. Table 7a.

[26] Bugryniec, P., Resendiz, E., Nwophoke, S., Khanna, S., James, C., Brown, S. *Review of gas emissions from lithium-ion battery thermal runaway failure — Considering toxic and flammable compounds*. Journal of Energy Storage. Volume 87. 2024. https://www.sciencedirect.com/science/article/pii/S2352152X24008739.

[27] Other salts include lithium tetrafluoroborate (LiBF4) or lithium difluoride sulfonimide (LiFSI) which have substantially less fluorine that $LiPF_6$. https://www.sciencedirect.com/topics/engineering/inorganic-lithium-salt#:~:text=At%20present%2C%20the%20lithium%20salt,SO2)2NLi).

[28] The study by Larsson et al showed that vapor phase emissions from LFP battery fires do not include POF_3[28]; this means that all six fluoride molecules in each molecule of $LiPF_6$ tend to be converted to six molecules of HF. Attachment 4 page 2.

[29] Claassen et al measured HF emissions ranging from 40 to 80 mg/Wh; the average is 60 mg/Wh. This converts to 60 kg/MWh [(60 mg/Wh) x (10^6Wh/MWh) x (1 kg/10^6 mg) = 60 kg/MWh].

[30] Bugryniec et al report an HF emission range of 50 g/kWh to 100 g/kWh (50 mg/Wh - 100 mg/Wh).

conservative emission capacity factor which is more protective of public health would be 75 mg/Wh (which is an average of Bugryniec's results and on the high end of Claassen's results). Nonetheless, if we rely on the 60 mg/Wh emission capacity factor, then each deflagration of a single PowerTitan unit (which has a 5.015 MWh storage capacity[31]) will emit *at least* 662 pounds of HF[32]. To calculate the minimum hourly HF emission rate, the 662 pounds of total HF emissions is divided by 28 hours (which is the length of time that the developer claims is required to fully burn a PowerTitan 2.0 unit[33]); this yields a minimum hourly HF emission rate of 23.6 pounds/hour[34]. These total and hourly HF emission rates (662 pounds and 23.6 lb/hr respectively) should be considered *lower bound values*; actual HF emissions from the BESS project are likely to be much higher because of the high fluorine content in the PowerTitan 2.0 electrolyte.

The BESS Developer's HF Emission rates Lack Evidentiary Support

According to page 1 of Attachment A in the developer's response to Data Request #5, the developer's health risk assessment assumes that each PowerTitan 2.0 deflagration event will release only 38.68 pounds of HF, and that the hourly HF emission rate is only 1.38 lbs/hr. When these values were input to the AERMOD risk assessment model, the resulting output showed a "Hazard Quotient" of only 0.63[35]. And, because the resulting Hazard Quotient is less than the adopted threshold of 1.0, the developer asserts that the public safety risk posed by HF emissions is "less than significant".

The problem is, the 38.68 pound HF emission factor assumed by the developer is 17 times smaller than the 662 pound HF emission factor that SORT derived based on the published literature discussed above. It is possible to calculate the developer's assumed HF emission capacity by reconciling the developer's assumed HF emission rate with the energy capacity of a PowerTitan 2.0 system as follows:

$$\left(\frac{38.68\ pounds}{5.015\ MWh}\right) \times \frac{1\ kg}{2.2\ pounds} \times \frac{1{,}000{,}000\ mg}{1\ kg} \times \frac{1\ MWh}{1{,}000{,}000\ Wh} = 3.5\ mg/Wh$$

As this equation shows, the developer's HF emission assumption of 38.68 pounds is equivalent to an emission capacity of only 3.5 mg/Wh, which is 11 to 22 times smaller

[31] https://info-support.sungrowpower.com/application/pdf/2024/12/07/ST5015UX-2H-US_ST5015UX-4H-US%20Datasheet.pdf.
[32] (60 mg/Wh) x (10^6Wh/MWh) x (1 kg/10^6 mg) x 5.015 MWh x (2.2 pounds/kg) = 661.89 pounds.
[33] Page 3 of the developer's response to data request #5 states that "the LSBT [Large Scale Burn Test] showed emissions over approximately 28.03 hours".
[34] 662 pounds ÷ 28 hours = 23.6 pounds per hour. This release rate is probably biased low because it is unlikely that the HF concentrations will remain constant throughout the entire deflagration cycle. In fact, it is more likely that deflagration will be initiated by a massive flame event that will release high HF concentrations which will eventually taper off. Therefore, ***actual*** HF emissions will at times be much higher than 23.6 pounds per hour.
[35] Table 5 of the developer's response to Data Request #5.

than what is reported in the Claassen study and 14 to 28 times smaller than what is reported in the Bugryniec study. In other words, the developer's assumed HF emission rate is *at least* an order of magnitude ***less*** than what was found in published studies! Accordingly, the HF emission rate assumed by the developer *is not* consistent with published literature and it *does not* comply with the Commission's directive issued in Data Request #5 to perform a toxic air contaminant impact analysis using "available representative data from the literature review". Moreover, if the developer's HF emission assumption is increased by a factor of 15 to make it more consistent with published literature, then the developer's 0.63 HF "Hazard Quotient" result must also be increased by a factor of 153 because concentration results scale linearly with emission rates in the AERMOD program[36]. This results in an HF Hazard Quotient of 9.45 which does indeed demonstrate the BESS project will have significant public safety impacts.

Very little of the information provided in the developer's hazard assessment o explains how the developer derived the 38.68 pound HF emission assumption. There is a footnote on page 1 of Attachment A stating "Emission concentrations from the experimental study on thermal runaway and fire behaviors of large format lithium iron phosphate battery, Liu et al 2021". However, the document that is cited in this footnote is only a partial copy of the Liu study, and it does not actually report any emission results (see Attachment 7). In fact, it appears to merely estimate what the HF concentration would be if LFP pouch-style battery cells were burned in an enclosed 50 m^3 (50 cubic meter) room. The developer does not explain how Liu's estimated HF concentrations in a closed room were used to derive the 38.68 pound HF emission assumption upon which the developer's risk assessment is based.

There is also a table in the lower right portion of page 1 of the developer's Attachment A that appears to pertain to HF emissions; it is labeled "Pouch to Cylindrical Reduction Factor" with a footnote that cites to the Larsson study discussed above. The table lists the range of HF emissions per unit of battery capacity reported by Larsson et al for both pouch and cylindrical LFP cell configurations, then it combines several of these HF values in a two-step averaging process. The table then reports a "calculated reduction factor" and a "modeled reduction factor". However, there is nothing in this table that explains how Larsson's HF data were used to derive the 38.68 pound HF emission assumption or how any of the "reduction factors" are utilized applied. In other words, there is simply nothing in Attachment A that corroborates or substantiates the developer's HF emission assumptions and, by extension, the developer's AERMOD results and HF Hazard Quotient conclusions; in fact, the developer's HF emission

[36] AERMOD utilizes a steady state plume model in which concentration results are linearly dependent on emission rates. See equation 51 in the EPA's "AERMOD Model Formulation" document published in 2024 and found here: https://gaftp.epa.gov/aqmg/SCRAM/models/preferred/aermod/aermod_mfd.pdf.

assumption appears to have been conjured from thin air and tailored to ensure that the HF Hazard Quotient result would remained slightly below 1.0. This constitutes a substantial deficiency, and it renders the developer's conclusions uncorroborated and unsubstantiated.

Because the developer does not quantitatively describe how the 38.68 pound HF emission assumption was derived or clearly explain where it came from, the 0.63 HF Hazard Quotient result that was derived from the 38.68 pound HF emission value is not valid and cannot be relied upon by the Commission to draw any public safety conclusions regarding the BESS project. Equally important, when the developer's HF emission assumption is properly adjusted to be consistent with published literature, then the resulting HF Hazard Quotient value substantially exceeds adopted acceptability thresholds. This means that the BESS project does indeed pose a public health risk.

SORT's contention that dangerous HF concentrations are generated downwind of a lithium BESS deflagration is supported by extensive anecdotal evidence. For instance, lithium BESS deflagrations in or near a populated area typically result in extensive "shelter in place" orders and even evacuations (as explained in prior comments submitted by SORT). Additionally, recent events clearly demonstrate that lithium battery fires can cause substantial health impacts. For example, firefighters responding to an electric vehicle fire in Sacramento in April of 2025 were severely injured when white misty smoke wafted into the area where they stood more than 200 feet away from the fire. The firefighters at that location had removed their self-contained breathing apparatus (SCBA) because it was thought the fire was out and they were a safe distance from the fire. Immediately upon inhaling the mist, they all complained of the vapor smell and taste. One of the firefighters began vomiting and was taken to the hospital; all the other firefighters experienced symptoms that required medical attention. Four of the firefighters have suffered from persistent respiratory problems, severe fatigue, and low exercise tolerance; some have experienced a 20% reduction in lung function. These outcomes are consistent with HF exposure which typically presents as "lingering chronic lung" problems[37]. As of October, four of the five firefighters had still not returned to work[38]. If these significantly adverse health effects can result from just an electric vehicle fire located more than 200 feet away, substantially worse health effects will be experienced by Acton residents who are near the BESS project when a Sungrow PowerTitan 2.0 unit ignites. And none of these impacts will be mitigated by the fire response measures recommended by "Fire & Risk Analysis."

[37] https://www.dir.ca.gov/dosh/dosh_publications/Hydrogen-Flouride-fs.pdf .
[38] Information pertaining to this exposure event and the resulting health outcomes are provided in a Stached video found here: https://www.youtube.com/watch?v=I-XFHdnN1tE. A transcript of this video can be provided upon request.

Page 11 of the developer's response to Data Request #5 includes a paragraph that provides a general discussion of HF data. However, the information provided in this paragraph does not explain or describe how the developer derived the 38.68 pound HF emission assumption that was used to calculate the HF Hazard Quotient, towit:

First, the developer identifies the HF study published by Larsson et al (described above) which expresses HF emissions from lithium batteries as a function of battery capacity (in watt-hour or Wh) and reports an HF emission capacity of 20 mg to 200 mg/Wh. Larsson et al concluded that this variation was likely due to differences in electrolyte materials and quantities, but that "information on those amounts are difficult to access for commercial batteries" (see page 2 of Attachment 4). Yet, the developer completely misrepresents the Larsson findings and even claims that Larsson et al concluded that HF yield is *not* dependent on battery capacity and is instead a function of "venting dynamics, construction, and sampling method". The developer's description of Larsson's findings is material incorrect because the Larsson study *does* report HF emissions as a function of battery capacity and not "venting dynamics" or "construction" or "sampling method"; such terms do not even appear in the Larsson study. Contrary to what the developer claims, the Larson study makes express findings regarding HF yield and its dependency on battery capacity because it specifically states:

> *Significant amounts of HF, ranging between 20 and 200 mg/Wh of nominal battery energy capacity, were detected from the burning Li-ion batteries. The measured HF levels, verified using two independent measurement methods, indicate that HF can pose a serious toxic threat, especially for large Li-ion batteries and in confined environments. The amounts of HF released from burning Li-ion batteries are presented as mg/Wh. If extrapolated for large battery packs the amounts would be 2–20 kg for a 100 kWh battery system, e.g. an electric vehicle and 20–200 kg for a 1000 kWh battery system, e.g. a small stationary energy storage. The immediate dangerous to life or health (IDLH) level for HF is 0.025 g/m3 (30 ppm) and the lethal 10 minutes HF toxicity value (AEGL-3) is 0.0139 g/m3 (170 ppm). The release of hydrogen fluoride from a Li-ion battery fire can therefore be a severe risk".*

Clearly, the Larsson study does not support the developer's claims. Equally important, the 3.5 mg/Wh HF emission capacity factor that is implicit in the developer's 38.68 pound HF emission assumption is substantially less than the 20-200 mg/Wh HF emission capacities measured by Larsson. Therefore, the Larsson report does not support the developer's 38.68 pound HF emission assumption or the 0.63 Hazard Quotient that is based upon the developer's 38.68 pound HF emission assumption.

Next, the developer discusses the analytical methodology employed by Larsson et al which involved a Fourier Transform Infrared (FTIR) analyzer to measure vapor phase HF. According to the developer, the Larsson study "adopts FTIR based yields for air dispersion modeling to avoid systematic overprediction of airborne HF". However, the Larsson study makes no recommendations regarding what measurement protocols are appropriate for air dispersion modeling. Furthermore, while SORT agrees that FTIR analysis can be an accurate method for measuring airborne HF concentrations, the use of an FTIR for airborne HF monitoring is not typical, and it is not the only method which provides accurate results. For instance, the airborne HF monitoring methodology adopted by OSHA for assessing worker safety uses a specially treated filter collection system that fuses vapor phase HF[39]. Therefore, it should not be presumed that non-FTIR sampling and analysis methodologies are not efficacious.

Next, the BESS developer asserts that, with respect to HF emissions, the Larsson study concludes "the cell-level results do not scale proportionally with nominal capacity; rather, they scale with electrolyte mass, electrode surface area, and total materials mass". ***None of this*** appears anywhere in the Larsson study! In fact, the Larsson study directly contradicts this claim because it reports HF emissions as a function of nominal capacity (specifically, 20-200 mg/Wh) and it expressly affirms that these results ***are*** scalable based on nominal capacity because it states categorically on page 6 that the 20 - 200 mg/Wh range of HF emission capacities measured for battery cells can be proportionally scaled up to 20 to 200 kg/MWhr for energy storage devices. This particular claim by the developer is utterly lacking in foundation.

Next, the developer points to a 380 page document prepared by the Environmental Protection Agency (EPA) in 1993 pursuant to the 1990 Clean Air Act Amendments, and declares that HF "is rapidly scavenged by fire suppression water, enclosure surfaces, and soot". The developer provides no page citation, and in reviewing the document, SORT found no information pertaining to how HF is "rapidly scavenged" by either "fire suppression water" or "enclosed surfaces" or "soot". However, page 104 states that "water spray systems could be effective in reducing airborne HF. At water to HF ratios of 40 to 1, water sprays have been documented as reducing the concentration of HF in the air by up to 90 percent". The document describes the water spray testing that was done, and it states that the water stream was "pointed at" the HF source; this means that, to achieve a 90% HF removal efficiency, large quantities of water must be applied directly to the HF emission source (see the report excerpt provided in Attachment 8). Clearly, this EPA document indicates that, for water to be an efficacious "HF scavenger" during a BESS fire, copious amounts must be continuously sprayed *directly onto the*

[39] See for example OSHA Method ID-110 for sampling HF in workplace atmospheres. https://www.osha.gov/sites/default/files/methods/osha-id110.pdf

burning BESS to ensure full coverage of all emanating HF vapors. Furthermore, the water must be applied to the BESS throughout the entire deflagration event. However, the developer's "Firefighting Water Supply Analysis" states that water *will not* be applied to the burning BESS, and Table 1 states that no water resources are even allocated to respond to a BESS fire. And, even if 1,000 gallons per minute of water were applied directly onto the BESS to suppress HF emission, the water would be gone in less than 2 hours (as explained above). Therefore, the developer's claim that fire suppression water can effectively "scavenge" vapor phase HF is entirely irrelevant.

Next, the developer states "Experimental studies of battery fires and industrial HF releases show that only a fraction of generated HF remains airborne". This statement is not supported by any citations, references, or evidence. More importantly, this statement is directly controverted by the published studies discussed above which all clearly show that significant quantities of airborne HF are released by burning LFP batteries. Accordingly, the Commission can accord no weight to this statement because it lacks evidentiary support and because it is directly controverted by substantial evidence provided in numerous published studies.

Next, the developer states "Larsson et al also observed that there was a 75% reduction in HF emissions in cylindrical cells compared to pouch, due to increased mechanical confinement, restricted vent paths, and partial retention or internal recombination of fluorinated species". However, no such conclusion is drawn in the Larsson study; in fact, the phrases "mechanical confinement", "restricted vent paths", "partial retention", and "internal recombination of fluorinated species" do not appear anywhere in the study. Furthermore, Larsson et al attribute the differences in HF emissions between LFP pouch batteries (at 43-198 mg/Wh) and LFP cylindrical batteries (at 12-52 mg/Wh) to the differing amounts of electrolyte material used in these batteries (page 4). Nothing in the Larsson study draws conclusions regarding the relationship between HF emissions and "increased mechanical confinement" or "restricted vent paths" or "partial retention" or "internal recombination of fluorinated species". This developer statement lacks foundation and appears to have been completely "made up".

Next, the developer asserts that, because the Larsson results are "based on pouch cells", a reduction factor of 0.5 (or 50%) is applied. However, Larsson et al measured HF emissions from both cylindrical *and* pouch LFP battery cells; this is specifically reported in Table 2 which shows that cylindrical battery HF emission capacities can be as high as 52 mg/Wh (which is consistent with the 60 mg/Wh value derived by averaging values reported in the Claassen study). Because the PowerTitan 2.0 BESS is constructed with cylindrical LFP batteries, and because Larsson et al specifically measured HF emissions from cylindrical LFP batteries, these results can be directly relied upon without a "reduction factor". Moreover, the developer fails to explain how the 0.5 reduction factor

was applied to calculate the 38.68 pound HF emission assumption and associated 1.38 pound per hour HF emission factor that was input to the AERMOD model. In short, nothing that the developer claims regarding the applicability of a reduction factor to Larsson's data is supported.

Finally, the developer asserts "the emission factor of 1,264 milligrams per cubic meter was included herein as the analysis of a 243Ah pouch cell is the most representative of the Project's chemistry and configuration". This assertion makes no sense for several reasons. First, the pouch cell *is not* the "most representative of the Project's chemistry and configuration" because the developer states categorically that the Sungrow PowerTitan 2.0 utilizes a cylindrical cell type[40]. Second, the "1,264 milligrams per cubic meter" cited by the developer is a *concentration value* and not an *emission rate;* therefore, it is cannot be used as a mass emission rate in the AERMOD program[41]. Third, the developer cites to a study published by Liu et al to justify this "1,264 milligrams per cubic meter" concentration value, but the link that is cited[42] produces only a portion of the study report (see Attachment 7); the full report must be purchased. Fourth, the portion of the Liu study report that is available to the public states that Liu et al only studied pouch LFP battery cells that were connected in parallel (see the highlighted portion of Attachment 7) and placed in a prismatic casing; however, the PowerTitan system uses cylindrical cells, not pouch cells. Because the Liu study did not analyze the type of cell that is used in the PowerTitan 2.0 system, it is not particularly relevant. Fifth, the developer does not provide a derivation of the 1,264 mg/m^3 value or even explain where it came from or how it relates to the results presented in the Liu study. Sixth, the developer fails to explain how the reported 1,264 mg/m^3 value was used to derive the 38.68 pound HF emission assumption that was the basis of the 1.38 lb/hr HF emission factor input to the AERMOD model.

To shed light on these deficiencies, SORT purchased the complete Liu study and found the only HF data that it provides is a tabulated estimate of a 162 mg/m^3 HF concentration; it appears to represent the concentration that would result if the pouch batteries were burned in a room that is 50 cubic meters in volume. Copyright protections prevent SORT from providing the Liu report; however, it can be purchased for $35.95[43]. Importantly, the developer never explains how Liu's 162 mg/m^3 hypothetical estimate was used to calculate the claimed 1,264 mg/m^3 "emission factor" or how any of these numbers relate to the 38.68 pound emission assumption. The Liu study provides no relevant data and how it was used is certainly unclear.

---

[40] See for example page 10 of the developer's response to Data Request #5.
[41] As shown on page 1 of Attachment A of the developer's response to Data Request #5, the HF input for the AERMOD model is a mass emission rate (pounds per hour), not a concentration (mg/m^3).
[42] https://www.sciencedirect.com/science/article/abs/pii/S1359431121003963.
[43] https://www.sciencedirect.com/getaccess/pii/S1359431121003963/purchase.

The facts presented above demonstrate that there is ***no*** evidence which supports or explains the developer's assumption that the total HF emissions from a full deflagration of a Sungrow PowerTitan 2.0 is only 38.68 pounds or that the hourly HF emission rate is only 1.38 lb/hour. Equally important, there is substantial evidence that invalidates these assumptions. Moreover, because the developer's hazard assessment is based on these invalid HF emission assumptions, they are themselves invalid and cannot be relied upon to draw any conclusions regarding the public safety impacts of the BESS project.

Additional Concerns with the Developer's Risk Assessment

SORT understands that, in the past, regulatory agencies have approved BESS projects without giving any thought to whether the public will be put at risk by the toxic emissions released from a deflagrating BESS; therefore, we appreciate that the Commission is giving due consideration to this concern. It is essential that such hazard assessments be based on sound technical assumptions and that the emission factors assumed in these assessments be properly documented and their derivation clearly set forth. These are not the circumstances presented by the developer's assessment which does not comply with the Commission's directive issued in Data Request #5 to "provide justification demonstrating that the assumptions are both representative and conservative to be protective of public health".

SORT's concerns regarding the developer's hazard assessment results are not limited to just the assumed HF emission rates. For example, the hazard analysis assumes the HCl emissions from a complete BESS deflagration is only 10.43 pounds, and the hourly emission assumption is only 0.37 pounds per hour; the developer states that these emission rates were derived from the same Liu study that was allegedly used to develop HF emission assumptions. However, the Liu study does not provide HCl mass emission data and the developer does not describe how HCl concentration estimates from the Liu study were used to calculate the 10.43 pound HCl emission assumption. In fact, the 10.43 pound HCL emission assumption is not corroborated or explained anywhere. Accordingly, the developer's HCl emission assumptions are not supported by substantial evidence and the hazard quotient results that are based upon these assumptions cannot be relied upon by the Commission to draw any conclusions regarding public safety impacts of the BESS Project.

Similarly, the hazard assessment assumes the HCN emissions from a complete BESS deflagration is only 10.5 pounds, and the hourly HCN emission assumption is only 0.37 pounds per hour; these values are allegedly based on a "Technical Reference" document posted on the "Safety4Sea" website. However, the link provided by the developer[44]

[44] The link is provided on page 21 of the developer's response to Data Request #5.

connects to a 71 page document[45] that offers no information regarding HCN emissions other than a line in Table 5-1 stating that 0.0182 liters of HCN is emitted per amp hour (a parameter that is utterly meaningless). The developer does not explain how the HCN emission assumptions were derived and does not provide the data that was used to derive them. Accordingly, the developer's HCN emission assumptions are not supported by substantial evidence and the hazard analysis results that are based upon these assumptions cannot be relied upon by the Commission to draw any conclusions regarding public safety impacts of the BESS Project.

Additionally, the developer asserts that the emission rates of several toxic compounds were estimated based on the results of a "Large Scale Burn Test" conducted on the Sungrow PowerTitan 2.0 BESS unit; however, the developer does not provide relevant information such as analytical methods, method detection limits, practical quantitation limits, reporting limits, and QA/QC data even though the Commission directed the developer to provide such information in Data Request #5[46]. Insofar as SORT can determine, the LSBT report has not even been introduced into the record; this makes it impossible to assess the accuracy or appropriateness of the toxic compound emission assumptions which are based on the report. Finally, the poor formatting of the AERMOD output files provided by the developer[47] makes it difficult to assess the efficacy and accuracy of the modeled outputs.

Unfortunately, SORT does not have the bandwidth to analyze in detail *all* the toxic emission assumptions and modeling inputs used by the developer's hazard assessment to determine whether they "are both representative and conservative to be protective of public health"; therefore, we must have faith that the Commission will conduct a critical analysis of these factors. However, the information provided herein is sufficiently detailed to prove that 1) HF emissions from a BESS fire are sufficient to pose a significant health risk and, by extension, a significant public health impact; and 2) the developer's risk assessment cannot be relied upon to assess the public safety impacts of the BESS project because, for at least some toxic compounds, the results are *not*

---

https://safety4sea.com/wp-content/uploads/2020/01/DNV-GL-Technical-Reference-for-Li-Ion-Battery-Explosion-Risk-and-Fire-Suppresion-2020_01.pdf

[45] According to the table of contents provided in the "Technical Reference", the document is nearly 200 pages in length, but the link provided by the developer only accesses the first 71 pages. Thus, it appears that most of the referenced study is not publicly available.

[46] Data Request #5 directs that, for emission factor data which is based on a BESS test, the developer provide "specific analytical method(s) for determining the presence of off-gassing constituents in the test, including sample collection methods, laboratory preparation methods, analytical methods, the MDL (method detection limit) or PQL (practical quantitation limit) or RL (reporting limit) for all measured constituents, and all QA/QC (quality assurance/quality control) data including results of a spiked sample.

[47] Instead of slightly shrinking the oversized spreadsheet output files and/or providing them in "landscape" mode, the developer provided them in "portrait" mode which makes them very difficult to follow.

supported by substantial evidence and in fact are actually controverted by substantial evidence. Finally, SORT notes that there are no mitigation measures which will reduce public safety risks posed by BESS deflagrations and that the only project alternatives which will be effective in this regard are if the project is 1) constructed with a non-lithium battery chemistry; or 2) is constructed at a location that is sufficiently separated from populated areas that the emission of HF and other toxics will not endanger any residences or businesses.

CONCERNS WITH THE NOP DISCUSSION ON PUBLIC SAFETY IMPACTS.

SORT is troubled by the discussion of public safety impacts that is presented in the NOP. For instance, the NOP states on page 10 that, in regards to potential public safety impacts of toxic air emissions, "CEC staff has not completed its analysis of the significance of the project's potential construction or operational impacts and is yet to reach a definitive conclusion". This is troubling because SORT has placed substantial evidence in the record showing that BESS deflagration events have the potential to emit unsafe levels of HF, HCl, and HCN; this evidence has not been controverted[48]. Accordingly, and consistent with Section 21082.2(a) of the CEQA Statute, the NOP should have simply identified the emission of toxic compounds as a potentially significant public safety impact. Instead, the NOP equivocates, and asserts that staff have not decided whether this impact is indeed significant. SORT notes that the purpose of the NOP is to identify impacts that are *potentially* significant; it is not supposed to reach any "definitive conclusions" regarding whether such impacts *are* significant. Definitive conclusions regarding the significance of an impact lie within the domain of the EIR, not the NOP. Furthermore, CEQA Guidelines Section 15064(g) directs the Commission to treat an effect as potentially "significant" even if there is disagreement among expert opinion supported by facts. In other words, even if the Commission has substantial record evidence showing that toxic emissions do not pose a potentially significant public safety impact, Section 15064(g) still requires the NOP to unequivocally identify public safety as a potentially significant impact because SORT has provided substantial record evidence showing that it is.

The NOP also states on page 10 that the EIR will address whether sensitive receptors will be exposed to toxic air contaminants during a BESS fire, but then declares that the EIR will "propose mitigation measures when necessary to reduce any health risks". This statement is very troubling because it presupposes that mitigation measures exist to address toxic emissions from a BESS fire; worse yet, it presumes that these mitigation measures will "reduce any health risks" *even though no record evidence supports such a*

[48] In fact, the developer has assiduously avoided the topic and did not address it until compelled to do so by the Commission in Data Request #5.

presumption. Moreover, there *are no* measures that reduce toxic emissions from a deflagrating lithium ion BESS; therefore, there *are no* mitigation measures that reduce the health risks posed by such events. For example, and as explained above, the only action that could effectively reduce HF emissions from a lithium ion BESS deflagration is to apply copious amounts of water directly onto the burning BESS. However, the BESS project does not allocate any water resources to a BESS fire response and "fogging" the area from the BESS yard perimeter with a 1¾ inch handline that is operated only intermittently at a 125 gpm flow rate (as recommended by "Fire & Risk Analysis") *will not* "reduce any health risks"

In an attempt to understand the mitigations measures alluded to in the NOP that will "reduce any health risks" from a BESS fire, SORT reviewed the Staff Assessment prepared for the recently approved Darden project[49] and analyzed the justifications, assumptions, and mitigation measures that the Commission relied upon to conclude that a BESS deflagration event on the Darden project will not result in any public safety impacts. In the following paragraphs, SORT examines each of the mitigation measures, justifications, and assumptions that formed the basis of the Commission's conclusion; we also show why none of them will "reduce any health risks" posed to Acton residents as a result of a deflagration event at the BESS project.

- "A BESS accidental release of hazardous materials" at the Darden project was found by the Commission to constitute a "less than significant" public safety impact because of the "distance separating the BESS facility from the public" (which was several miles wide). However, and unlike the Darden project, the BESS project is located immediately adjacent to existing residences in Acton. Because there is no "distance separating the BESS facility from the public", this rationalization does not apply to Acton, and distance separation will not "reduce any health risks".
- "Provide that fire lanes exist down the length and width of the BESS units wide enough to allow for fire engine access". This provision will not mitigate public safety impacts because, according to "Fire & Risk Alliance", fire engines will not even enter the BESS yard during a BESS fire (instead, firefighters will remain outside the perimeter wall and "fog" the area from more than 100 feet away using one 1¾ inch handline operating at 125 gpm). More importantly, the BESS yard is so tightly packed that most of the BESS rows are less than 10 feet apart [see for example Figure PSR-BE-100 provided in the developer's most recent site plan); thus, the BESS project does not allow fire engine access down the "length and width" of BESS units.

[49] According to page 4.4-22 and 5.7-33, a BESS fire on the Darden project was found to not pose any significant risk because of "the distance separating the BESS facility from the public" and because of the imposition of three "Conditions of Certification": "WORKER SAFETY-7", "WORKER SAFETY-8", and "HAZ-9". NOTE: only those measures that are applicable to the BESS yard are addressed herein.

- "Provide at least two gates into the BESS facility wide enough for emergency access". The BESS project is configured with multiple access gates, but this configuration does not mitigate public risk because according to "Fire & Risk Alliance", firefighters will remain outside the BESS yard. And, even if they did enter the BESS yard, the BESS are stacked too closely together to be fully accessible by a fire truck.

- "Install remote fire or heat sensors at sufficient locations to cover the entire BESS facility (e.g., thermal infrared)". Fire and heat sensors are useful in notifying off-site operators that a BESS is deflagrating so that they can contact firefighters and HAZMAT teams to respond. However, the sensors will not "reduce any health risks" posed by toxic mist emanating from a BESS fire which will persist even after firefighters are onsite and applying water. Therefore, fire and heat sensors do not "reduce any risk" of a BESS fire. Moreover, even after the firefighters arrive in response to what the fire and heat sensors report, there will not be enough water to operate the high flow equipment needed to lay down water to cool surrounding. Thus, nothing will prevent additional BESS fires and more toxic emissions.

- "Place fire hydrants at the corners and midline location along the two east to west lengths of the facility". The BESS project includes equally spaced hydrants within the BESS yard approximately 50 feet from the perimeter wall; thus, they will not be accessible to the firefighters who, according to "Fire & Risk Alliance", will be staged outside the perimeter wall. And, even if the fire hydrants are placed outside of the perimeter wall and thus accessible to firefighters, the 1¾ inch handlines operating at 125 gpm will be incapable of reaching the burning BESS. And, even if high flow firefighting equipment is brought in, the water will quickly run out, and nothing will prevent additional BESS fires and more toxic emissions.

- "Provide fire water flow of at least 2,500 gallons per minute". If the fire hydrants could deliver a fire flow of 2,500 gallons per minute and were accessible from outside the BESS yard, this mitigation measure will ensure that firefighters could use a "Deck gun" to reach any area in the BESS yard from outside the perimeter. However, the 2,500 gpm fire flow will deplete all onsite water supplies within half an hour[50], after which nothing will prevent BESS fire spread and additional toxic emissions. And, even if 2,500 gpm could be sustained throughout the BESS deflagration event, HF emissions would still not be reduced because efficacious HF suppression requires that copious quantities water be "pointed at" the HF source. Given that firefighters will avoid spraying the burning BESS, the Commission cannot

[50] 80,000 gallons ÷ 2,500 gallons per minute = 32 minutes.

assume that firefighting efforts will "reduce any health risks" because such a finding would be purely speculative and thus impermissible under CEQA[51].

- "Install closed-circuit television (CCTV) cameras with Pan, Tilt, Zoom (PTZ), and low-light capability that cover the entire area of the BESS and which would have their own separate power supply". These cameras will not "reduce any health risks" for the same reasons that the heat and fire sensors described above will not reduce health risks. Cameras are helpful to notify off-site operators that a BESS fire is initiated so that firefighters and HAZMAT teams can be contacted; however, they will not eliminate the toxic mist emanating from the BESS fire which will persist even after firefighter arrival.

- "Establish a Command and Control Protocol for staff to perform emergency duties and responsibilities during the detection, initiation, and escalation of a BESS fire". While this is an important firefighting protocol, it does not "reduce any health risks" posed by toxic mists emanating from a burning BESS.

- "Establish remote telemetry and CCTV viewing in a Command and Control Center located at a safe distance from the BESS facility for an Incident Commander to use". While this is an important firefighting protocol, it does not "reduce any health risks" posed by toxic mists emanating from a burning BESS.

- "Establish an annual joint training program with the FCFPD that includes tabletop exercises for a BESS fire". While firefighter training and "tabletop exercises" are important in deciding how to approach BESS fires when they occur, they do nothing to "reduce any health risks" posed by toxic mists emanating from a burning BESS.

- "Prepare and submit a Root Cause analysis of any incident at the BESS facility (including but not limited to fire, malfunction, leak, or thermal runaway of any cell, module, or unit) to the CPM". "Root Cause" analyses are useful "after action" tools, but they do not "reduce any health risks" posed by toxic mists emanating from a burning BESS.

- "Consult with the FCFPD in preparing the fire protection system specifications and drawings for the Operations and Maintenance Building to ensure an adequate water supply for the fire suppression systems for the BESS facility as well as for occupied buildings". What is particularly troubling about this "mitigation measure" is that the

[51] A CEQA finding that an impact is mitigated to a level that is "less than significant" must be supported by substantial evidence [CEQA Guidelines Section 1509(b)]. Substantial evidence is defined by CEQA as "facts, reasonable assumptions predicated upon facts, and expert opinion supported by facts"; it is not "argument, speculation, unsubstantiated opinion or narrative, evidence which is clearly inaccurate or erroneous, or evidence of social or economic impacts which do not contribute to, or are not caused by, physical impacts on the environment" [Section 21082.2(c) of the CEQA statute].

fire department consultations it establishes should have been conducted ***before*** the Commission approved the Darden project, and the requirements established by this consultation *should be deemed "Conditions of Certification"*. The analysis above demonstrates how critical it is that consultation occur between Commission staff and Fire Department staff and Public Works staff to assess whether the project has sufficient fire protection facilities.

- "Implement the final provisions of CPUC GO 167-C". While GO 167-C is useful in ensuring that BESS facilities maintain log books and maintenance plans and operating plans and comply with maintenance and operating standards[52], the implementation of GO 167-C will not reduce the toxic mists that emanate from a burning BESS and endanger the public. This is because BESS fires can be triggered for any number of reasons (see Attachment 9); thus, no amount of "planning" can reduce these fires. As the CPUC points out, every component of a lithium BESS unit is "a potential **point of failure**—the risk of which can be minimized via quality control, testing, and ongoing monitoring and maintenance ***but cannot be entirely eliminated***"[53]. Accordingly, implementation of GO 167-C does not "mitigate any health risks" posed by the BESS project.

In short, *none* of the justifications and mitigation measures applied by the Commission to conclude that the Darden project would not pose any public safety risks are applicable to the BESS project. Moreover, because there is no record evidence to support a finding that mitigation measures will "reduce any health risks" posed by a BESS fire, the NOP errs in presupposing that such mitigation measures exist and that they are sufficiently efficacious to address any risks.

VISUAL RESOURCES AND AESTHETICS.

The visual resource impacts created by the BESS project are significant because the BESS project introduces an enormous, unsightly, industrial land use in an area that is designated as a "scenic resource" by the County General Plan and the Antelope Valley Area Plan. This is because the project is adjacent to two "priority scenic drives": the 14 freeway located just north of the project and Soledad Canyon Road that runs right through the project. The BESS project site is a designated scenic resource because:

- The County General Plan establishes that "scenic resources" include "scenic viewsheds" which are defined as a "scenic vista from a given location, such as a

[52] CPUC General Order 167-C became effective September 2, 2025 and can be found here: https://docs.cpuc.ca.gov/PublishedDocs/Published/G000/M567/K474/567474805.pdf

[53] *CPUC Energy Storage Procurement Study: Safety Best Practices*. Attachment F at page F-6. https://www.cpuc.ca.gov/-/media/cpuc-website/divisions/energy-division/documents/energy-storage/2023-05-31_lumen_energy-storage-procurement-study-report-attf.pdf

highway, a park, a hiking trail, river/waterway, or even from a particular neighborhood. The boundaries of a viewshed are defined by the field of view to the nearest ridgeline. Scenic viewsheds vary by location and community and can include ridgelines, unique rock outcroppings, waterfalls, ocean views or various other unusual or scenic landforms" [page 160]. The project site is within the boundaries of a "scenic resource" as that term is defined by the County General Plan because it is within the "field of view" of a freeway and several major highways "to the nearest ridgeline" of the San Gabriel Mountains National Monument to the south and of the Sierra Pelona mountains to the north and northwest. Accordingly, the project site is a "scenic resource".

- The Antelope Valley Area Plan (AV Plan) establishes that "scenic resources" include mapped "scenic drives" [page COS-5]; these "scenic drives" are precisely designated on Map No. 4.2 of the AV Area Plan[54] and they include Soledad Canyon Road and the 14 freeway. The BESS project site is immediately adjacent to Soledad Canyon Road and the 14 Freeway (in fact, it is located *between* these two scenic drives) and, if approved, it will dominate the viewshed from both.

It is an indisputable fact that the project is a massive, high density, unsightly industrial use that is completely "at odds with" with its rural agricultural surroundings:

- The project is massive because it stretches for more than a mile throughout Acton's rural countryside. This fact is proven by Figure PSR-SE-101[55].

- The project is high density because it consists of more than two thousand shipping containers that are packed so closely together that they resemble a container storage yard at a major shipping port. And, because the project is in a valley, it will be visible from all the homes and businesses located on the surrounding hillsides.

- The project has an unsightly industrial appearance because of the massive BESS container yard that will be surrounded by a block wall topped with concertina wire and because of the enormous outdoor transmission substation consisting of large 500 kV transformers, busbar facilities exceeding 150 feet in height, and enormous transmission infrastructure that will be highly visible from miles away.

- The project is completely out of character with its rural surroundings because its high density industrial "barbed wire" characteristic is substantially incongruent with the rural, low density agricultural and residential uses that surround it. This fact is proven by Figure 1-5a provided with the developer's application[56].

[54] https://planning.lacounty.gov/long-range-planning/antelope-valley-area-plan/
[55] https://efiling.energy.ca.gov/GetDocument.aspx?tn=266806&DocumentContentId=103897
[56] https://efiling.energy.ca.gov/GetDocument.aspx?tn=264413&DocumentContentId=101199

As SORT has previously remarked, the visual resource impact analysis and visual simulations provided in the developer's application fail to properly describe the BESS project's significant visual resource impacts[57]. For instance, there are no visual simulations of the 500 kV substation portion from either the 14 Freeway or Soledad Canyon Road and there are no visual simulations from any of the homes and businesses that will look down on the project from north of the 14 freeway. Despite these deficiencies, the few visual simulations provided by the developer clearly show that the visual resource impacts created by the BESS project are significant. The EIR that will be prepared for the BESS project must not perpetrate the errors found in the developer's visual analysis; rather, it must provide an accurate and comprehensive set of visual simulations that properly reflect the significant aesthetic impacts of the BESS project from not only the adjacent scenic drives, but also from the homes and businesses that will be forced to endure the visual blight created by the BESS project.

One project alternative and two mitigation measures are available to reduce the significant visual resource impacts of the project. The project alternative is to locate the project outside of a designated scenic resource by placing it outside of the viewshed of a designated scenic drive. The first mitigation measure is to place all the BESS facilities in enclosures that are designed with a western aesthetic (as required by the Acton Community Standards District[58]) to "camouflage" them as much as possible. Of course, this mitigation measure will require the use of a non-lithium battery chemistry, but it will also effectively eliminate the public safety and water resource impacts posed by the Sungrow PowerTitan 2.0 lithium system. Using non-lithium batteries to mitigate visual resource impacts would also allow the battery units to be "stacked" and thereby reduce the project footprint and, by extension, further reduce visual resource impacts. The second mitigation measure is to utilize gas-insulated switchgear (GIS) for the 500 kV substation which will substantially reduce the height and footprint of the substation and allow it to be fully enclosed and "camouflaged". This is a feasible alternative, because new and environmentally benign GIS systems have been developed that operate at 500 kV and do not depend on harmful sulfur hexafluoride (SF_6)[59]. SORT understands that the Commission may not consider a non-lithium battery technology to be a "feasible" mitigation measure as that term is contemplated by CEQA; however, there is no reason to find that the GIS substation mitigation measure is infeasible because the technology works and the marginal cost to construct a GIS substation rather than an open air

[57] SORT letter dated August 18, 2025. https://efiling.energy.ca.gov/GetDocument.aspx?tn=265680&DocumentContentId=102530 at 51-57.
[58] https://library.municode.com/ca/los_angeles_county/codes/code_of_ordinances?nodeId=TIT22PLZO_DIV10PLARCOSTDI_CH22.302ACCOSTDI_APXIACCOSTDIARSTGU
[59] For example, Hitachi has developed an SF6 free GIS switchgear that operates up to 550 kV [https://www.hitachienergy.com/us/en/news-and-events/press-releases/2025/05/hitachi-energy-to-deliver-the-world-s-first-sf6-free-550-kv-gas-insulated-switchgear].

substation is so small compared to the cost of the whole project that a reasonable developer would still proceed with the project if it includes a GIS substation rather than an open air substation. This is the standard established by *Uphold Our Heritage v. Town of Woodside* (2007) 147 Cal.App.4th, and it is applicable here.

SORT appreciates that the NOP recognizes the 14 Freeway as a "priority scenic drive"; however, careful inspection of the "Town and Country Scenic Drives" Map provided in the AV Area Plan (specifically, Map 4.2) shows that Soledad Canyon Road (which runs through the BESS project) is also a "priority scenic drive". This is demonstrated in Figure 3. SORT asks that the EIR prepared for the BESS Project recognize that Soledad Canyon Road is also a "priority scenic drive" and that construction of an enormous, tall, and unsightly industrial 500 kV substation along Soledad Canyon Road will particularly and devastatingly mar this important scenic resource in Acton.

Figure 3. Excerpt from the AV Area Plan "Scenic Drives Map" Showing Soledad Canyon Road is a "Priority Scenic Drive.

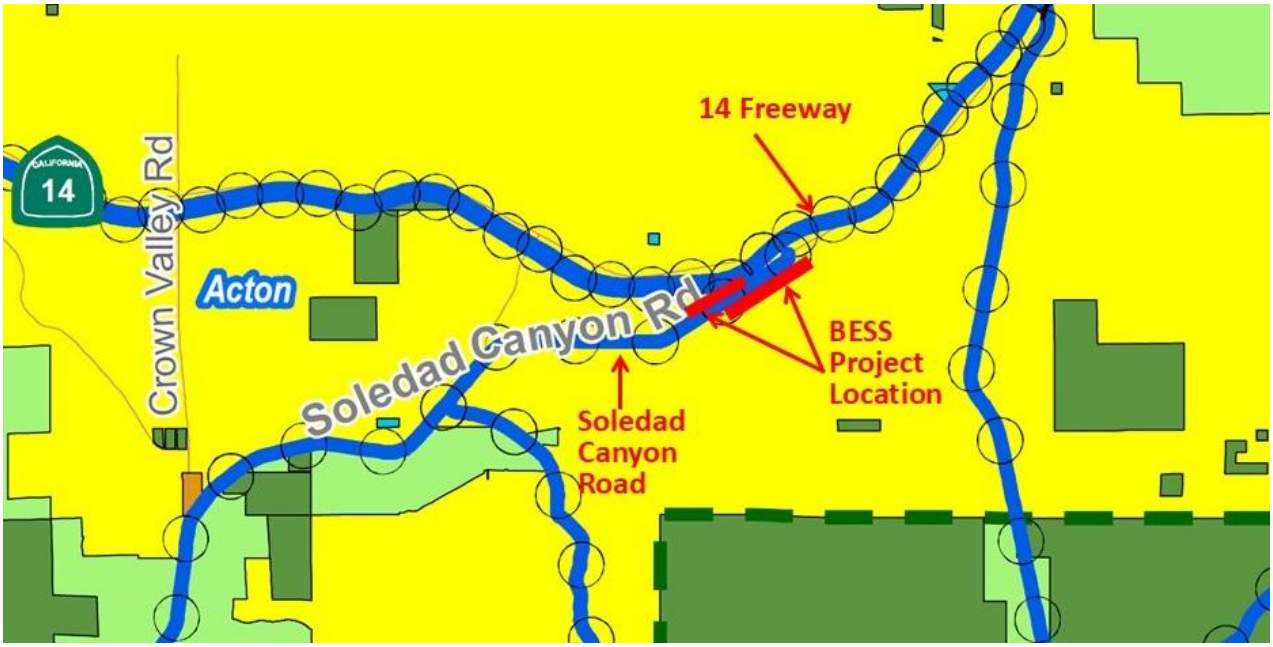

Additionally, the EIR prepared for the BESS project must consider visual resource impacts to the existing trails that both traverse and surround the project site as well as mapped trail routes adopted in the County General Plan[60]. For instance, one mapped trail along Carson Mesa Road is along the southern boundary of the project and it is traversed by the 500 kV transmission line that will connect the project to the Vincent

[60] The mapped trail routes are found in Figure 10.1 of the County General Plan found here: https://planning.lacounty.gov/long-range-planning/general-plan/

Substation. The EIR must also address the fact that the 12 foot high block wall topped with razor wire will *completely block viewsheds* and eliminate what is now a broad and expansive viewscape of the east Acton Valley from the "Scenic Drive" that is Soledad Canyon Road. Finally, the EIR must properly address the cumulative impact of the BESS project in combination with other BESS developments that have been proposed in East Acton, including, but not limited to, the Humidor BESS and the Maathai BESS (both of which have been presented to the Community of Acton by the project developer[61] and both of which the project owner intends to develop). The Humidor Project is located on Assessor parcel numbers 3056004044 and 3056004058; the Maathai project is on Assessor Parcel number 3056012008.

Finally, the Commission must ensure that all lighting on the project faces only downward and is recessed and not just fully shielded. This is the only way to ensure that project lighting is only incident on the project site and that there is ***no*** light trespass onto other properties. Acton is a "Dark Skies" community, and all development in Acton is subject to the County's "Dark Skies" Ordinance enumerated in Chapter 22.80 of the County Code.

NOISE.

The BESS project will result in significant noise impacts both during construction and operation; these impacts must be properly assessed in the BESS project EIR.

Project Construction Noise: Because project construction will extend beyond 10 days, the BESS project is not eligible for the 75 dBA construction noise standard established by Section 12.08.440 of the Los Angeles County Code (which applies only to "short term" construction projects[62]). The reason is simple: 75 dBA is an exceedingly loud noise level[63], and because of this, the County Board of Supervisors determined that only short term construction projects could avail themselves of this exceedingly high 75 dBA noise standard; this ensured that construction projects did not become too burdensome on surrounding properties. Because the BESS project is ineligible for the 75 dBA construction noise standard, the more restrictive "Exterior Noise Standard" set forth in Section 12.08.390 of the County Code applies to the construction phase of the BESS

[61] The Humidor Project has been approved by the County of Los Angeles; however, this approval was challenged in Court and rejected. An appeal of this decision is now pending. The Maathai project was presented at a community meeting in August, 2025.

[62] Section 12.08.440 states 75 dBA is the "Maximum noise level for nonscheduled, intermittent, short-term operation (less than 10 days) of mobile equipment" for construction near single family residences [https://library.municode.com/ca/los_angeles_county/codes/code_of_ordinances?nodeId=TIT12ENPR_CH12.08NOCO_PT4SPNORE_12.08.440CONO]

[63] It is equivalent to the noise generated by the operation of a powerful upright corded vacuum. https://ehs.yale.edu/sites/default/files/files/decibel-level-chart.pdf https://www.ecovacs.com/us/blog/how-many-decibels-does-a-vacuum-cleaner-produce

project (as well as the operation phase of the BESS project). The "Exterior Noise Standard" is based on *actual* "Noise Levels" ("L_N") that occur at the property line of adjacent parcels[64] and is broken down into 5 separate Noise Level "L_N" standards:

- The "L50" standard is a noise level that may not be exceeded at the property line for a cumulative period of more than 30 minutes in any hour. It is referred to as the "L50" standard because it is the noise level that cannot be exceeded more than 50% of the time. For residential properties, the daytime L50 standard is 50 dBA[65].
- The "L25" standard is a noise level that may not be exceeded at the property line for a cumulative period of more than 15 minutes in any hour. It is referred to as the "L25" standard because it is the noise level that cannot be exceeded more than 25% of the time. For residential properties, the daytime L25 standard is 55 dBA[66].
- The "L8.3" standard is a noise level that may not be exceeded at the property line for a cumulative period of more than 5 minutes in any hour. It is referred to as the "L8.3" standard because it is the noise level that cannot be exceeded more than 8.3% of the time. For residential properties, the daytime L8.3 standard is 60 dBA[67].
- The "L1.8" standard is a noise level that may not be exceeded at the property line for a cumulative period of more than 1 minutes in any hour. It is referred to as the "L1.8" standard because it is the noise level that cannot be exceeded more than 1.8% of the time. For residential properties, the daytime L1.8 standard is 65 dBA[68].
- The "L0" standard is the maximum permissible exterior noise level that may not be exceeded at the property line for any period of time. It is referred to as the ""L0" standard because it is the noise level that can never be exceeded (i.e. 0% of the time). For residential properties, the daytime "L0" standard is 70 dBA[69].

The EIR must apply these noise standards in both the construction noise analysis and the operation noise analysis that is prepared for the BESS project EIR because these are the applicable noise standards per the County Code. Furthermore, all baseline noise measurements that are collected in the vicinity of the project to establish existing noise profiles must be reported as L50, L25, L8.3, L1.8 and maximum L0 values, and all projected noise levels must also be reported as L50, L25, L8.3, L1.8 and maximum L0

[64] Section 12.08.390.B states "no person shall operate or cause to be operated, any source of sound at any location within the unincorporated county, or allow the creation of any noise on property owned, leased, occupied or otherwise controlled by such person which causes the noise level, when measured on any other property".
[65] If the existing L50 noise level exceeds 50 dBA, then the measured L50 value is the applicable standard.
[66] If the existing L25 noise level exceeds 55 dBA, then the measured L25 value is the applicable standard.
[67] If the existing L8.3 noise level exceeds 60 dBA, then the measured L8.3 value is the applicable standard.
[68] If the existing L1.8 noise level exceeds 65 dBA, then the measured L1.8 value is the applicable standard.
[69] If the existing L0 noise level exceeds 70 dBA, then the measured L0 value is the applicable standard.

values; this is essential for ensuring a proper comparison of project noise impacts to baseline conditions.

SORT notes that the developer's noise analysis submitted with the BESS project application does not utilize the proper "Noise Level" ("L_N") standards adopted by the County Code; in fact, SORT prepared a detailed assessment of the developer's noise analysis which identified numerous errors and deficiencies[70]. For example, the developer improperly applied a 75 dBA noise standard to the construction activities and even cited Section 12.08.440 of the County Code as justification *even though Section 12.08.440 clearly states that the 75 dBA standard only applies to short term construction projects that operate less than 10 days*. Worse yet, the developer "interprets" the County's 75 dBA construction noise standard to be an "equivalent" noise standard (referred to as "L_{eq}") in which all noise events that occur over an 8 hour period are averaged together; with this "interpretation", deafeningly loud construction activities (such as pile driver operations that regularly exceed 90 dBA) are "averaged out" so that the resulting *equivalent* noise value remains below 75 dBA even though the *actual* noise level greatly exceeds 75 dBA. The Commission cannot repeat the mistakes embodied in the developer's noise analysis:

- The 75 dBA construction noise standard is not an "equivalent" L_{eq} standard; to the contrary, it is an actual maximum noise level that may not be exceeded at any time.
- The 75 dBA construction noise standard does not apply to the BESS project anyway because construction activities will exceed 10 days.
- All baseline noise measurements must be reported only as L50, L25, L8.3, L1.8 and maximum L0 values.
- All projected noise levels must be reported as reported as L50, L25, L8.3, L1.8 and maximum L0 values.

SORT notes that the project construction noise reported in the EIR that the Commission prepared for the Darden project utilized the equivalent L_{eq} methodology to average all noise insults and concluded that noise levels would be 80 dBA [see page 5.9-8]. This conveniently masks the actual 100+ dBA noise level that adjacent residences will experience during construction due to pile driver operations (which the EIR attempts to mitigate to some extent[71]). SORT understands that the Commission utilized the L_{eq}

[70] SORT letter dated August 18, 2025. https://efiling.energy.ca.gov/GetDocument.aspx?tn=265680&DocumentContentId=102530 at 39-46.
[71] The Darden developer is required to use plywood pads or impact cushions, dampened driving, and vibratory drivers or hydraulic pile pushers. However, noise insults will still be significant (>80 dBA). The EIR dismisses this concern by stating that the impact is "temporary"; this controverts CEQA which does not permit a lead agency to dismiss a significant impact simply because it is temporary.

methodology because the Fresno County Noise ordinance exempts construction activities from compliance [page 5.9-7] and therefore the Commission had no established construction noise standard to work with; this is also why the Commission found that construction noise impacts did not exceed adopted standards and were thus "less than significant" [page 5.9-9]. In contrast, the Los Angeles County Noise Ordinance does not exempt construction activities and it is not based on an equivalent L_{eq} methodology. Accordingly, an entirely different methodology will have to be applied to the BESS project noise impact assessment.

Project Operation Noise:

BESS project operations will result in noise impacts because BESS inverters and 500 kV transformers all have a direct "line of site" to surrounding residential uses. SORT understands that the Commission will assess these impacts and the extent to which the BESS project comports with the County's "Exterior Noise Standard" described above.

However, the Commission must also assess the significant "low frequency" noise impacts that will result from BESS project operations. As SORT has previously explained[72], utility scale BESS facilities (inverters, transformers, power control systems, etc.) generate significant levels of low frequency noise (<1,000 Hertz) which are constant and highly disturbing. Low frequency noise insults present themselves as a background hum that verges on a low vibration which the body "senses" more than the ear "hears". A person can actually be unaware of the low frequency noise insults that their body perceives until the noise is curtained at which time they experience an immediate sense of relief. Low frequency sound is often characterized as an "annoyance" because of the way it affects the human body. And, because adopted noise standards and noise reporting procedures are based on the A-weighted scale, they fail to capture or address significant noise insults that occur in the low frequency range. According to a publication posted by the National Institutes of Health and the National Library, low frequency noise is a "special environmental noise problem, particularly to sensitive people in their homes"[73]; the article further points out that "conventional methods of assessing annoyance, typically based on [an] A-weighted equivalent level, *are inadequate for low frequency noise* and *lead to incorrect decisions by regulatory authorities* (emphasis added).

[72] SORT letter dated August 18, 2025. https://efiling.energy.ca.gov/GetDocument.aspx?tn=265680&DocumentContentId=102530 at 43-44.

[73] Leventhall H. G. Low frequency noise and annoyance. Noise Health. 2004 Apr-Jun;6(23):59-72. A copy is provided in Attachment 10.

Equally important, low frequency noise are not effectively attenuated with barriers[74], and while vegetation and ground cover can provide a limited amount of absorption in the low frequency range, Acton lacks sufficient vegetation to make any difference. In other words, the low frequency noise impacts that will be caused by the BESS project *cannot be mitigated*, and noise reduction will only occur via geometric attenuation. A noise propagation analysis prepared by SORT indicates that *all* the homes surrounding the BESS Project will be subject to continuous and substantial low frequency noise insults that will exceed 80 dB; even the homes that are north of the 14 Freeway along San Gabriel Avenue will experience continuous low frequency noise levels exceeding 70 dB. Accordingly, it is essential that the noise analysis prepared for the BESS Project EIR include an assessment of low frequency noise impacts which, according to information provided by the developer's application, will be significant[75].

SORT understands that low frequency noise impacts are not typically addressed in environmental reviews; this is because most projects do not generate low frequency noise insults. In fact, and insofar as SORT is aware, only three types of developments tend to generate continuous and significant low frequency noise: 1) Energy system infrastructure (such as the BESS project); 2) high speed transportation systems (particularly trains traveling at speeds exceeding 160 miles per hour[76]); and 3) manufacturing facilities with significant HVAC, compressor, and/or mechanical equipment operations. However, a core purpose of the CEQA scoping process is to ensure that the Lead Agency is fully appraised of significant project effects that warrant in depth analyses in an EIR [Guidelines Section 15083] even if such effects are unique to the project and not typically addressed. These are the circumstances here: because the BESS project will result in significant low frequency noise impacts, such impacts must be fully addressed in the EIR that is prepared for the project.

Finally, SORT notes that, while most EIRs tend to assess noise impacts based on *average* equivalent noise values (L_{eq}) rather than *actual* noise levels (L_N), it would be improper to apply an L_{eq} equivalent noise standard to the BESS project because the Los Angeles County Noise Ordinance is not based on any L_{eq} standard (as explained above). Moreover, because CEQA requires the Commission to assess the "direct effects" of the BESS project and because CEQA defines "direct effects" as effects that are "caused by

---

[74] The FRA Noise Manual states low frequencies "are inherently difficult to shield with a barrier". [https://railroads.dot.gov/sites/fra.dot.gov/files/fra_net/2680/20120220_FRA_HSR_NV_Manual_FINAL_102412.pdf].

[75] The last page of Appendix 3-7 reports that peak low frequency noise levels from the PCS and the transformers are 96.9 and 108 dB, respectively

[76] As the train speed exceeds 180 mph, aerodynamic noise effects begin to dwarf mechanical noise (steel wheels on rails, engines, etc.); the dominant frequency band in aerodynamic noise is 500 Hz and less. [https://railroads.dot.gov/sites/fra.dot.gov/files/fra_net/2680/20120220_FRA_HSR_NV_Manual_FINAL_102412.pdf at 2-11].

the project and occur at the same time and place" as the project [Guidelines Section 15358], the Commission is precluded from utilizing an "equivalent" L_{eq} noise parameter to assess "direct" noise effects because L_{eq} merely represents the average of all noise events and ***does not*** represent *actual* noise effects at the "time and place" in which they occur. However, the "equivalent" L_{eq} noise parameter may perhaps be used to assess the indirect noise effects of a project[77].

LAND USE.

As SORT has explained in previous comment letters, approval of the BESS project on agriculturally zoned land in Acton's rural town area will result in numerous and substantial land use conflicts and thus create significant land use impacts. For instance, in a letter dated August 18, 2025 SORT explained that the BESS project controverts the Los Angeles Zoning Code which expressly prohibits the construction of energy storage devices as a principal use on agricultural zones. In a letter dated November 5, 2025, SORT explained that the developer was incorrect to claim that an "Interpretation Memorandum" issued by the Department of Regional Planning permits the BESS project and we provided court documents which showed that this "Interpretation Memorandum" cannot be applied in a manner that is contrary to the Zoning Code. Since November, SORT has commenced another legal action to challenge a second BESS approval issued by Regional Planning that was based on this "Interpretation Memorandum"[78].

The November letter also explained how the BESS project is inconsistent with many policies, goals, and development objectives set forth in the County General Plan and the AV Area plan. The Courts have long held that an inconsistency between a proposed project and an adopted General Plan policy, goal, or development objective constitutes a potentially significant environmental impact when the policy, goal, or objective was adopted for the purpose of mitigating environmental impacts. [*Joshua Tree Downtown Business Alliance v. County of San Bernardino* 1 Cal.App.5th 677, *Pocket Protectors v. City Of Sacramento* (2004) 124 Cal.App.4th 903]. SORT has evaluated all the plan policies, goals, and development objectives that were adopted to mitigate environmental impacts, and found that more than 60 of them are controverted by the BESS project; these policies, goals, and development objectives are provided in Attachment 11. Accordingly, the EIR that is prepared for the BESS project must address ***each*** of these controverted plan policies, goals, and development objectives as a separate and distinct significant environmental impact.

---

[77] Indirect effects are defined by CEQA as effects "which are caused by the project and are later in time or farther removed in distance, but are still reasonably foreseeable" [CEQA Guidelines 15358].

[78] The second legal challenge pertains to a ministerial BESS approved in the unincorporated rural community of Castaic. Los Angeles County Superior Court Case No. 25STCP04792.

Finally, SORT observes that the BESS project is intrinsically incompatible with the rural residential and agricultural development that surrounds the project. At its core, "land use compatibility" means the capacity for different land uses to coexist in close proximity in a harmonious way without adverse effects. The BESS project is not a "compatible land use" by definition because it brings only disharmony and significant adverse effects into an existing rural residential area. For example, the BESS project endangers surrounding residents because of the toxic contaminants that will be released with each BESS deflagration event; these toxic emissions cannot be eliminated or even reduced. The BESS project will also produce a constant and significant low frequency noise that will be highly disturbing to the surrounding neighborhood; this persistent and highly disturbing low frequency noise cannot be eliminated or reduced. The BESS project also introduces an immense, mile long, high density, and unsightly industrial use into Acton's bucolic east side which consists of a massive 500 kV transmission substation and an enormous BESS yard surrounded by a block wall and concertina wire; the visual blight cannot be eliminated or even reduced. The BESS project also eliminates large, undisturbed open spaces with Juniper Woodland, Joshua trees, cholla, sage, rabbitbrush, and other vegetation that provide extensive habitat for many wildlife species (both common and endangered). The visual blight, noise, and public safety risk introduced by the BESS project into an existing rural, residential, and agricultural neighborhood represents the very essence of "incompatible land use"; thus, these incompatibilities constitute significant impacts that must be fully explored in the EIR.

HAZARDOUS MATERIALS AND HAZARDOUS WASTE.

Hazardous waste is defined in Section 261.3 of Title 40 of the Code of Federal Regulations (40 CFR § 261.3) as a solid waste that is not exempt under § 261.4(b) and has one or specific characteristics, including "ignitibility" which, as set forth in § 261.21 (a) (2) includes non-liquid waste that, "when ignited, burns so vigorously and persistently that it creates a hazard". Spent BESS devices ***are not*** exempt from a hazardous waste designation under § 261.4(b) and when ignited, spent BESS devices ***do*** "burn so vigorously and persistently that it creates a hazard". This is because waste BESS devices are just lithium ion battery cells that are not connected to any fire suppression or battery management systems and which contain large quantities of highly flammable and reactive electrolyte. Accordingly, every spent Sungrow PowerTitan 2.0 lithium battery cell that is produced by the BESS project ***is*** hazardous waste because it meets the definition of hazardous waste.

SORT understands that spent BESS batteries are often regarded as "universal waste" because energy developers always claim that they will be recycled and not disposed of. Remarkably, regulators just accept these claims and assume that all BESS batteries will be recycled; they never assess whether such developer claims are true or investigate

whether the requisite recycling facilities actually exist or where they are or if they have sufficient capacity to recycle all the battery waste that the project generates. The BESS project is no different; in fact, the developer refuses to even acknowledge that the spent battery cells are indeed "hazardous waste"[79]. Instead, the developer just states that batteries "will be recycled *to the extent feasible*" (emphasis added) and that "the project alone is not expected to generate quantities of waste such that the surrounding accepting facilities cannot accommodate the additional materials"[80]. However, and as explained in SORT's comment letter dated August 18, 2026, there are no "surrounding accepting facilities" for lithium battery waste; in fact, and insofar as SORT is aware, there are no such facilities in the State of California and most are thousands of miles away[81]. The allegation that spent battery cells will be recycled "to the extent feasible" is a legal fig leaf that the developer uses to sidestep any obligation to properly address spent batteries as the hazardous waste stream that it is. As proof of this, one need only recognize that the developer does not identify the lithium battery recycling facilities that will be used for the BESS project *because there are none*. Yet, the mere claim that battery cells will be recycled is apparently sufficient to insulate the developer from properly addressing them as hazardous waste; this conclusion is based on the fact that the NOP does not identify ***any*** hazardous waste streams generated by the project.

As SORT explained in detail in the comment letter dated August 18, 2026, the BESS project will begin generating significant volumes of hazardous waste within 5-10 years of commissioning because that is the lifecycle for lithium BESS devices. The developer admits that 60 tons of spent lithium battery cells will be produced *each year*[82], and ***all of it*** is hazardous waste. Yet, and incredibly, this input has been completely ignored because the NOP does not even acknowledge that BESS project operations will continually generate significant volumes of hazardous battery cell waste. The EIR must deal with this problem "head on" by addressing whether there is (or will be) sufficient capacities at battery recycling facilities to process the 60 tons per year of hazardous battery cell waste that will be generated by the BESS project and identify where these recycling facilities are and what transportation and air quality impacts will result from their transport and processing. And, if there is not (or will not be) sufficient recycling capacity for the BESS project *then the BESS project cannot be approved* because the hazardous battery cell waste that will "pile up" will pose a *significant and unmitigable public safety risk wherever it is stored*. For example, a storage facility for spent lithium batteries in Morris, IL went up in flames in 2021 and resulted in a 4-day evacuation of

[79] Page 3.14- 7 of the Application.
[80] Page 3.14-8 of the Application.
[81] An excerpt from SORT's comment letter that addresses his concern is provided in Attachment 13; this excerpt provides evidence that the BESS project will generate significant amounts of hazardous waste.
[82] Table 3.14-3 of the Application.

all areas within half a mile[83]. The transportation, storage, and processing of the hazardous lithium battery cell waste stream generated by the BESS project will result in potentially significant waste handling and public safety impacts that must be addressed by the EIR.

TRANSPORTATION.

The NOP indicates that the Commission does not anticipate that transportation impacts of the BESS project will be significant because any such impacts can be mitigated. SORT respectfully disagrees. The transportation of thousands of lithium ion BESS containers to and from the project site on freeways, highways, and local roads *does* pose potentially significant transportation impacts (as well as public safety risks) because a single BESS transportation mishap can result in closures along these transportation corridors that last for days[84]. Additionally, the deflagration of a BESS unit at the project site will require the closure of surrounding roads, highways, freeways and rail corridors which also constitutes a significant transportation impact. The only alternative that will significantly reduce these transportation impacts is to utilize a non-lithium battery chemistry for the BESS project.

SORT understands that a transportation mitigation measure implemented for the Darden project was to require BESS units to be shipped at a state of charge that does not exceed 30%. Citing a 2018 study by the U.S. Department of Transportation for the FAA Reauthorization Act of 2018 which addresses the air transport of battery cells, the Commission opined that this measure would reduce any BESS transportation hazard to a level that is less than significant because lowering the state of charge (SOC) "during transportation reduces the severity of the thermal runaway, slows or eliminates propagation of the thermal runaway, and reduces the volume of flammable gasses vented during thermal runaway"[85]. However, this study pertains solely to air transport systems which differ substantially from ground transport systems. Air transport systems do not experience dangerous road conditions, unsafe drivers, on-road mechanical failures, and other difficulties that are the cause of so many BESS transportation fires and explosions. And, since this 2018 study was released, many accidents involving lithium BESS have occurred during ground transportation which caused numerous and substantial impacts. This is because a lithium ion BESS is perfectly capable of experiencing thermal runaway, sustaining thermal runaway, and

[83] https://response.epa.gov/MorrisLithiumBatteryFire#:~:text=The%20Morris%20Lithium%20Battery%20Fire%20occurred%20on,a%201/2%20mile%20evacuation%20of%20nearby%20residents .

[84] In 2024, the Vincent Thomas bridge was closed for more than 30 hours because a BESS unit exploded after a traffic mishap. And, when a BESS container caught fire during transport in July, 2024, officials were compelled to close the 15 Freeway in San Bernardino County for almost 48 hours. This particular incident involved an LFP BESS.

[85] Darden Clean Energy Project Staff Assessment at 4.4-20.

releasing flammable and toxic gases at *any* state of charge *including a 30% SOC*. Accordingly, SORT challenges the conclusion adopted by the Commission in prior proceedings that transportation impacts will be less than significant if the BESS is transported at an SOC that is less than 30%; history shows this conclusion is simply not true.

Additionally, a deflagration event at the BESS project site will result in significant transportation impacts because of the lengthy closure of adjacent freeway, highway, roadway, and rail corridors that will be initiated due to the release of toxic emissions. SORT notes that an email dated January 21, 2026 from LACoFD staff was entered into the docket by the developer which states that the staff member does not anticipate any rail or highway closures as a result of "localized emergency incidents related to this project" [TN # 268304]. However, and as explained in the responsive comment letter submitted by SORT on January 27, 2026, the developer provided LACoFD with erroneous information regarding the proximity of highway and rail corridors. For instance, the developer told the LACoFD staff member that the project is "setback" more than "444 feet from the nearest highway" and that it was "approximately 200 feet from the closest rail line". These statements are categorically false. Soledad Canyon Road actually runs through the BESS project,and there is *no setback* between this highway and the project site. Additionally, the entire southern boundary of the BESS project site shares a common property line with the existing rail corridor, so there is no separation between the BESS project site and the rail corridor. Equally damning, the developer never even told the LACoFD staff member that the BESS project is adjacent to the 14 freeway, which is a major transportation corridor that serves up to 105,000 travelers per day[86] and connects Southern California to Northern California, Arizona, and beyond. Simply put, the LACoFD staff member was relying on patently false information provided by the developer when he opined that rail or highway closures were not anticipated in the event of "localized emergency incidents"; therefore, the Commission cannot rely upon this opinion in ascertaining the significance of traffic impacts resulting from the BESS project. Moreover, and given that BESS fires cause lengthy evacuations, and "shelter in place" orders within half a mile or more, it is a *certainty* that the BESS project will result in road closures every time a BESS deflagration event occurs.

Finally, the developer's site plan indicates that the block wall surrounding the BESS yard is less than 25 feet from Soledad Canyon Road (a designated "Major Highway" in the County Road System); therefore, Soledad Canyon Road will have to be closed so that firetrucks and firefighters can freely access and safely stage outside the block wall enclosure when responding to a BESS fire.

[86] https://dot.ca.gov/-/media/dot-media/programs/traffic-operations/documents/census/2023/2023-traffic-volumes-ca-a11y.xlsx

SORT notes that the transportation impacts identified above were not considered in prior environmental assessments prepared by the Commission for projects that include lithium ion battery systems; this is because the Commission's assessment was limited to standard "CEQA Checklist" items and only addressed whether the project:

1. Conflicts with a program, plan, ordinance or policy addressing the circulation system, including transit, roadway, bicycle and pedestrian facilities?
2. Conflicts or is inconsistent with CEQA Guidelines, section 15064.3, subdivision (b)?
3. Will substantially increase hazards due to a geometric design feature (e.g., sharp curves or dangerous intersections) or incompatible uses (e.g., farm equipment)?
4. Will result in inadequate emergency access?

The unusual circumstances surrounding the hazardous BESS devices utilized by the project and their propensity to trigger road closures when they deflagrate during transportation or operation warrants a "broadening" of the spectrum of transportation impacts that will be considered in the EIR. This is appropriate, given that a core purpose of CEQA scoping is to identify "significant effects to be analyzed in depth in an EIR" if such claims of significant impacts are supported by substantial evidence [CEQA Guidelines 15083]. The evidence placed in the record by SORT and others regarding the adverse transportation impacts described above is sufficiently substantial to warrant consideration of these impacts in the EIR. Accordingly, they must be addressed.

WILDFIRE.

As explained above, the BESS devices proposed for the project are susceptible to the type of violent deflagration event and flame characteristics that are pictured in Figure 1. This, coupled with the fact that the BESS project is in a designated Very High Fire Hazard Severity Zone which also happens to regularly experience very high winds, is certainly indicative of a significant wildfire risk. This risk is substantially amplified by the fact that the developer does not intent to actively respond to any BESS fires, and has not provided any water resources to actively respond to a BESS fire. Together, these factors demonstrate that the BESS project will result in significant wildfire impacts which can only be mitigated by utilizing non-lithium batteries in place of the Sungrow PowerTitan 2.0 system.

CONCERNS REGARDING BESS PROJECT OBJECTIVES.

The developer has identified 13 "basic project objectives" for the BESS project. Several of these objectives are consistent with CEQA Guidelines Section 15124 because they

properly reflect the underlying purpose of the BESS project [87]; examples include the development of new energy storage capacity to meet California's renewable energy, climate change, procurement, and greenhouse gas reduction goals and to provide grid benefits. However, nearly half of the developer's objectives do not reflect the project's underlying purpose; instead, they impose conditions that merely benefit the developer and they are so artificially constrained that the only alternative which is capable of achieving them is the proposed BESS project (or slight variations of it). These project objectives include:

- "Secure a location to allow the stored energy to relieve grid congestion, and enhance electricity reliability, without requiring the construction of substantial new regional transmission infrastructure or network upgrades."
- "Develop an electricity storage facility in close proximity to a utility grid-connected substation with existing capacity …"
- "Develop an energy storage project that is in close proximity to existing electrical infrastructure and the Vincent Substation…"
- "Locate a site to accommodate a gen-tie line of reasonable length to the POI (point of interconnection) …."
- "Locate near existing roadways and related infrastructure where available and feasible for construction and O&M access."

These objectives are not necessary to achieve the renewable energy integration and grid enhancement purposes of the BESS project. Rather, they simply ensure that the BESS project will be constructed near the Vincent substation in Acton; this allows the developer to construct a shorter transmission line and thus avoid the cost and hassle of developing more lengthy transmission facilities. There is no evidentiary support for these project objectives because the underlying project purpose can be fully achieved if the BESS project is located in a remote and unpopulated area outside of Acton. And frankly, the environmental impacts of constructing a line that connects to such a location (particularly if it utilizes an existing transmission corridor) will be far less significant than the BESS project's noise, land use, public safety, visual, transportation, and water resource impacts that will persist in Acton for at least 40 years. Many large remote BESS facilities have been successfully interconnected to the grid despite the fact that they are located miles from infrastructure. For example, the Sanborn project is the largest BESS constructed to date, and it is located 11 miles away from its grid connection at the Windhub substation. Given that "CEQA establishes a duty for public agencies to

[87] § 15124 of the CEQA Guidelines states "The statement of objectives should include the underlying purpose of the project and may discuss the project benefits".

avoid or minimize environmental damage where feasible" and requires agencies "to give major consideration to preventing environmental damage" [Guidelines Section 15021], it is axiomatic that placing the BESS project in a remote and unpopulated area is preferred because it eliminates 40 years of significant noise, land use, water resource, visual resource, wildfire, and public safety impacts in Acton. Fortunately for Acton, CEQA does not permit the inclusion of project objectives that are so narrowly defined that they impermissibly constrain the range of project alternatives and preclude alternatives that avoid or substantially lessen the project's significant environmental effects. Accordingly, the project objectives listed above must not be included in the EIR.

Finally, SORT appreciates that the Darden project objectives included: "Design, construct, and operate the facility in a manner that respects the local community, its values, and its economy" and "Operate the facility in a manner that protects the safety of on-site staff and off-site members of the public.". SORT respectfully requests that similar "community protective" project objectives be established for the BESS project.

ALTERNATIVES TO THE BESS PROJECT.

CEQA directs lead agencies to consider "alternatives to the project or its location which are capable of avoiding or substantially lessening any significant effects of the project, even if these alternatives would impede to some degree the attainment of the project objectives, or would be more costly" [CEQA Guidelines Section 15126.6(b)]. CEQA also establishes that the alternatives considered in an EIR "shall be limited to ones that would avoid or substantially lessen any of the significant effects of the project" [CEQA Guidelines Section 15126.6(f)]. In other words, CEQA precludes the consideration of alternatives that do not "avoid or substantially lessen any of the significant effects of the project".

As explained in detail in the comment letter submitted on January 5, 2026 (see Attachment 12), SORT has carefully reviewed the BESS project alternatives proposed by the developer[88], and note that they all place the BESS development adjacent to residential areas in High or Very High Fire Hazard Severity Zones and on land that is not zoned for BESS uses. As such, the alternatives proposed by the developer will create the same significant noise, public safety, visual, land use, water resource, hazardous waste, and transportation impacts as the BESS project and not "avoid or substantially lessen" any of them. Accordingly, the alternatives proposed by the developer do not comport with CEQA and cannot be considered in the EIR that the Commission prepares for the BESS project.

[88] SORT comment letter dated January 5, 2026. Pages 1-5.

SORT has developed a range of system alternatives that should be included in the BESS Project EIR because they "avoid or substantially lessen" the public safety, water resource, transportation, and hazardous waste impacts created by the project. These system alternatives are discussed in SORT's comment letter dated January 5, 2026[89] and they involve non-lithium battery chemistries (Iron Flow, Vanadium Redox, Aqueous Zinc, etc.) that are not susceptible to deflagration and toxic release. These alternatives may also be able to substantially reduce the visual impacts of the BESS yard because unlike lithium BESS, non-lithium BESS can be stacked and operated indoors; this will allow them to be somewhat "camouflaged" by an indoor configuration and attractive landscaping.

Finally, SORT has developed a range of location alternatives that should also be included in the BESS Project EIR because the locations are:

- Outside of fire hazard zones (which substantially reduces wildfire risk);
- Zoned for BESS uses (which substantially reduces land use impacts); and
- Away from homes (which substantially reduces noise, visual resource, and public safety impacts).

These alternatives are discussed in detail in SORT's letter dated January 5, 2026 which, for convenience, is provided in Attachment 12.

DECOMMISSIONING.

As explained in the SORT comment letter dated August 18, 2025, AV Area Plan policy COS 13.3 was adopted for the purpose of mitigating environmental effects, and it requires the BESS site to be restored to its "natural condition". Therefore, decommissioning the BESS project in a manner that is consistent with this policy is a key consideration, and a lack of consistency with this policy would constitute a significant environmental impact that must be mitigated if feasible [§ 21002 of the CEQA statute]. It is certainly feasible to fully decommission the BESS project and remove all BESS facilities from the project site (including concrete foundations) and there is no reason why the developer cannot do so. Nonetheless, the developer has stated that the BESS project site will not be returned to its original condition and that the only equipment and infrastructure to be removed is that which is above ground or shallowly placed[90]; this will prevent the eventual re-establishment of keystone species

[89] Id at 6-7.

[90] As SORT previously pointed out, the developer's Draft Decommission Plan states that material which is 3 feet or more below the surface will be left behind and even indicates that foundations and cables will be abandoned in place.

and critical vegetation communities that provide essential habitat[91]. The developer's decommissioning plan is unacceptable, and if approved, it will result in significant environmental impacts that are not mitigated despite the fact that full mitigation is entirely feasible. The NOP does not mention the developer's draft decommissioning plan, or the fact that its implementation will preclude the reestablishment of keystone species and critical vegetation communities and therefore result in permanent and significant environmental effects. Nonetheless, all of these concerns must be addressed in the EIR, and it must include mitigation measures which ensures that the BESS site is fully rehabilitated with all copper cables and concrete foundations removed.

SORT is not alone in having concerns that the developer will not properly decommission the BESS project site; several commenters at the Scoping Meeting expressed concern that, once the developer finds the project to be either not sustainable or not profitable, they will simply walk away and abandon infrastructure in place. It happens everywhere all the time, including in Acton[92]. Thus, residents have little faith in commitments made by government agencies and developers that project sites will be restored upon project decommissioning. Our mistrust is amplified by the fact that the developer claims the BESS project is consistent with AV Area Plan policies (which means that the BESS project site will be fully restored to a "natural state" as required by Policy COS 13.3) but then drafts a Decommissioning Plan which states that anything below 3 feet in depth will be abandoned in place; this will preclude the reestablishment of keystone native species and result in the leaching of copper into the soil once the sheathing that surrounds abandoned cables is broken down.

SORT has reviewed the Staff Assessment prepared for the Darden project, and we find that our concerns are not allayed. For instance, the Staff Assessment states that the Darden project developer is only required to restore the site "to the extent practicable"[93].

---

[91] Abandoned detritus on the BESS site will prevent re-establishment of native vegetation communities including Big Sagebrush, California Juniper Woodland, California Buckwheat scrub, and Rubber Rabbitbrush scrub. These vegetation communities rely on keystone species that develop deep taproots extending beyond 3 feet. Accordingly, the abandonment of extensive concrete foundations will inhibit the reestablishment of these species by preventing taproot development. Also, root growth is likely to be inhibited by the vast network of abandoned cables that will leach copper into the soil upon disintegration of their protective sheaths (which typically occurs within 50 years of construction).

[92] For example, in 2007, a developer initiated the construction of a large residential neighborhood with more than 100 homes in the heart of Acton, and began grading activities that destroyed juniper woodland, altered drainage patterns, and caused problems for "downhill" residences. The County reassured the community that the site would be fully restored to initial conditions if the developer was unable to finish the drainage infrastructure needed for the project because the County had required the developer to post a bond that was sufficiently large to ensure full site restoration. Then, the developer simply abandoned the project in 2008 and did not restore the site or the native drainage patterns. When the County called upon the developer's bonding company to provide the funds needed to restore the site, the bonding company declared bankruptcy. As a result, the County did nothing, the site was not restored, and Acton residents "downhill" of the project site had to contend with the drainage problems that all of this created.

[93] Page 3-24 of the Final Staff Assessment.

The phrase "to the extent practicable" is highly subjective, and if the decision regarding what is "practicable" is left to the discretion of the developer, then only minimal restoration efforts will be undertaken. Furthermore, the Darden Staff Assessment only briefly addresses decommissioning[94], and it vaguely avers that concrete foundations and equipment pads "can" be crushed and recycled if they are removed, but it does not *require* that they be crushed and recycled; it does not even require that they be removed! Equally disturbing, the Darden EIR does not substantively address decommissioning of the Darden BESS yard. For instance, it does not even acknowledge that the spent BESS units constitute hazardous waste or address how this hazardous waste will be recycled/disposed of or whether there are sufficient existing or proposed facilities that are capable of processing it.

The Darden Staff Analysis also indicates that the Commission does not incorporate any "backstop" provisions in any conditions of certification to ensure that hazardous BESS waste is properly disposed of or that the site is properly restored if the developer walks away. SORT observes that the BESS project is wholly owned by "Prairie Song Reliability Project, LLC" which is a Delaware "Limited Liability Corporation" that has no track record or project portfolio. There is nothing to prevent the shareholders of "Prairie Song Reliability Project, LLC" from dissolving the corporation and just walking away at the end of the BESS project life. During the Scoping meeting, the developer's presentation persistently referred to "Coval" as the entity responsible for the BESS project, but environmental responsibility for the project rests solely with "Prairie Song Reliability Project, LLC" and not "Coval". "Prairie Song Reliability Project, LLC" is described as a wholly owned subsidiary of "Coval Infrastructure DevCo LLC" which is another Delaware LLC that was formed less than two years ago[95] and which, insofar as SORT can determine, does not have an extensive track record or project portfolio in California. With this relationship, Coval's environmental responsibility for the project is removed and held at "arm's length". This concern must be factored into the Commission's consideration of the BESS project and addressed through the inclusion of backstop provisions sufficient to remove all vestiges of development from the site because that is the only way to ensure that the site can return to its natural state. Moreover, simply requiring a "bond" is not sufficient because surety companies can (and do) absolve themselves of financial responsibility through bankruptcy.

VULNERABILITY TO VANDALISM AND EXTREMIST ATTACK.

During the Scoping Meeting, at least one commenter pointed out that the BESS project is highly vulnerable to attack, and should one occur, Acton residents will be endangered.

[94] Pages 3-23 to 3-24 of the Final Staff Assessment.

[95] According to the State of Delaware, "Coval Infrastructure DevCo LLC" incorporated on March 14, 2024.

SORT has carefully considered this, and concluded that the configuration of the BESS project does indeed make it highly vulnerable to an attack which can initiate numerous and simultaneous BESS deflagrations. For example, the BESS project has an "open air" configuration with densely packed, deflagration prone battery containers, and its location in a valley surrounded by hillsides render it incredibly defenseless against even crude and unsophisticated attacks. Any projectile that pierces a battery cell will cause an immediate short circuit, and projectiles that pierce liquid cooling systems (such as those used by the PowerTitan 2.0) will immediately cause coolant leaks and overheating. Such circumstances will pose a significant public safety risk to the residents of Acton, and as such, they must be addressed in the BESS project EIR.

CONCLUSION.

SORT respectfully requests that the Commission consider the environmental impacts, mitigation measures, and project alternatives presented above and incorporate them into the EIR that is prepared for the BESS project. If you have any questions or require clarification regarding the matters raised herein, please do not hesitate to contact us at SORTActon@gmail.com.

Sincerely;

/S/ Jacqueline Ayer
Jacqueline Ayer, Director
Save Our Rural Town

ATTACHMENT 1

RECOMMENDATIONS BY THE INTERNATIONAL ASSOCIATION OF FIRE CHIEFS (IAFC)

Recommended Fire Department Response to Energy Storage Systems (ESS) Part 1

Events involving ESS Systems with Lithium-ion batteries can be extremely dangerous. All fire crews must follow department policy, and train all staff on response to incidents involving ESS. Compromised lithium-ion batteries can produce significant amounts of flammable gases with potential risk of deflagration and fire.

1. If a commercial or utility install, follow pre-plan and do not enter structure.
2. Residential setting response, control power to the unit, ventilate the area, and protect exposures.
3. In all cases contact manufacture technical support as soon as possible.

This guide serves as a resource for emergency responders with regards to safety surrounding lithium ion Energy Storage Systems (ESS). Each manufacturer has specific response guidelines that should be made available to first responders prior to activation.

ESS systems come in many shapes and sizes. They may be affiliated with renewable systems (wind, photovoltaic systems, etc) or used as standby power. ESS Systems can be installed in single family homes too large commercial and utility applications.

Pre-Incident

Modify or establish your department policy or standard response guideline to ESS incidents. Include guidelines for mitigation of the event which may include a defensive operations such as non-intervention and manage fire propagation or protect exposures.

Review installation procedures for systems with the various code officials including Building, Fire, and Electrical

ESS systems must be installed per the adopted fire and building codes in the region.

For the 2015 editions of the International Fire Code and NFPA 1 Fire Code and earlier editions the necessary safety requirements are not present (Consider language in 2021 Fire Codes or NFPA 855).

Ensure pre-incident plans are covering location, type, disconnect, and other contact information

Pre-incident plans should provide rapid response resources for company officers specific to your area and region including OEM emergency contact information

Train on department policy and perform practical scenarios which support the response plan

INCIDENT ACTIONS

The fire crew should allow the battery to burn itself out, during which it is recommended to apply water spray to neighboring battery enclosures and exposures to further mitigate the spread of the hazards rather than directly onto the burning unit.

Applying water directly to the affected enclosure will not stop the thermal runaway event, as the fire will be located behind several layers of steel material, and direct application of water has shown to only delay the eventual combustion of the entire unit.

- Firefighters must wear full personal protective equipment, including SCBA with face-piece.
- If identified in pre-incident plan, shut off the unit/system by operating any visible disconnects or E-stops (shutting off the disconnect does not remove the energy from the battery). To isolate any PV system and ESS in an emergency, multiple disconnects may need to be shut off. This could include circuit breakers, knife-blade disconnects, or other switches.
- Lithium ion batteries that are in thermal runaway or off gasing will create hazardous atmospheres. Firefighters must stay out of the vapor cloud and not rely on gas monitors (without consideration of cross contamination of the gas sensors)
- Due to construction of the unit, thermal imaging cameras may not give true thermal conditions.

Events can occur from damage, exterior fire, or a malfunction. Smoke or suspicious odor from an ESS system can be an indication of a hazardous condition. When batteries or cells enter thermal runaway, there is typically a period of smoke (may be under pressure). The smoke is most likely flammable and may ignite at any time.

Responding to a venting ESS product

- Evacuate the area. **Never open any doors or remove panels to ESS units.**
- Contact vendor-specific technical support for assistance including BMS data.
- Residential units that are located inside a dwelling unit or garage, the space should be properly ventilated with charged hand-lines in place.
- Maintain a safe distance from the ESS and monitor. A remote FDC may be present on larger commercial or utility ESS to support a sprinkler system inside the enclosure.
- Each manufacturer will have a recommended time for a battery pack to cool down. This can be near a full work cycle of 12 hours or more.
- Defensive Firefighting. Water spray is the preferred agent for response to lithium-ion battery fires *(Lithium-ion is not water reactive)*.
    - If a fire has not developed and only smoke is visible, take a defensive stance toward the system and be prepared to apply water spray.
    - If a fire develops, take a defensive stance toward the burning unit and apply water spray to neighboring battery enclosures and exposures.
- Maintaining a safe distance from the unit involved (large commercial systems, at least 300').
- Response crews should allow the battery to burn out. Water should be applied to adjacent battery enclosures and exposures (building).

ATTACHMENT 2

UL 9540A TEST PROTOCOL

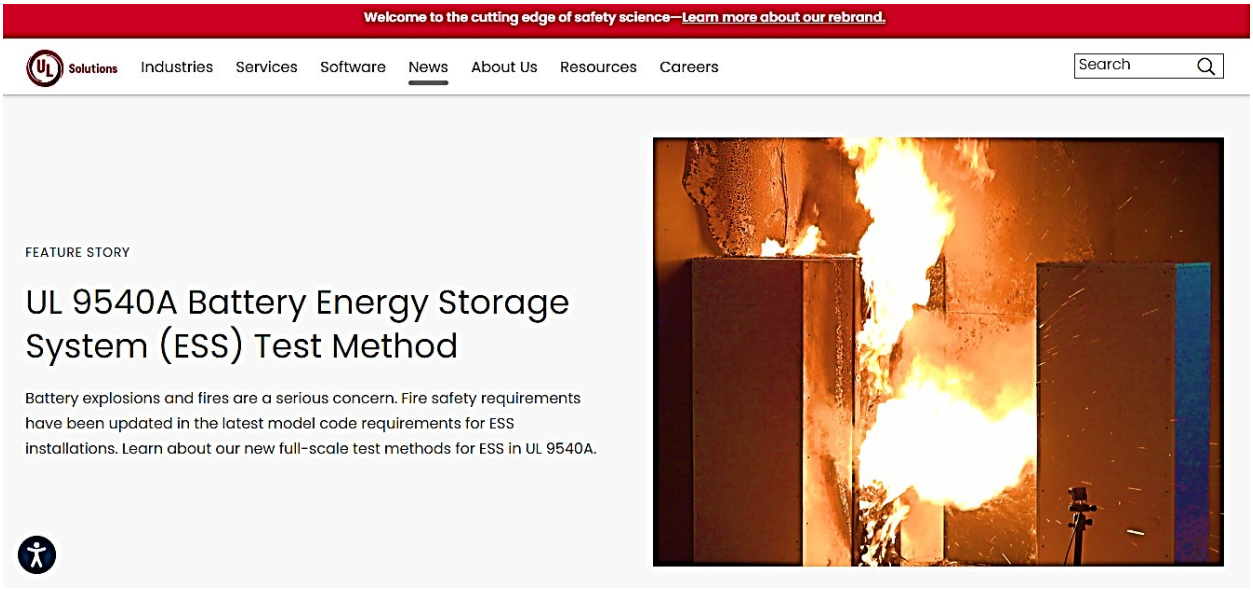

December 2, 2019

Authored by Howard D. Hopper, FPE - Global Regulatory Services Manager. Contributions by Adam Barowy, Research Engineer

In 2015 work began on developing fire safety requirements in U.S. fire codes to address modern energy storage systems (ESS). This effort focused on mitigating the potential hazards of large indoor and outdoor lithium-ion battery ESS installations. The greatest concern for ESS installations was thermal runaway in a battery module that could propagate to a significant fire or explosion, especially since there were no proven methods for controlling or suppressing a fire or mitigating a potential explosion. At the time there was a lack of research and fire performance data to use as a basis for developing protection solutions.

Size (electrical capacity in a unit), separation and maximum allowable quantity (total electrical capacity in one space) requirements were introduced in the 2018 International Fire Code and the NFPA 1 Fire Code to address uncertainty with thermal runaway and fire propagation of battery ESS. The size and electrical energy density of ESS installations were limited by these requirements. However, the codes allowed ESS installations with

larger capacities or smaller separation distances when approved by the code authority using large-scale fire and fault condition testing results from an approved testing laboratory. This testing needed to demonstrate that a fire involving one ESS unit would not propagate to an adjacent unit and would be contained within a battery room.

UL stepped up to meet the needs of the ESS industry and code authorities by developing a methodology for conducting battery ESS fire tests by publishing UL 9540A[1], Test Method for Evaluating Thermal Runaway Fire Propagation in Battery Energy Storage Systems in November 2017. The requirements were designed to evaluate the fire characteristics of a battery ESS that undergoes thermal runaway. The data generated was intended to be used to determine the fire and explosion protection required for an installation of a battery energy storage system. It also meets the objectives of the International Fire Code (IFC) and NFPA 1 relative to fire propagation hazards and fire mitigation methods from a single battery energy storage system unit.

UL 9540A included a series of progressively larger fire tests, beginning at the cell level and progressing to the module level, unit level, and finally the installation level. Each test generated specific data used to evaluate thermal runaway characteristics and fire propagation without specific pass/fail test criteria. Instead, the complete data package was provided to code authorities so they could evaluate the suitability of a battery ESS installation.

As fire codes evolved, and UL gained additional experience with battery ESS fire propagation testing, thermal runaway characteristic, and the data needed by code authorities, UL 9540A was updated in rapid succession with a second edition published in January 2018 and a third edition published in June 2018. With the technical foundation for battery ESS large-scale fire testing firmly in place, UL engaged Standard Technical Panel 9540 in 2019 to develop a binational edition of the test method. The fourth edition of

ANSI/CAN/UL 9540A was published November 12, 2019 and is an ANSI and SCC (Standards Council of Canada) accredited standard.

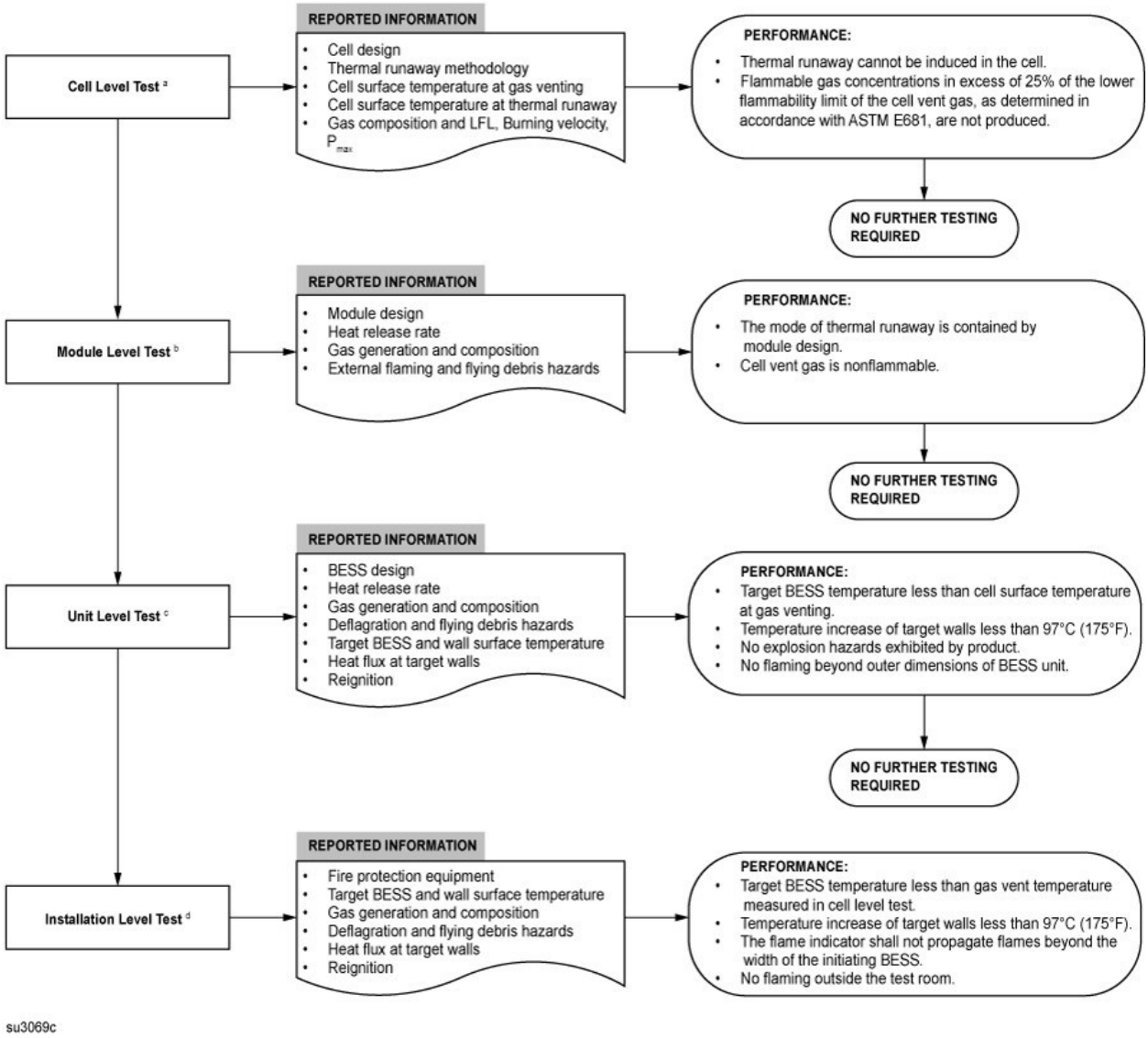

A few of the significant changes introduced into the fourth edition of UL 9540A include:

- Criteria introduced to the cell level, module level, and unit level tests that identify when progressively larger tests are unnecessary,

essentially establishing acceptance criteria for the tests. The flow chart accompanying this article provides details on the test sequence UL 9540A[1].

- Enhancements to the unit level test to include specific test criteria for testing indoor floor mounted battery energy storage systems (BESS), outdoor ground mounted BESS, indoor wall mounted BESS and outdoor wall mounted BESS. All of these types of systems are covered by specific installation requirements in the latest editions of the IFC, NFPA 1 and NFPA 855.

UL 9540A will continue to evolve to reflect changes in ESS installation requirements, advancements in fire science, and the needs of the ESS industry and code authorities. For additional information on UL 9540A, visit www.UL.com/batteries.

[1.] Adapted from UL 9540A copyright © 2019 Underwriters Laboratories Inc.

ATTACHMENT 3

REPORT OF TECHNICAL FINDINGS: VICTORIAN BIG BATTERY FIRE: JULY 30, 2021

January 25, 2022

Victorian Big Battery Fire: July 30, 2021

REPORT OF TECHNICAL FINDINGS

ANDY BLUM, PE, CFEI
SENIOR FIRE PROTECTION ENGINEER

TOM BENSEN, PRINCIPAL FOUNDER
PAUL ROGERS, PRINCIPAL FOUNDER
CASEY GRANT, PE, SENIOR CONSULTANT
GEORGE HOUGH, SENIOR CONSULTANT

Fisher Engineering, Inc.
10475 MEDLOCK BRIDGE ROAD
SUITE 520
JOHNS CREEK GA 30097

Energy Safety Response Group
8350 US HIGHWAY N 23
DELAWARE OHIO 43015

Background

The Victorian Big Battery (VBB) is a 300-Megawatt (MW)/450-Megawatt hour (MWh) grid-scale battery storage project in Geelong, Australia. VBB is one of the largest battery installations in the world and can power over one million Victorian homes for 30 minutes during critical peak load situations.[1] It is designed to support the renewable energy industry by charging during times of excess renewable generation. The VBB is fitted with 212 Tesla Megapacks to provide the 300-MW/450-MWh of energy storage. The Megapack is a lithium-ion battery energy storage system (BESS) consisting of battery modules, power electronics, a thermal management system, and control systems all pre-manufactured within a single cabinet that is approximately 7.2 meters (m) in length, 1.6 m deep and 2.5 m in height (23.5 feet [ft] x 5.4 ft x 8.3 ft).

On Friday, July 30th, 2021, a single Megapack at VBB caught fire and spread to a neighboring Megapack during the initial installation and commissioning of the Megapacks. The fire did not spread beyond these two Megapacks and they burned themselves out over the course of approximately six hours. There were no injuries to the general public, to site personnel or to emergency first responders as the Megapacks failed safely (i.e., slowly burned themselves out with no explosions or deflagrations), as they are designed to do in the event of a fire. Per the guidance in Tesla's Lithium-Ion Battery Emergency Response Guide[2] (ERG), emergency responders permitted the Megapack to burn and consume itself while nearby exposures were being monitored at a safe distance. The total impact to the site was two out of the 212 Megapacks were fire damaged, or less than 1% of the BESS.

Following the emergency response, a detailed, multi-entity fire investigation commenced on August 3, 2021. The investigation process included local regulatory entities, Tesla, outside third-party engineers and subject matter experts. The investigation process involved analyzing both the fire origin and cause as well as the root cause of the fire propagation to the neighbor Megapack. In addition, given this is the first fire event in a Megapack installation to date, a review of the emergency response has been performed to identify any lessons learned from this fire event.

This report summarizes those investigations and analyses and has been prepared by Fisher Engineering, Inc. (FEI) and Energy Safety Response Group (ESRG), two independent engineering and energy storage fire safety consulting firms. In addition, this report provides a list of lessons learned from the fire and also highlights the procedural, software and hardware changes that have been implemented based on those lessons learned.

Incident Timeline

At the time of the fire, the VBB was fitted with approximately one-half of the 212 total Megapacks intended for the site. The Megapacks that were installed at VBB were undergoing routine testing and commissioning on the day of the fire. At 7:20 AM Australian Eastern Standard Time (AEST) on the morning of July 30, 2021, commissioning and testing of a number of Megapacks commenced. One such Megapack (denoted herein as MP-1), was not going to be tested that day and was therefore shut off manually by means of the keylock switch.[3] At the time MP-1 was shut down via the keylock switch, the unit displayed no abnormal conditions to site personnel. Around 10:00 AM, smoke was observed emitting from MP-1 by site personnel. Site personnel

[1] https://victorianbigbattery.com.au/

[2] https://www.tesla.com/sites/default/files/downloads/Lithium-Ion_Battery_Emergency_Response_Guide_en.pdf

[3] The keylock switch is a type of "lock out tag out" switch on the front of the Megapack that safely powers down the unit for servicing.

electrically isolated all the Megapacks on-site and called emergency services: Country Fire Authority (CFA). The CFA arrived shortly thereafter and set up a 25 m (82 ft) perimeter around MP-1. They also began applying cooling water to nearby exposures as recommended in Tesla's ERG. The fire eventually spread into a neighbor Megapack (MP-2) installed 15 centimeters (cm), or 6 inches (in), behind MP-1. The CFA permitted MP-1 and MP-2 to burn themselves out and did not directly apply water into or onto either Megapack, as recommended in Tesla's ERG. By 4:00 PM (approximately six hours after the start of the event), visible fire had subdued and a fire watch was instituted. The CFA monitored the site for the next three days before deeming it under control on August 2, 2021, at which time, the CFA handed the site over for the fire investigation to begin.

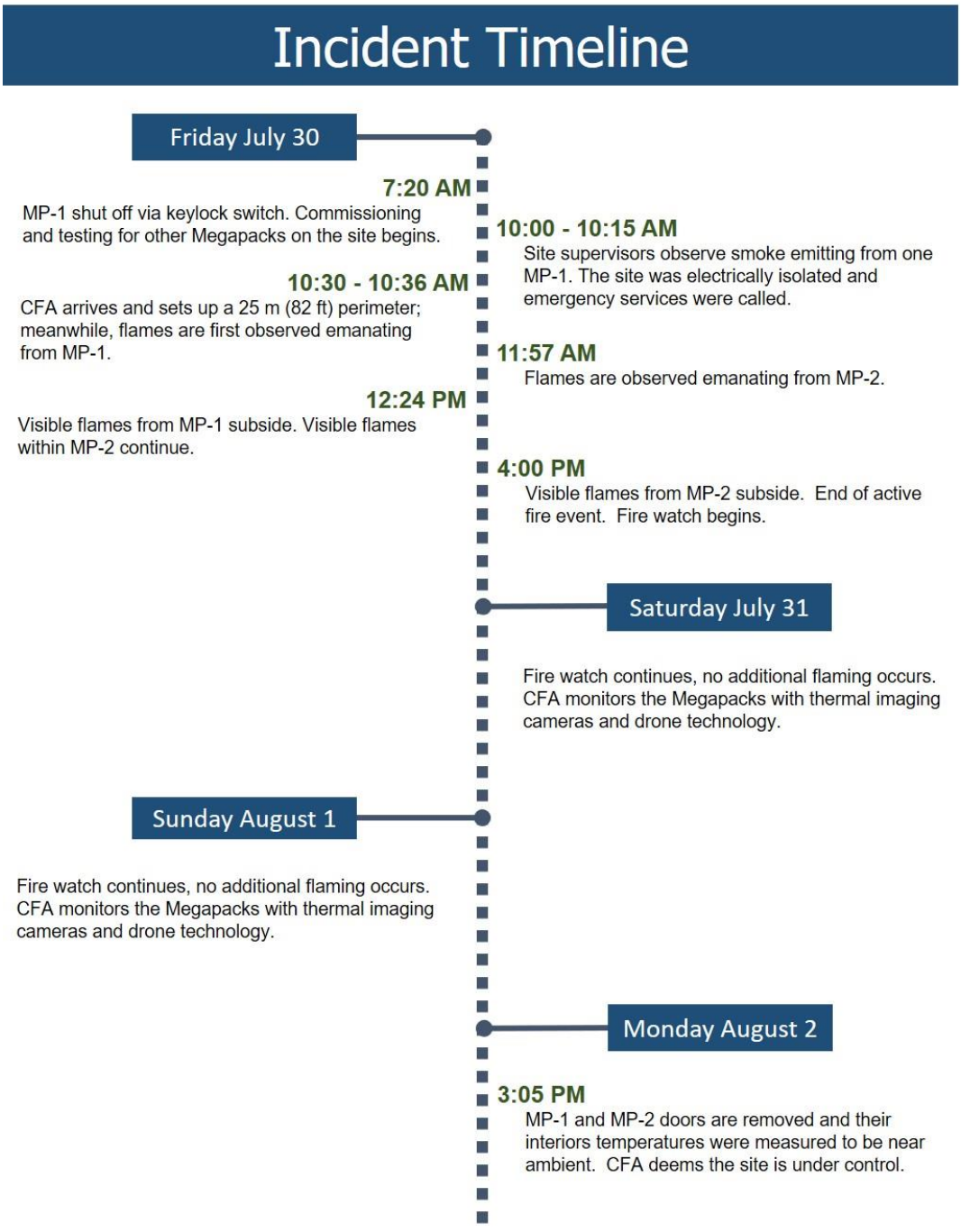

Note: The time stamp is AEST (UTC+10) which is 19 hours ahead of USA PDT (UTC-7)

Investigation

A multi-entity fire investigation commenced on August 3, 2021. The VBB fire investigation process involved analyzing both the root cause of the initial fire in MP-1 as well as the root cause of the fire propagation into MP-2. The investigations included on-site inspections of MP-1 and MP-2 by the CFA, Energy Safe Victoria[4] (ESV), Work Safety Victoria[5] (WSV), local Tesla engineering/service teams and a local third-party independent engineering firm. In addition to the on-site work immediately after the incident, the root cause investigations also included data analysis, thermal modeling and physical testing (electrical and fire) performed by Tesla at their headquarters in California, USA and their fire test facility in Nevada, USA.

Fire Cause Investigation

On-site inspections commenced on August 3, 2021 and concluded on August 12, 2021. MP-1 and MP-2 were documented, inspected and preserved for future examinations, if necessary. Concurrently, all available telemetry data (such as internal temperatures and fault alarms) from MP-1 and MP-2 were analyzed and a series of electrical fault and fire tests were performed. The on-site investigation findings, the telemetry data analysis, electrical fault tests and fire tests, when combined, identified a very specific series of fault conditions present on July 30, 2021 that could lead to a fire event.

Fire Origin and Cause Determination

The origin of the fire was MP-1 and the most likely root cause of the fire was a leak within the liquid cooling system of MP-1 causing arcing in the power electronics of the Megapack's battery modules. This resulted in heating of the battery module's lithium-ion cells that led to a propagating thermal runaway event and the fire.

Other possible fire causes were considered during the fire cause investigation; however, the above sequence of events was the only fire cause scenario that fits all the evidence collected and analyzed to date.

Contributory Factors

A number of factors contributed to this incident. Had these contributory factors not been present, the initial fault condition would likely have been identified and interrupted (either manually or automatically) before it escalated into a fire event. These contributory factors include:

1. The supervisory control and data acquisition (SCADA) system for a Megapack required 24 hours to setup a connection for new equipment (i.e., a new Megapack) to provide full telemetry data functionality and remote monitoring by Tesla operators. Since VBB was still in the installation and commissioning phase of the project (i.e., not in operation), MP-1 had only been in service for 13 hours prior to being switched off via the keylock switch on the morning of the fire. As such, MP-1 had not been on-line for the required 24 hours, which prevented this unit from transmitting telemetry data (internal temperatures, fault alarms, etc.) to Tesla's off-site control facility on the morning of the fire.
2. The keylock switch for MP-1 was operated correctly on the morning of the fire to turn MP-1 off as the unit was not required for commissioning and testing that morning; however, this action caused telemetry systems, fault monitoring, and electrical fault safety devices[6] to be disabled or operate with

[4] Victoria's energy safety regulator

[5] Victoria's health and safety regulator

[6] These elements include, among other devices, fuses at the cell and module level for localized fault current interruption and a battery module pyro disconnect that severs the electrical connection of the battery module when a fault current is passing through the battery module.

only limited functionality. This prevented some of the safety features of MP-1 from actively monitoring and interrupting the electrical fault conditions before escalating into a fire event.

3. The exposure of liquid coolant onto the battery modules likely disabled the power supply to the circuit that actuates the pyro disconnect.[7] With a power supply failure, the pyro disconnect would not receive a signal to sever and would not be able to interrupt a fault current passing through the battery module prior to it escalating into a fire event.

Fire Propagation Investigation

The VBB fire investigation process involved analyzing not only the root cause of the initial fire in MP-1 but also the root cause of the fire propagation into MP-2. The Megapack has been designed to be installed in close proximity to each other without fire propagating to adjacent units. The design objective of the Megapack in terms of limiting fire propagation was mainly reliant on the thermal insulation of the Megapack's exterior vertical steel panels and the sheer mass of the battery modules acting as a heat sink (i.e., they are difficult to heat up). With this thermal insulation, the Megapack spacing can be as close as 15 cm (6 in) to the sides and back of each unit with 2.4 m (8 ft) aisles in front of each Megapack, as shown in Figure 1. This product spacing has been validated in UL9540A unit level tests.[8] Similar to the fire origin and cause investigation, the on-site inspections were supported simultaneously with an analysis of telemetry data (such as internal temperatures) from MP-2 and fire testing. The on-site investigation findings, the telemetry data analysis and fire tests, when combined, identified a scenario where Megapack to Megapack fire propagation can occur.

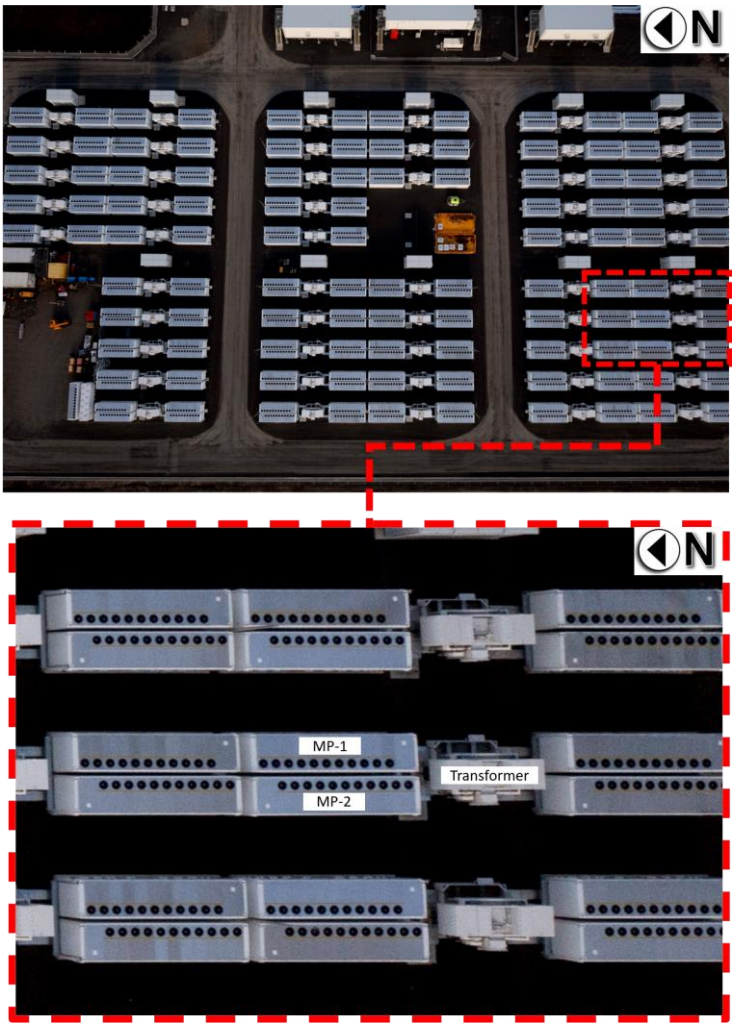

Figure 1 VBB Megapack layout (top) and area of fire origin (bottom)

[7] The pyro disconnect is a Tesla proprietary shunt-controlled pyrotechnic fuse that allows for rapid one-time actuation. There is one pyro disconnect per battery module.

[8] UL9540A, *Test Method for Evaluating Thermal Runaway Fire Propagation in Battery Energy Storage Systems*. UL9540A is a test method developed by UL to address fire safety concerns with BESS. The test method provides a method to evaluate thermal runaway and fire propagation at the cell level, module level, and unit level. In addition to cell and module level tests, Tesla performed unit level tests to evaluate, among other fire safety characteristics, the potential for fire propagation from Megapack-to-Megapack. During unit level testing, fire propagation did not occur between Megapacks when they were installed with a spacing of 15 cm (6 in) to the sides and back of each unit.

Fire Propagation Determination

Flames exiting the roof of MP-1 were significantly impacted by the wind conditions at the time of the fire. Wind speeds were recorded between 20-30 knots[9] which pushed the flames exiting the roof of MP-1 towards the roof of MP-2. This direct flame impingement on the top of the thermal roof of MP-2 ignited the internal components of MP-2, most notably, the plastic overpressure vents that seal the battery bay[10] from the thermal roof. Once ignited, the overpressure vents provided a direct path for flames and hot gases to enter into the battery bays, thus exposing the battery modules of MP-2 to fire and/or elevated temperatures. Exposed to temperatures above their thermal runaway threshold of 139°C (282°F), the cells within the battery modules eventually failed and became involved in the fire.

Other possible fire propagation root causes were considered during the investigation; however, the above sequence of events was the only fire propagation scenario that fits all the evidence collected and analyzed to date. Of note, at the time when fire was observed within the thermal roof of MP-2, internal cell temperature readings of MP-2 had only increased by 1°C (1.8°F) from 40°C to 41°C (104°F to 105.8°F)[11] Around the same time that fire was observed within the thermal roof of MP-2, around 11:57 AM (approximately 2 hours into the fire event), communication was lost to the unit and no additional telemetry data was transmitted. However, given the internal cell temperatures of MP-2 had only recorded a 1°C (1.8°F) temperature rise 2 hours into the fire event and while the unit's roof was actively on fire, fire propagation across the 15 cm (6 in) gap via heat transfer is not the root cause of the fire propagation. Furthermore, this telemetry data from MP-2 demonstrates that the Megapack's thermal insulation can provide significant thermal protection in the event of a fire within an adjacent Megapack installed only 15 cm (6 in) away.

Contributory Factors

The wind was the dominant contributory factor in the propagation of fire from MP-1 to MP-2. At the time of the fire, a 20-30 knot (37-56 km/hr, 23-35 mph) wind was recorded out of the north. The wind conditions at the time of the fire pushed the flames exiting out of the top of MP-1 towards the top of MP-2 leading to direct flame impingement on the thermal roof of MP-2. This type of flame behavior was not observed during previous product testing or regulatory testing per UL9540A. In UL9540A unit level testing, the maximum wind speed permitted[12] during the test is 10.4 knots (19.3 km/hr, 12.0 mph); whereas, wind conditions during the VBB fire were two to three times greater in magnitude. As such, the wind conditions during the VBB fire appear to have identified a weakness in the Megapack's thermal roof design (unprotected, plastic overpressure vents in the ceiling of the battery bays) that allows Megapack-to-Megapack fire propagation. This weakness was not identified previously during product or regulatory testing and does not invalidate the Megapack's UL9540A certification, as the cause of fire propagation was primarily due to an environmental condition (wind) that is not captured in the UL9540A test method.

---

9 This equates to 37-56 kilometers per hour (km/hr) or 23-35 miles per hour (mph).

10 The battery bay is an IP66 enclosure that houses the battery modules. It is distinct from the thermal roof installed above it. Plastic overpressure vents are installed in the ceiling of the battery bay, sealing the two enclosures from one another.

11 As a reference, the Megapack's normal operating cell temperature is between 20-50°C and cell thermal runaway does not occur until 139°C (98°C above cell temperatures of MP-2 before telemetry data was lost).

12 This threshold is necessary for test reliability and reproducibility. If wind conditions are not bounded in some fashion in an outdoor fire test, large variances on product performance could be introduced due to varying wind conditions.

Mitigations

The investigation of the VBB fire identified several gaps in Tesla's commissioning procedures, electrical fault protection devices and thermal roof design. Since the fire, Tesla has implemented a number of procedural, firmware, and hardware mitigations to address these gaps. These mitigations have been applied to all existing and any future Megapack installations and include:

Procedural Mitigations:

- Improved inspection of the coolant system for leaks during Megapack assembly and during end-of-line testing to reduce the likelihood of future coolant leaks.
- Reduce the telemetry setup connection time for new Megapacks from 24 hours to 1 hour to ensure new equipment is transmitting telemetry data (internal temperatures, fault alarms, etc.) to Tesla's off-site control facility for remote monitoring.
- Avoid utilizing the Megapack's keylock switch during commissioning or operation unless the unit is actively being serviced. This procedural mitigation ensures telemetry, fault monitoring, and electrical fault safety devices (such as the pyro disconnect) are active while the Megapack is idle (such as during testing and commissioning).

Firmware Mitigations:

- Added additional alarms to the coolant system's telemetry data to identify and respond (either manually or automatically) to a possible coolant leak.
- Keep all electrical safety protection devices active, regardless of keylock switch position or system state. This firmware mitigation allows electrical safety protection devices (such as the pyro disconnect) to remain in an active mode, capable of actuating when electrical faults occur at the battery modules, no matter what the system status is.
- Active monitoring and control of the pyro disconnect's power supply circuit. In the event of a power supply failure (either through an external event such as a coolant exposure or some other means), the Megapack will automatically actuate the pyro disconnect prior to the loss of its power supply.

Hardware Mitigations

- Installation of newly designed, thermally insulated steel vent shields within the thermal roof of all Megapacks. These vent shields protect the plastic overpressure vents from direct flame impingement or hot gas intrusion, thus keeping the IP66 battery bay enclosures isolated from a fire above in the thermal roof. Their performance was validated through a series of fire tests, including unit level fire testing of entire Megapack units.[13] The vent shields are placed over the top of the overpressure vents and will come standard on all new Megapack installations. For existing Megapacks, the vent shields can be installed in the field (retrofit) with minimal effort or disruption to the unit. At the time of this report, the vent shields are nearing production stage and will be retrofitted to applicable Megapack sites shortly.

[13] The tests confirmed that, even with the entire thermal roof fully involved in fire, the overpressure vents will not ignite and the battery modules below remain relatively unaffected by the fire above. For instance, the cells within the battery modules saw a less than 1°C temperature rise while the entire thermal roof was fully involved in fire.

Emergency Response

Beyond the origin and cause and propagation investigations, another key aspect of the VBB fire was the emergency response. The CFA is the responsible fire service organization for VBB, and the facility is in their initial response jurisdiction. The location of the VBB facility is in a semi-rural location. The nearest fire station is the CFA Lovely Banks, approximately 4 km (2.5 miles) distance from VBB and thus relatively close, though other resources had more extended travel distances.

Upon arrival around 10:30 AM, CFA immediately established incident command (IC) in accordance with their protocols, and the IC worked closely with the facility representatives and subject matter experts (SMEs). This close coordination continued throughout the entire event. The facility was evacuated and all-site personnel accounted-for upon notification of the emergency event and the commencement of fire service operations. A 25 m (82 ft) perimeter was established around MP-1 while water application and cooling strategies were discussed with facility representatives and subject matter experts (SMEs). The decision was made to provide exposure protection to Megapacks and transformers adjacent to MP-1 and MP-2 using water hose lines, as recommended in Tesla's ERG. The fire eventually propagated into MP-2; however, flame spread did not advance any further than MP-1 and MP-2. The two Megapacks were permitted to burn themselves out, during which time the CFA did not directly apply water into or onto either Megapack. By 4:00 PM (approximately six hours after the start of the event), visible flames had subdued and a fire watch was instituted. The CFA continued to monitor the site for the next three days before deeming it under control on August 2, 2021, at which time, the fire investigation began.

Key Takeaways

A thorough review of the VBB fire emergency response yielded the following key takeaways:

- Effective Pre-incident Planning: VBB had both an Emergency Action Plan (EAP) and an Emergency Response Plan (ERP). Both plans were available to emergency responders and were effectively used during the VBB fire. For example, all site employees and contractors followed proper evacuation protocols during the fire and as a result, no injuries occurred to those personnel.
- Coordination with SMEs: VBB had thorough pre-incident plans that clearly identified the SMEs, how to contact them, their role and other key tasks. It was reported that the facility SMEs stayed in close contact with the CFA IC throughout the VBB fire, providing valuable information and expertise for the CFA to draw upon. For example, site representatives and SMEs worked closely with the CFA in determining water application and cooling strategies of adjacent exposures.
- Water Application: A key question regarding water application is the necessary amount and duration for effective fire containment. Tesla's design philosophy is based on inherent passive protection (i.e., thermal insulation), with minimal dependence on active firefighting measures like external hose lines. As such, water was not aimed at suppressing the fire but rather protecting the exposures as directed by Tesla's ERG and the SMEs on site. All available data and visual observations of the fire indicates water had limited effectiveness in terms of reducing or stopping fire propagation from Megapack-to-Megapack. The thermal insulation appears to be the dominant factor in reducing heat transfer between adjacent Megapacks. However, water was effectively used on other exposures

(transformers, electrical equipment, etc.) to protect that equipment, which are not designed with the same level of protection as a Megapack is (i.e., thermal insulation).[14]

- The fire protection design approach of the Megapack has inherent advantages over other BESS designs in terms of safety to emergency responders. The Megapack approach minimizes the likelihood of fire spread using passive compartmentation and separation, eliminates the danger to fire fighters of an overpressure event due to design features and a lack of confinement (e.g., outdoor versus indoor), does not rely on active firefighting measures like external hose lines and minimizes the dangers from stranded electrical energy to those involved with overhaul and de-commissioning with a fire response approach permitting the Megapack to burn itself out.

Environmental Concerns

The Environment Protection Authority Victoria (EPA) deployed two mobile air quality monitors within 2 km (1.2 miles) of the VBB site. Locations were chosen where there was potential to impact the local community. The EPA monitors confirmed "good air quality in the local community" after the incident; however, the measurements were not taken during the peak of the fire event. They were sampled around 6:00 PM, or approximately 2 hours after the fire was out. Therefore, the data cannot be used to understand the airborne hazards during the actual fire event. The data does demonstrate that two hours after the fire event, the air quality in the surrounding area was "good" and no long-lasting air quality concerns arose from the fire event.[15]

During the fire event, the CFA coordinated with site personnel to control the water run-off from fire hoses into a catchment. Water samples, collected by Tesla site personnel under the supervision of CFA, were extracted from the catchment. Laboratory results from those samples indicated that the likelihood of the fire having a material impact on the water was minimal. After the incident, as a precaution, the water was removed from the catchment, via suction trucks, and was transported to a licensed waste facility for treatment and disposal. It is estimated that approximately 900,000 liters of water was disposed of from the site after the event.

Community Concerns

Neoen, the project developer and owner, pro-actively engaged with the local community during and following the VBB fire. These engagements included door-to-door visits, phone calls and emails with the residential and agricultural properties within a 2-3 km (1.2-1.9 mile) radius of the VBB site. Neoen found their prior community outreach during the project planning stages to be invaluable as this outreach provided up-to-date contact information for Neoen when reaching out to the local community during and following the fire. In addition, Neoen formed an executive stakeholder steering committee compromising of key organizations within 24 hours of the incident. With multiple parties involved in the emergency response to the fire event

[14] At the time of this report, final fire department reports were not available for review and inclusion. As that information becomes available, additional information regarding water usage and effectiveness may require inclusion in this report. Although the effectiveness of external water in a Megapack fire may be limited, water should still be made available for exposure protection and other unanticipated events in the future, as required by any applicable regulatory requirements.

[15] It should be noted that prior regulatory testing (UL 9540A module level fire testing) has shown that the products of combustion of a Megapack battery module can include flammable and nonflammable gases. Based on those regulatory tests, the flammable gases were found to be below their lower flammable limit (LFL) and would not pose a deflagration or explosion risk to first responders or the general public. The nonflammable gases were found to be comparable to the smoke you would encounter in a typical Class A structure fire and do not contain any unique, or atypical, gases beyond what you would find in the combustion of modern combustible materials.

actively participating in the steering committee, this helped ensure that from the outset communication was timely, efficient, well-coordinated across different organizations and accurate.

In addition to the community outreach, Neoen and Tesla also briefed multiple industry, State and Federal Government Departments and Agencies immediately following the VBB fire and at the conclusion of the investigation process. These briefings helped ensure the wider energy sector with interests in BESS were able to be kept directly informed as information became available.

Overhaul and Remediation

On July 29, 2021 nearly half of the Megapacks had been installed and the site was in the testing and commissioning stage of the project. Following the fire event on July 30, 2021, fire department personnel, regulatory agencies and other emergency responders remained on-site for precautionary purposes until August 2, 2021. At that time the site was turned over for regulatory fire investigations to begin. On-site fire investigations started on August 3, 2021 and continued until August 12, 2021. During this time, starting on August 6, 2021, the site was permitted to continue the installation of Megapacks while the area around MP-1 remained cordoned off for the investigation. On September 23rd, 2021, less than two months after the fire, VBB was re-energized and testing and commissioning restarted. Remediation of the damaged equipment followed shortly after, and lasted a total of three days. All testing and commissioning efforts were completed without any further incidents and on December 8, 2021, VBB officially opened.

Lessons Learned

The VBB fire exposed a number of unlikely factors that, when combined, contributed to the fire initiation as well as its propagation to a neighboring unit. This collection of factors had never before been encountered during previous Megapack installations, operation and/or regulatory product testing. This section summarizes those factors as well as the emergency response to the fire, discusses the lessons learned from this fire event, and highlights the mitigations Tesla has implemented in response.

1. Commissioning Procedures

Lessons learned related to commissioning procedures include: (1) limited supervision/monitoring of telemetry data during the first 24 hours of commissioning and (2) the use of the keylock switch during commissioning and testing. These two factors prevented MP-1 from transmitting telemetry data (internal temperatures, fault alarms, etc.) to Tesla's control facility and placed critical electrical fault safety devices (such as the pyro disconnect) in a state of limited functionality, reducing the Megapack's ability to actively monitor and interrupt electrical fault conditions prior to them escalating into a fire event.

Since the VBB fire, Tesla has modified their commissioning procedures to reduce the telemetry setup connection time for new Megapacks from 24 hours to 1 hour and to avoid utilizing the Megapack's keylock switch unless the unit is actively being serviced.

2. Electrical Fault Protection Devices

Lessons learned related to electrical fault protection devices include: (1) coolant leak alarms; (2) the pyro disconnect being unable to interrupt fault currents when the Megapack is off via the keylock switch and (3) the pyro disconnect likely being disabled due to a power supply loss to the circuit that actuates it. These three factors prevented the pyro disconnect of MP-1 from actively monitoring and interrupting the electrical fault conditions before escalating into a fire event.

Since the VBB fire, Tesla has implemented a number of firmware mitigations that keep all electrical safety protection devices active, regardless of keylock switch position or system state, and to actively monitor and control the pyro disconnect's power supply circuit. Furthermore, Tesla has added additional alarms to better identify and respond (either manually or automatically) to coolant leaks. Additionally, although this fire event was likely initiated by a coolant leak, unexpected failures of other internal components of the Megapack could create similar damage to the battery modules. These new firmware mitigations do not only address damage from a coolant leak. They also permit the Megapack to better identify, respond, contain and isolate issues within the battery modules due to failures of other internal components, should they occur in the future.

3. Fire Propagation

Lessons learned related to fire propagation include: (1) the significant role external, environmental conditions (such as wind) can have on a Megapack fire and (2) the identification of a weakness in the thermal roof design that permits Megapack-to-Megapack fire propagation. These two factors led to direct flame impingement on the plastic overpressure vents that seal the battery bay from the thermal roof. With a direct path for flames and hot gases to enter into the battery bays, the cells within the battery modules of MP-2 failed and became involved in the fire.

Since the VBB fire, Tesla has devised (and validated through extensive testing) a hardware mitigation that protects the overpressure vents from direct flame impingement or hot gas intrusion via the installation of new, thermally insulated, steel vent shields. The vent shields are placed on top of the overpressure vents and will come standard on all new Megapack installations. For existing Megapacks, the vent shields can be easily installed in the field. At the time of this report, the vent shields are nearing production stage and will be retrofitted to applicable Megapack sites shortly.

4. Megapack Spacing

Lessons learned related to Megapack spacing include: no changes are required to the installation practices of the Megapack with the vent shield mitigation (as described above) in place. Based on an analysis of telemetry data within MP-2 during the VBB fire, the Megapack's thermal insulation can provide significant thermal protection in the event of a fire within an adjacent Megapack installed 15 cm (6 in) away. The internal cell temperatures of MP-2 only increased by 1°C (1.8°F), from 40°C to 41°C (104°F to 105.8°F), before communication was lost to the unit, presumably due to fire, around 11:57 AM (approximately 2 hours into the fire event). Fire propagation was triggered by the weakness in the thermal roof, as described above in #3, and not due to heat transfer via the 15 cm (6 in) gap between Megapacks. With the vent shield mitigation in place, the weakness has been addressed and validated through unit level fire testing (i.e., tests involving the ignition of the Megapack's thermal roof). These tests confirmed that, even with the thermal roof fully involved in a fire, the overpressure vents will not ignite and the battery modules remain relatively unaffected with internal cell temperatures rising less than 1°C.

5. Emergency Response

Lessons learned from the emergency response to the VBB fire include: (1) effective pre-incident planning is invaluable and can reduce the likelihood of injuries; (2) coordination with SMEs, either on site or remotely, can provide critical expertise and system information for emergency responders to draw upon; (3) the effectiveness of applying water directly to adjacent Megapacks appears to provide limited benefits; however, water application to other electrical equipment, with inherently less fire protection built into their designs (such as transformers), can be a useful tactic to protect that equipment; (4) the fire protection design

approach of the Megapack has inherent advantages over other BESS designs in terms of safety to emergency responders; (5) the EPA indicated that there was “good” air quality 2 hours after the fire demonstrating that no long-lasting air quality concerns arose from the fire event; (6) water samples indicated that the likelihood of the fire having a material impact on firefighting water was minimal; (7) prior community engagement during the project planning stages is invaluable as it enabled Neoen to quickly update the local community and address immediate questions and concerns; (8) early, factual and where possible, face-to-face engagement with the local community is essential when a fire event is unfolding to keep the general public informed; (9) an executive stakeholder steering committee from the key organizations involved in the emergency response can help ensure that any pubic communications are timely, efficient, coordinated and accurate; and (10) effective coordination between stakeholders at the site allowed for rapid and thorough handover process after the incident, the swift and safe decommissioning of the damaged units and the site’s quick return to service.

In summary, the VBB fire event proceeded in accordance with its fire protection design and pre-incident planning. It presented no unusual, unexpected, or surprising characteristics (i.e., explosions) or resulted in any injuries to site personnel, the general public or emergency responders. It was isolated to the units directly involved, had minimal environmental impact, did not adversely impact the electrical grid, and had appreciably short mission interruption.

ATTACHMENT 4

TOXIC FLUORIDE GAS EMISSIONS FROM LITHIUM-ION BATTERY FIRES

SCIENTIFIC REPORTS

Correction: Author Correction

OPEN

Toxic fluoride gas emissions from lithium-ion battery fires

Fredrik Larsson[1,2], Petra Andersson[2], Per Blomqvist[2] & Bengt-Erik Mellander[1]

Received: 11 April 2017
Accepted: 28 July 2017
Published online: 30 August 2017

Lithium-ion battery fires generate intense heat and considerable amounts of gas and smoke. Although the emission of toxic gases can be a larger threat than the heat, the knowledge of such emissions is limited. This paper presents quantitative measurements of heat release and fluoride gas emissions during battery fires for seven different types of commercial lithium-ion batteries. The results have been validated using two independent measurement techniques and show that large amounts of hydrogen fluoride (HF) may be generated, ranging between 20 and 200 mg/Wh of nominal battery energy capacity. In addition, 15–22 mg/Wh of another potentially toxic gas, phosphoryl fluoride (POF_3), was measured in some of the fire tests. Gas emissions when using water mist as extinguishing agent were also investigated. Fluoride gas emission can pose a serious toxic threat and the results are crucial findings for risk assessment and management, especially for large Li-ion battery packs.

Lithium-ion batteries are a technical and a commercial success enabling a number of applications from cellular phones to electric vehicles and large scale electrical energy storage plants. The occasional occurrences of battery fires have, however, caused some concern especially regarding the risk for spontaneous fires and the intense heat generated by such fires[1–5]. While the fire itself and the heat it generates may be a serious threat in many situations, the risks associated with gas and smoke emissions from malfunctioning lithium-ion batteries may in some circumstances be a larger threat, especially in confined environments where people are present, such as in an aircraft, a submarine, a mine shaft, a spacecraft or in a home equipped with a battery energy storage system. The gas emissions has however only been studied to a very limited extent.

An irreversible thermal event in a lithium-ion battery can be initiated in several ways, by spontaneous internal or external short-circuit, overcharging, external heating or fire, mechanical abuse etc. This may result in a thermal runaway caused by the exothermal reactions in the battery[6–10], eventually resulting in a fire and/or explosion. The consequences of such an event in a large Li-ion battery pack can be severe due to the risk for failure propagation[11–13]. The electrolyte in a lithium-ion battery is flammable and generally contains lithium hexafluorophosphate ($LiPF_6$) or other Li-salts containing fluorine. In the event of overheating the electrolyte will evaporate and eventually be vented out from the battery cells. The gases may or may not be ignited immediately. In case the emitted gas is not immediately ignited the risk for a gas explosion at a later stage may be imminent. Li-ion batteries release a various number of toxic substances[14–16] as well as e.g. CO (an asphyxiant gas) and CO_2 (induces anoxia) during heating and fire. At elevated temperature the fluorine content of the electrolyte and, to some extent, other parts of the battery such as the polyvinylidene fluoride (PVdF) binder in the electrodes, may form gases such as hydrogen fluoride HF, phosphorus pentafluoride (PF_5) and phosphoryl fluoride (POF_3). Compounds containing fluorine can also be present as e.g. flame retardants in electrolyte and/or separator[17], in additives and in the electrode materials, e.g. fluorophosphates[18,19], adding additional sources of fluorine.

The decomposition of $LiPF_6$ is promoted by the presence of water/humidity according to the following reactions[20,21];

$$LiPF_6 \rightarrow LiF + PF_5 \quad (1)$$

$$PF_5 + H_2O \rightarrow POF_3 + 2HF \quad (2)$$

$$LiPF_6 + H_2O \rightarrow LiF + POF_3 + 2HF \quad (3)$$

[1]Department of Physics, Chalmers University of Technology, Kemivagen 9, SE-41296, Gothenburg, Sweden. [2]Safety and Transport, RISE Research Institutes of Sweden, Brinellgatan 4, SE-50115, Boras, Sweden. Correspondence and requests for materials should be addressed to F.L. (email: vegan@chalmers.se)

Battery	Numbers of batteries per test	Type	Nominal capacity per battery (Ah)	Nominal voltage per battery (V)	Cell packaging
A	5–10	LCO ($LiCoO_2$)	6.8	3.75	Prismatic hard Al-can
B	2	LFP ($LiFePO_4$)	20	3.2	Pouch
C	5	LFP ($LiFePO_4$)	7	3.2	Pouch
D	9	LFP ($LiFePO_4$)	3.2	3.2	Cylindrical
E	5	LFP ($LiFePO_4$)	8	3.3	Cylindrical
F	2	NCA-LATP ($LiNiCoAlO_2$-$LiAlTiPO_4$)	30	2.3	Pouch
G	2	Laptop pack*	5.6	11.1	Cylindrical

Table 1. Details of the tested Li-ion battery cells. *Each laptop battery pack has 6 cells of type 18650; arranged 2 in parallel and 3 in series.

Of these PF_5 is rather short lived. The toxicity of HF and the derivate hydrofluoric acid is well known[22–24] while there is no toxicity data available for POF_3, which is a reactive intermediate[25] that will either react with other organic materials or with water finally generating HF. Judging from its chlorine analogy $POCl_3$/HCl[24], POF_3 may even be more toxic than HF. The decomposition of fluorine containing compounds is complex and many other toxic fluoride gases might also be emitted in these situations, however, this study focuses on analysis of HF and POF_3.

Although a number of qualitative and semi-quantitative attempts have been made in order to measure HF from Li-ion batteries under abuse conditions, most studies do not report time dependent rates or total amounts of HF and other fluorine containing gases for different battery types, battery chemistries and state-of-charge (SOC). In some measurements reported, HF has been found, within limited SOC-variations, during the abuse of Li-ion battery cells[15,16,26], as well as detected during the abuse of battery packs[27]. However, time-resolved quantitative HF gas emission measurements from complete Li-ion battery cells undergoing an abusive situation have until now only been studied to a limited extend; for a few SOC-values, including larger commercial cells[28,29], a smaller-size commercial cell[30] and a research cell (i.e. non-commercial cell)[31]. Time-resolved quantitative HF measurements on the gas release from complete electric vehicles including their Li-ion battery packs during an external fire have also been performed[32]. Other types of gas emissions from Li-ion cells during abuse have been the subject of a somewhat larger number of investigations[33–41]. Since the electrolyte typically is the primary source of fluorine, measurements of fluorine emissions from battery type electrolytes have been studied. For example, fire or external heating abuse tests have been performed on electrolytes[42–46] and the quantitative amounts of HF and POF_3 have been measured in some cases[45,46]. Other studies of electrolytes exposed to moderate temperatures, 50–85 °C, show the generation of various fluorine compounds[20,21,47–49] and some studies include both electrolyte and electrode material[50,51,52].

Our quantitative study of the emission gases from Li-ion battery fires covers a wide range of battery types. We found that commercial lithium-ion batteries can emit considerable amounts of HF during a fire and that the emission rates vary for different types of batteries and SOC levels. POF_3, on the other hand, was found only in one of the cell types and only at 0% SOC. The use of water mist as an extinguishing agent may promote the formation of unwanted gases as in eqs (2)–(3) and our limited measurements show an increase of HF production rate during the application of water mist, however, no significant difference in the total amount of HF formed with or without the use of water mist.

Lithium-ion battery fire tests. The experiments were performed using an external propane burner for the purpose of heating and igniting the battery cells as described in the Methods section. Seven different types of batteries, type A-G, were investigated, from seven manufacturers and with different capacity, packaging type, design and cell chemistry, as specified in Table 1. Type A had a lithium cobalt oxide (LCO) cathode and carbon anode, types B to E had lithium-iron phosphate (LFP) cathode and carbon anode, type F had nickel cobalt aluminum oxide (NCA) and lithium aluminum titanium phosphate (LATP) electrodes while type G was a laptop battery pack with unspecified battery chemistry. All electrolytes contained $LiPF_6$. Most of the cells were tested for different SOC levels, from fully charged, 100% SOC, to fully discharged, 0% SOC. The study included large-sized automotive-classed cells, i.e. series production cells of high industry quality, with long life time etc.

The heat release rate (HRR) and the emitted HF for B-type cells with different SOC values are shown in Fig. 1. Only the 100% SOC cells show several distinct peaks, corresponding to intense flares, when the cells vented and the emitted gas burn, for all other cells the heat release as a function of time is more smooth. These behaviors are reproducible also for the other tested cell types, e.g., only the 100% SOC cells show the more violent heat release peaks with intense flares.

The measurements of the gas emissions during the fire tests show that the production of HF is correlated to the increase in HRR although somewhat delayed. From Fig. 1b it is evident that the higher SOC value, the higher values for the peak HF release rate. The total amount of HF varies considerably for the different battery types, see Fig. 2a. The amount of HF produced, expressed in mg/Wh, where Wh is the nominal battery energy capacity, is approximately 10 times higher for the cell with the highest values compared to the cells with the lowest values. The different relative amount of electrolyte and filler materials in the cells could be the simple explanation of this variation but information on those amounts are difficult to access for commercial batteries. The highest HF values are found for the pouch cells, a possible explanation would be that hard prismatic and cylindrical cells can build a

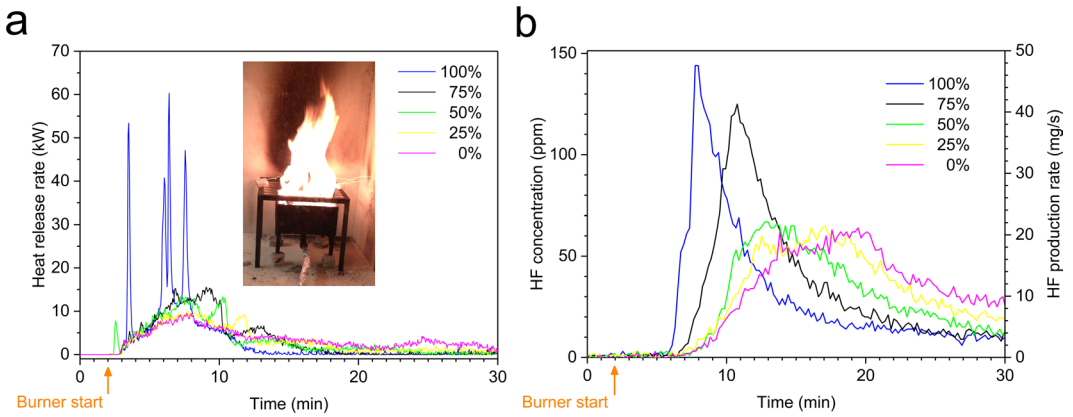

Figure 1. Results for type B cells, for 0–100% SOC with intermediate SOC-steps of 25%, exposed to an external propane fire; (**a**) showing the heat release rate (burner HRR contribution is subtracted), the inset photo shows burning battery cells during the test; (**b**) showing the HF release both as the measured concentrations as well as the calculated HF production rates. The HF production rates are calculated from the measured HF concentration by the Ideal gas law taking into account the ventilation flow, see Methods. The starting time of the heating process is marked on the time axis.

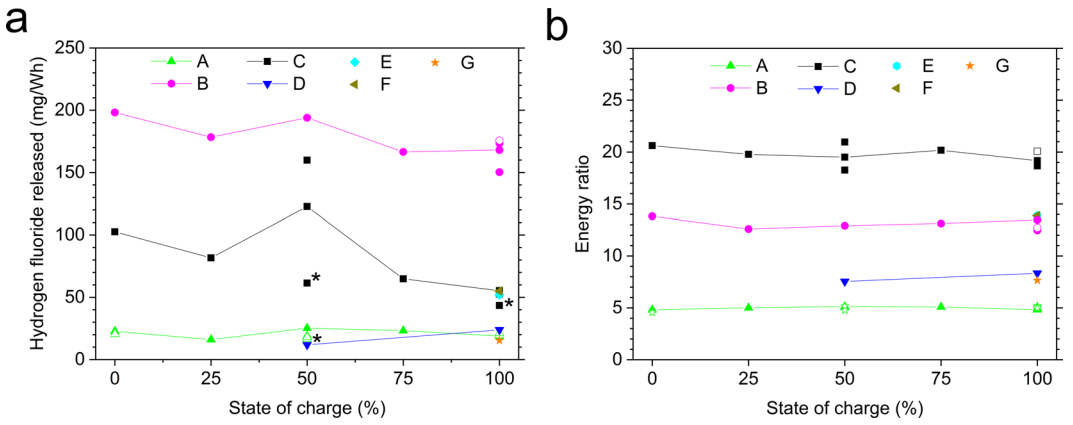

Figure 2. Total amount of HF measured by FTIR, normalized to nominal electrical energy capacity (**a**) and the energy ratio (**b**), for seven types of Li-ion battery cells and with various state of charge levels. Non-filled symbols indicate a repetition variant, e.g. applying water mist. The lines are intended as a guide for the eye. The energy ratio is a dimensionless value calculated by taking the total heat release from the battery fire divided by the nominal electrical energy capacity. Note that for 100% SOC the values are overlapping for type C, E and F as well as for type A, D and G in (**a**) and type B, E and F in (**b**). *Low value for type C at 50% and 100% SOC and type D at 50% SOC due to that a pre HF-saturation was not applied, therefore a part of the HF release was likely to be saturated in the gas sampling system, see Methods.

higher pressure before bursting, rapidly releasing a high amount of gases/vapors from the electrolyte. Due to the high velocity of the release and thus the short reaction time, combustion reactions might be incomplete and less reaction products might be produced. In the test involving type G the cylindrical cells were layered horizontally, thus having a different venting direction and possibly increased wall losses, which combined with a very energetic response, might suggest why HF was detected only from the filter analysis and not detected by FTIR-analysis. The tested pouch cells of type B and C burned for longer time and with less intensity. The pouch cell of type F, however, burned faster, possibly due to its different electrode materials. The SOC influence on the HF release was less significant and the trend in Fig. 2a shows higher HF values for 0% than for 100% SOC, however with clear peaks at 50% SOC. Although these results are reproducible, they are difficult to explain. In other studies[30,31], significantly narrower in test scope, involving smaller-sized cells and using a somewhat different abuse method, it was found that the total amount of HF measured by real-time FTIR was higher for decreasing SOC (tests conducted at 100%, 50% and 0% SOC).

The HRR curve is used to calculate the total heat release (THR) which corresponds to the energy released from the burning battery. THR is obtained by integrating the measured HRR (with the burner contribution subtracted) over the complete test time. Fig. 2b shows the energy ratio, that is how much energy is produced by the burning

Battery	Nominal energy capacity (Wh)	Normalized total HF detected with FTIR (mg/Wh)	Normalized maximum HRR (W/Wh)	Normalized THR (kJ/Wh)
A	128	15–25	243–729	17–19
B	128	150–198	78–633	45–50
C	112	43–160	116–491	66–75
D	92	12–24	207–315	27–30
E	132	52	235	50
F	138	55	384	50
G	124	15	460	28

Table 2. Main test results normalized to nominal energy capacity, when applicable including various SOC-levels.

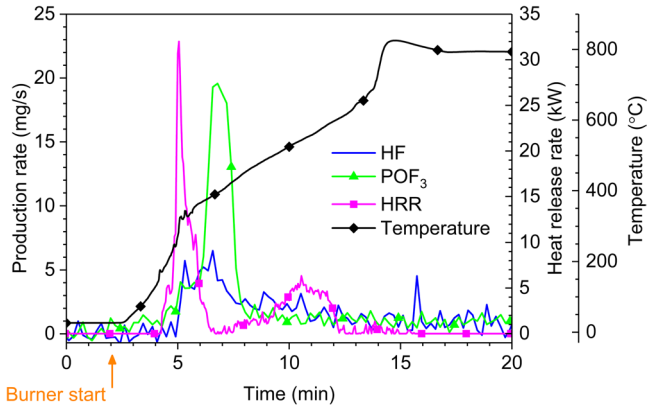

Figure 3. Results for a test with 5 type A cells at 0% SOC showing HF and POF_3, HRR and average surface temperature of the battery cells.

battery, compared to the amount of nominal electrical energy capacity a fully charged battery can deliver to an external circuit. The energy ratio is therefore a comparison between the chemical and the electrical energy of the Li-ion battery cell. The energy ratio varies considerably for the different cell types but is approximately constant for each cell, independent of SOC level. There are some similarities in Fig. 2a and b for the pouch cells, type B and C, which give the highest values in both cases, although in reverse order. This might indicate a higher amount of combustibles, e.g. electrolyte, in these cells compared to the other cells. It is also interesting to see that the energy ratio varies significantly between the tested cells, ranging from 5 to 21. This is important knowledge for fire protection and fire fighting. The energy ratio thus refers to a nominal fully charged battery while in normal use only a part of the SOC-window is used, for example half (50%) of the SOC-window (corresponding to cycling the battery between e.g. 30% and 80% SOC). If instead, the total heat release divided by the used electric battery capacity in the specific application is considered, higher energy ratio values are obtained. A summary of the results is shown in Table 2.

The measured heat release from an overheated battery may include several aspects, e.g. the battery temperature increase and the combustion of released gases. Variations due to the type of battery cell, the initiation method, e.g. if the test is done as an external fire test, an external heating or an overcharge test, and the test method, e.g. access to ambient oxygen (inert, under-ventilated or well-ventilated fire), and the presence of an external igniter, can greatly affect the amount of measured heat release. Energy release from a internal cell event in a confined environment can, for example, be lower than the energy release from the same cell in case of external fire. Thus energy ratios published using other methods and other types of Li-ion cells can be significantly different[7,52,53].

For all tested battert types and selected SOC-levels, POF_3 could only be measured quantitatively for type A battery cells at 0% SOC. Repeated measurements confirmed the presence of POF_3 only for type A and only for 0% SOC. No POF_3 could thus be detected in any of the other tests. POF_3 is an intermediate compound and the local combustion conditions in every test, will influence the amounts of POF_3 generated. This shows the importance of investigating many different set-ups when evaluating emitted gases.

In Fig. 3 the HRR, the average surface temperature of the five cells as well as the HF and POF_3 production rates are shown for type A cells at 0% SOC. The POF_3 curve is less noisy than the HF curve due to different signal-to-noise ratios of the FTIR instrumentation at the different wavenumbers. There is a secondary peak in HRR approximately 5 minutes after the main heat event, this peak does not correspond to any peaks in the mass flow of HF or POF_3. The explanation for this could be that the second peak in the heat release rate involves burning of mainly non-fluorine containing compounds. The temperature curve shows a rapid increase above the

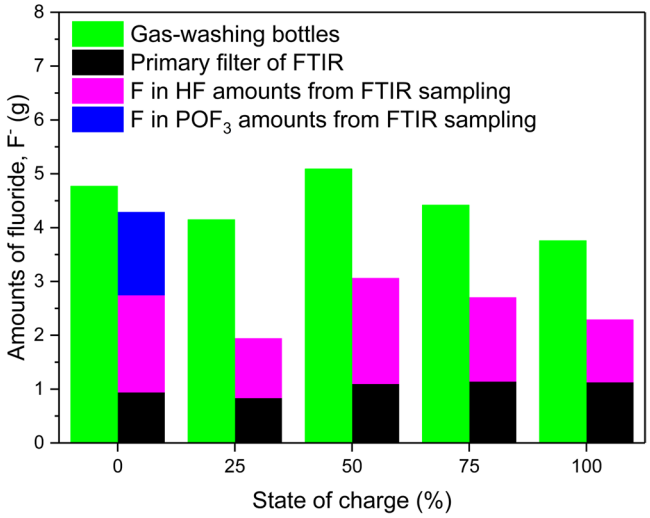

Figure 4. Total amount of measured fluoride, F^-, for type A, for 0–100% SOC with intermediate steps of 25%. The amount of F^- from the FTIR is calculated from the measurement results for POF_3 and HF, while the amount of fluoride from gas-washing bottles and primary filter analyses is measured as water soluble fluoride.

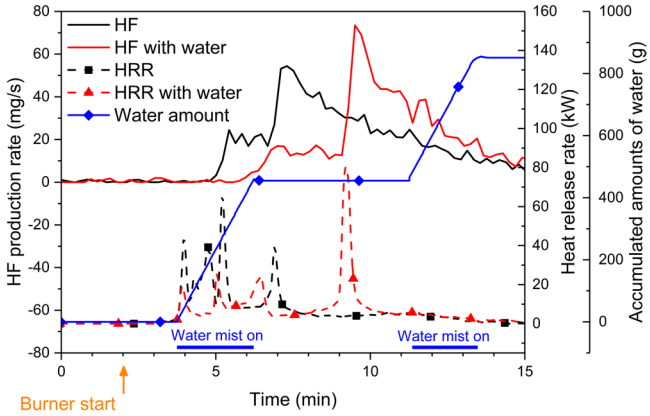

Figure 5. Results for type B cells at 100% SOC with and without the use of water mist.

melting temperature of the alumina cell case at about 660 °C. At these temperatures the alumina is molten and has formed a puddle on the burner bed beneath the battery cells. The thermal conditions in and around the thermocouples and the remains of the batteries have therefore changed considerably causing the apparent temperature increase.

In addition to the time resolved measurements with the FTIR, gas-washing bottles were used to determine the total fluorine content in the gas emissions during the tests. A comparison between the different measurement methods used can be seen in Fig. 4 for type A cells. Note that the FTIR measurements are performed only to detect HF and POF_3, other fluoride compounds are not included. It is interesting to note that for 0% SOC the total amount of fluoride measured by the gas-washing bottle technique matches rather well with the FTIR and primary filter analysis. For other SOC values the fluoride content is higher from the gas-washing bottle measurements. Still, the general trend observed in the FTIR measurements for different SOC values is more or less confirmed by the gas-washing bottle measurements.

Gas-washing bottles were also used for some of the tests involving battery types B and C. These batteries showed higher amounts of released HF compared to type A. The ratio between the total values of released flouride from FTIR plus filter analysis and from the gas-washing bottles for type B and C was between 0.89 and 1.02, indicating a better correlation between FTIR and gas-washing bottles measurement when HF gas emissions are higher.

The total amount of POF_3 measured by FTIR for type A at 0% SOC was 2.8 g (for 5-cells) and 3.9 g (for 10 cells). Hence, the normalized total POF_3 production was 15–22 mg/Wh of nominal battery energy capacity. Abuse studies measuring POF_3 are few, Andersson *et al.*[46] found both HF and POF_3 when burning mixtures of propane and Li-ion battery electrolytes with a HF:POF_3 production ratio between 8:1 and 53:1. Besides HF and POF_3 measurements, several distinct non-assigned peaks were found in the FTIR measurements, e.g. at 1027 cm^{-1}

Battery	SOC (%)	Number of tests	Normalized total HF detected (mg/Wh)		Normalized maximum HRR (W/Wh)	Normalized THR (kJ/Wh)
			From FTIR	From gas-washing bottles		
A	100	6	19.8 ± 1.2 [3]	29.1 ± 3.1 [5]	612 ± 102	18.1 ± 0.46
	50	7	18.5 ± 3.9 [6]	36.7 ± 3.3 [6]	416 ± 39 [6]	18.0 ± 0.61 [6]
	0	2	21.6 ± 1.5	38.3 ± 1.6	214 ± 53	16.8 ± 0.66
B	100	4	166.8 ± 11.5	191.3 ± 11.3 [2]	538 ± 77	46.9 ± 1.9
C	100	3	53.9 ± 2.0 [2]*	N/A	461 ± 27	69.5 ± 2.6
	50	3	141.3 ± 26.3 [2]*	N/A	149 ± 5	70.5 ± 4.9

Table 3. Detailed results for all available repetitions. Values presented as mean values followed by the standard deviation, in case the data parameter was not measured in all tests the value in bracket declares the number of available tests used for the specific data parameter value. *For FTIR data for battery type C, one data point of 50% and one data point at 100% SOC are excluded as outliers since they were low due to that a pre HF-saturation was not applied in the test, see Methods.

and 1034 cm^{-1}, which have also been seen in other studies[46]. They are compatible with the typical C-O stretching energies of low molecular weight alcohols in gas phase but also with in-plane stretching of aromatic compounds. This indicates the complexity and the limited knowledge in this area.

Water mist measurements. In order to study the effects of water on gas emissions, fire tests have also been performed where a water mist was applied during the fire. The reason for this experiment is that water is the preferred extinguishing agent for a lithium-ion battery fire. The intention in this study was however not to extinguish the fire completely. One potential problem regarding the use of water mist is that the addition of water may, in principle, increase the rate of formation of HF, see Eqs (2) and (3).

Figure 5 shows the results for type B cells with and without exposure to water mist, note that both the HRR and HF production are delayed when water mist is used. In this limited study, the peak of the HF production rate increased by 35% when using water, however no significant change in the total amounts of the HF release could be seen. A similar result has been reported in a previous study[28]. The water mist was applied during two different periods of time, as marked in Fig. 5, adding a total of 851 g of water in the reaction zone, however, several other large sources of water were also present in the experiment, i.e. water production from the propane combustion and from humidity in the air. The water mist is cooling the fire and the top surface of the pouch cell was for some time partly covered with liquid water; this is the reason that the battery fire is delayed as seen in Fig. 5. The water mist might actually also clean the air by collecting fume particles and HF can be bound to water droplets, thus possibly lowering the amount of HF in the smoke duct and increasing the non-measured amount of very toxic hydrofluoric acid on the test area surfaces (e.g. walls, floor, smoke duct walls).

Repeatability

Repeated tests were performed for battery types A-C for selected SOC-levels. Some of the repetitions included a variant, e.g. including water mist; see Methods. In Fig. 2 all available test data are presented. Since the test repetitions are not clearly observable in Fig. 2 the results are also presented in Table 3 showing the mean values and standard deviations and the number of performed tests. While the ranges in Table 2 include data for all tested SOC-values, Table 3 shows test data for repeated measurements including repetition variants.

Figure 6 shows the repeatability results for four tests of battery type B for 100% SOC. The time evolution of HRR varies in the fire tests as seen in Fig. 6a. In fire tests there are always natural variations, however comparing the tests with 100% SOC, in Fig. 6a, with those with lower SOC-values presented in Fig. 1a, the repeatability of the 100% SOC tests is significant. The third repetition (black line) in Fig. 6a is delayed due to that it included an application of water mist, as discussed above. Although the appearance of the HRR plots of the four tests differs in Fig. 6a the THR (the integrated HRR) values are rather similar. Fig. 6b shows the HF release for the same four tests of type B at 100% SOC. Repetition 2 and 3 were performed in the third test period, without secondary FTIR filter, and therefore Repetition 2 occurs earlier while Repetition 3 is delayed due to the applied water mist, as discussed above. For the four tests of type B at 100% SOC the mean value of the total FTIR detected HF release is 166.8 mg/Wh with a standard deviation of 11.5 mg/Wh, as seen in Table 3. Comparing Fig. 1b and Fig. 6b, shows that for 100% SOC the HF release is faster and reaches a higher value. Repetition 1 in Fig. 6b shows lower HF release peak values, however, the total HF release value from the FTIR measurement of 168 mg/Wh is close to the average value (166.8 mg/Wh, as seen in Table 3).

Conclusions

This study covered a broad range of commercial Li-ion battery cells with different chemistry, cell design and size and included large-sized automotive-classed cells, undergoing fire tests. The method was successful in evaluating fluoride gas emissions for a large variety of battery types and for various test setups.

Significant amounts of HF, ranging between 20 and 200 mg/Wh of nominal battery energy capacity, were detected from the burning Li-ion batteries. The measured HF levels, verified using two independent measurement methods, indicate that HF can pose a serious toxic threat, especially for large Li-ion batteries and in confined environments. The amounts of HF released from burning Li-ion batteries are presented as mg/Wh. If extrapolated for large battery packs the amounts would be 2–20 kg for a 100 kWh battery system, e.g. an electric

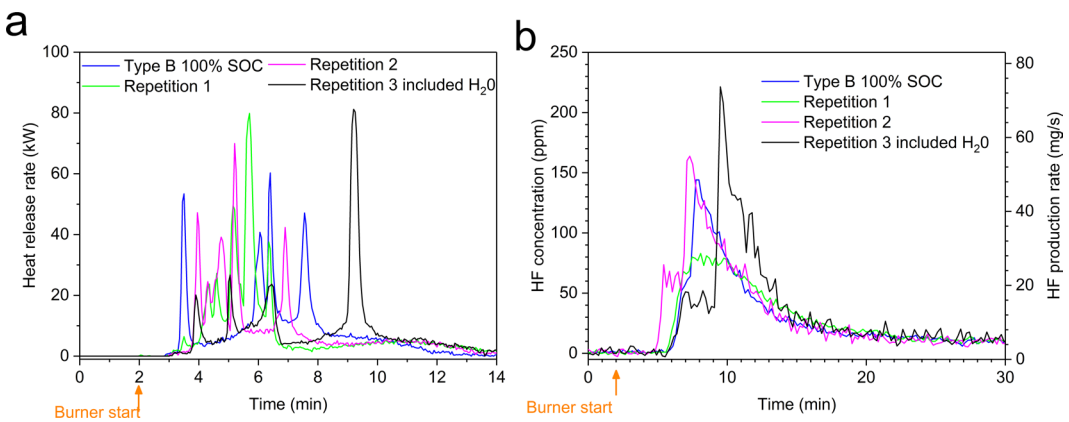

Figure 6. Repeatability for four tests of type B cells at 100% SOC, (**a**) shows the heat release rate (burner HRR contribution is subtracted) and (**b**) shows the HF release, both as the measured concentrations as well as the calculated HF production rates.

vehicle and 20–200 kg for a 1000 kWh battery system, e.g. a small stationary energy storage. The immediate dangerous to life or health (IDLH) level for HF is 0.025 g/m^3 (30 ppm)[22] and the lethal 10 minutes HF toxicity value (AEGL-3) is 0.0139 g/m^3 (170 ppm)[23]. The release of hydrogen fluoride from a Li-ion battery fire can therefore be a severe risk and an even greater risk in confined or semi-confined spaces.

This is the first paper to report measurements of POF_3, 15–22 mg/Wh, from commercial Li-ion battery cells undergoing abuse. However, we could only detect POF_3 for one of the battery types and only at 0% SOC, showing the complexity of the parameters influencing the gas emission. No POF_3 could be detected in any of the other tests.

Using water mist resulted in a temporarily increased production rate of HF but the application of water mist had no significant effect on the total amount of released HF.

The research area of Li-ion battery toxic gas emissions needs considerable more attention. Results as those presented here are crucial to be able to conduct a risk assessment that takes toxic HF gas into account. The results also enable strategies to be investigated for counteractions and safety handling, in order to achieve a high safety level for Li-ion battery applications. Today we have a rapid technology and market introduction of large Li-ion batteries but the risks associated with gas emissions have this far not been possible to take into consideration due to the lack of data.

Methods

Seven types of Li-ion batteries were exposed to an external propane fire. Fire characteristics, gas emissions, battery temperatures and cell voltages were measured. In total 39 fire tests were conducted of which 20 were within the base test matrix, 19 were repeated measurements of selected battery types and SOC-levels of which 10 included a variant, e.g. water mist for fire-fighting. The amounts of emitted fluoride gases were measured with two parallel and independent techniques, FTIR (time resolved concentration measurements and total values achieved by integration of the time resolved curve) and gas-washing bottles (total values). The experimental setup is schematically shown in Fig. 7. The gas collecting system and measurement system of the *Single Burning Item (SBI) method* (EN 13823[54]), which is normally used for reaction-to-fire classification of construction products according to EN 13501-1[55] was used in the tests. The tests were performed in three different test periods; the second test period was conducted about 1 year after the first and the third test period was conducted about 2.5 years after the first. Each test period involved several days of testing. The measurement equipment, as specified in the text below, was somewhat varying between the three test periods.

Batteries. Six different types of Li-ion battery cells, type A-F, and one Li-ion battery pack, type G, were tested as seen in Table 1. The number of cells used in each test was varied in order to achieve similar electrical energy capacity per test. The batteries were placed on wire gratings just above a 16 kW propane burner. The wire grating was made of steel wire about 2 mm thick over a surface of about 300 × 300 mm. The quadrants of the grating were 40 × 100 mm. The cells were not electrically connected to each other (except the laptop packs of type G, see note in Table 1). Type A-F was pure battery cells while type G was a complete laptop battery pack which included plastics box, electronics and cables. The chemical content of the polymer materials in the auxiliary components of the battery pack of battery type G is not known. It is possible, however not likely, that fluorine was included in some of the components, which in that case could have resulted in the production of HF. For battery type A, 5 cells/test was used except in two variant tests in which 10 cells/test were used.

The influence of different state of charge was investigated, for some battery types the complete SOC-window ranging from 0% to 100%, with intermediate steps of 25%, was investigated. The SOC levels included for each battery type and the numbers of repetitions per test type, i.e. the fire test matrix, is seen in Table 4. All parameters were not measured in all of the tests. Measurement of HRR and corresponding THR was conducted in 38 tests, FTIR in 35 tests and gas-washing bottles were used in 19 tests.

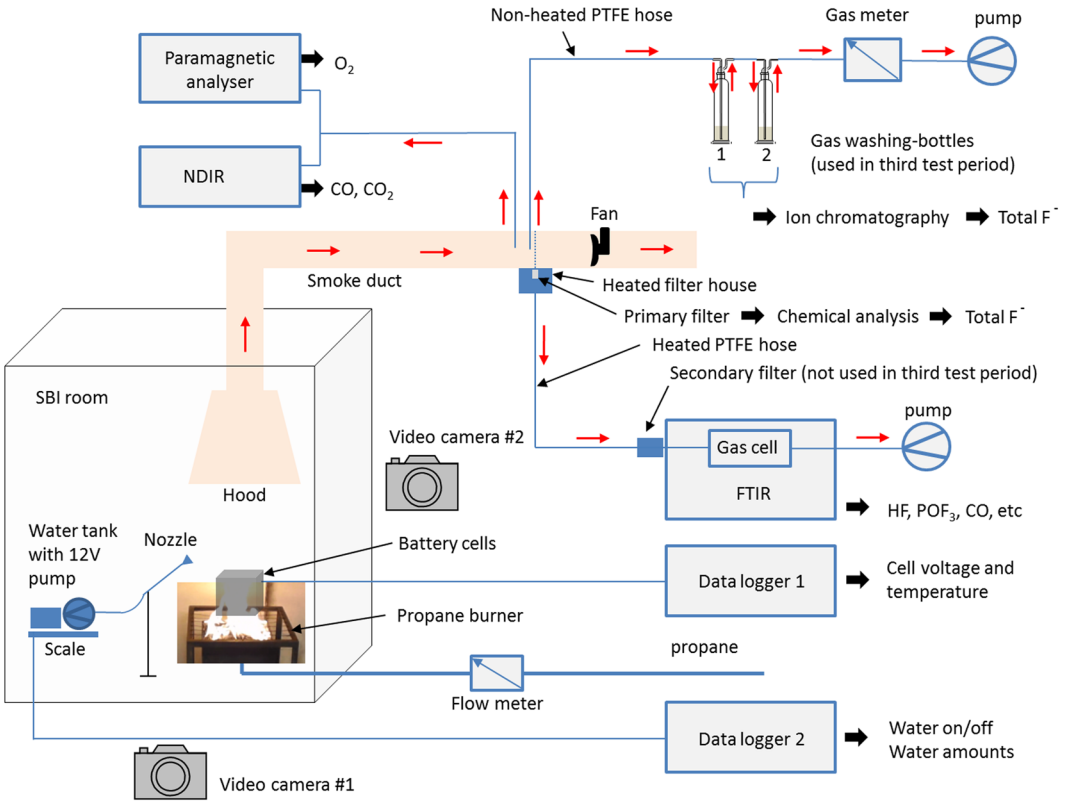

Figure 7. Schematic illustration of the experimental setup.

Battery	Number of tests per SOC-level					Number of tests
	0%	25%	50%	75%	100%	
A	1 + 1*	1	3 + 4*	1	3 + 3*	17
B	1	1	1	1	3 + 1*	8
C	1	1	3	1	2 + 1*	9
D			1		1	2
E					1	1
F					1	1
G					1	1
Total number of tests						39

Table 4. Detailed test matrix of the fire tests. *repetition includes a variant, e.g. water mist or 2 × 5-cell-pack (for battery type A).

The selected SOC level in each test was set using a charge/discharge procedure using ordinary laboratory equipment as well as dedicated battery test equipment, i.e. a *Digatron battery tester* and *Metrohm Autolab PGSTAT302N* with 20 A booster module. The cells were first fully charged by constant current followed by constant voltage (CC-CV) according to the manufacturer's instructions. For cells intended for tests with less than 100% SOC, the cell was discharged to the selected SOC level, using constant discharge current (CC). A relative low current rate, about C/5, was used and voltage and current rates were within the manufacturer limits. In most cases each battery type was tested during the same test period. However, the tests for type C and D were split in several test periods, for type C repetitions on 50% SOC were conducted in all three test periods, and for type B repetitions at 100% SOC were made in two test periods, the latter one included a water mist test.

All batteries were unused and the calendar life time of the cells before the tests were approximately 6–12 months for type A, F and G and between approximately 2–3 years for type B-E. The pouch cells; type B, C and F was mechanically tied together with steel wires (0.8 mm diameter). The type A hard prismatic cells were tight together in packs of five cells, "5-cell-pack", using steel straps (1 × 13 mm). The hard prismatic and cylindrical cells were placed in boxes to protect test personnel from potential projectile hazards in case of cell explosions due to excessive pressure. The 5-cell-pack of type A was placed standing up, with the cell safety vents releasing straight upright in direction to the hood and smoke duct, inside a custom-made steel-net-box, see Fig. 8. Additionally, the 5-cell-pack of type A was fastened to the bottom of the steel-net-box with steel wire (0.8 mm diameter) in the

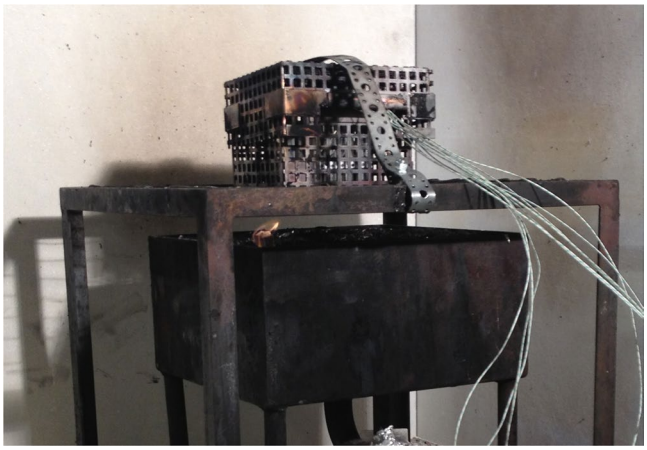

Figure 8. Photo of test type A, showing the 5-cell-pack inside a steel-net-box placed on the wire gratings. The sand bed for the propane burner is underneath the wire grating, a pilot flame (seen in front left corner of the burner) is used to ignite the propane gas.

corners to avoid it moving around due to e.g. explosion/rupture/venting. Type D and E cells were placed standing up in custom-made boxes made of non-combustible silica board and steel net at the top and bottom. Type G was placed in a steel net. The protective boxes and steel net were fastened in the wire gratings with steel wire and steel straps to avoid movement due to response to the fire. Care was taken to avoid external short circuiting when placing the battery on the wire gratings as well as avoiding accidental external electrical inter-cell-connections, e.g. for pouch cells the electrical tab terminals were cut. Still the battery test setup allowed that the separators and electrical insulation in the cells could melt due to the heat exposure which could cause various internal and external electrical contacts.

The battery surface temperature was measured with several type K thermocouples; the number of sensors varied for the different battery types. Battery cell surface temperature values presented in this paper are average values over the cell. Cell voltages were measured for type A, B, C and F battery tests. Cell voltage and thermocouple readings was sampled with 1 Hz using two types of data loggers, *Agilent 34972 A using an Agilent 34902 A reed multiplexer module* (for the third test period) and *Pico Technology ADC-24* (for the first and second test period).

Test procedure. The propane burner was started 2 minutes into each test, as indicated with arrows in the result figures in the paper. The burner was active as long as there was a heat contribution from the burning batteries; therefore, the burner was active for different durations of time for different batteries and SOC-levels. When the heat release from the batteries was no longer detectable, the power of the propane burner was doubled, i.e. to 32 kW, in order to be sure to fully burn out any residues of the batteries, for increased personnel safety. The fire emissions were collected in the hood and transferred in the smoke duct having a ventilation flow of 0.4 m^3/s, with the exception that 0.6 m^3/s was used in two tests with 100% SOC for type C. For these cases the values were scaled down to the lower flow values making the results from the two flow rates comparable. The SBI-room, see Fig. 7, had a ventilation inlet from an adjacent indoor laboratory hall (which had fresh air inlet from the ventilation system in the building), supplying ambient air with temperature about 20 °C entering beneath the propane burner. We consider the amount of ambient air to be sufficient to provide an oxygen-rich environment and thereby consider the battery fire as well-ventilated. However for some tests, during the rapid and energetic gas outbursts, a full combustion might not have occurred in these short time periods.

All tests were video recorded and for the majority of the tests an additional camera was used set at 90 degree angle from the other video camera, allowing simultaneous recording from two sides of the battery fire.

A part of the smoke duct flow was sampled to a *Servomex 4100 Gas purity analyser* where the oxygen content was measured by a *paramagnetic analyser* and CO and CO_2 were measured by a *non-dispersive infrared sensor (NDIR)*. By combing these two measurements, the heat release rate (HRR) is calculated using the oxygen consumption method corrected by CO_2[54]. Each test day started with a blank test, i.e. using only the propane burner, to measure the HRR of the burner alone and measure blanks for FTIR and gas-washing bottles. In the presented HRR values of the battery tests the burner contribution to the HRR (about 16 kW, with slight daily variations, established by the blank tests) has been subtracted. The combined expanded uncertainty is ±5 kW for the HRR-values. By integrating the HRR values over the entire test, subtracting the HRR from the burner, the total heat release (THR) from the battery cells could be established. The oxygen consumption method is common in fire calorimetry, however when using it with batteries, the joule heating from electrical discharge within the cells is not accounted for, therefore the values of HRR and THR do not include the Joule heating. During the external fire tests, it is difficult to measure how much a battery cell is electrically discharged when the separator is melting. The energy ratios presented in Fig. 2b do not include any Joule heating as clearly stated by its definition. For 0% SOC the influence from Joule heating is in principle zero, however small amounts of joule heating might possibly be liberated when going to zero voltage even though other processes might occur. Li-ion cells can also release oxygen during thermal runaway and this could affect the measured O_2 levels. The amount of oxygen release varies

Spectral bands (cm^{-1})	Type of band
POF_3	
868–874	P-F symmetric stretching mode[20]
1413–1418	P-O stretching mode[20]
HF	
4172–4175	HF R-branch stretching mode[58]
4202–4203	HF R-branch stretching mode[58]

Table 5. FTIR spectral band used for measurements of POF_3 and HF.

for different electrode materials, e.g. LFP typically releases less oxygen than LCO. However, the ventilation flow is large and the O_2 released from the battery cells is regarded as negligible.

Gas measurements. Besides the gas measurements in the SBI apparatus, measurements of gases were also conducted by online Fourier transform infrared spectroscopy (FTIR). The FTIR offers broad and diverse spectra of gases, the focus was however on fluoride gas emissions. The FTIR used was a *Thermo Scientific Antaris IGS analyzer (Nicolet)* with a gas cell. The gas cell was heated to 180 °C and had a volume of 0.2 L, 2.0 m path length and a cell pressure of 86.7 kPa which was maintained during the tests. The spectral resolution of the FTIR was 0.5 cm^{-1} (accuracy 0.01 cm^{-1}) and 10 scans where used to collect a spectrum every 12 s, giving both accurate intensity, as well as relatively rapid measurements with its five spectrum per minute rate. A part of the duct flow, taken along the full duct pipe width (in the mid height of the pipe) from around 15 sampling holes (about 2 mm diameter, directed opposite to flow, pipe end was closed), was taken to online FTIR measurement. This sub-flow was extracted through a primary filter inside a heated filter house (180 °C) and then extracted through an 8.5 m sampling PTFE hose, heated to 180 °C, and then through a secondary filter and finally through the gas cell of the FTIR. The sub-flow was selected to be 3.5 L/min using a pump located after the FTIR gas cell. Between each test the FTIR sampling system was flushed with N_2 gas and a new background spectrum was measured. There is a natural delay time between the FTIR and the heat release measurement. In order to time synchronize them the (CO_2 measurements from both the FTIR and the NDIR) part of the heat release rate measurement, were overlayed.

One primary filter (M&C ceramic filter, type "F-2K") was used per test and was chemically analysed for fluoride content after the test. It is known that HF may be partly adsorbed by this type of filter[56]. The fluoride amount absorbed by the filter was determined by leaching the filter in an ultrasonic water bath for at least 10 min and thereafter the fluoride content in the water was measured by ion chromatography with a conductive detector, according to the method B.1 (b) of the SS-ISO 19702:2006 Annex B standard. The amount of HF is calculated by assuming that all fluoride ions present in the filter derives from HF. The secondary filter (M&C sintered steel filter), heated to 180 °C, was the same in all tests in the first and second test period. In the third test period the secondary filter was removed in order to decrease delay time and losses. The third test period started with burning 10 cells of type A in order to saturate the FTIR sampling system with HF and it was conducted because in the first and the second test period the first tests had indicated low HF values, HF was potentially lost during saturation of the gas collecting system.

The FTIR was calibrated[29,57] for HF and POF_3. The minimum detection limit (MDL) for HF was 1.7 ppm and the limit of quantification (LOQ) was established to 5.7 ppm. The detection limit for POF_3 was 6 ppm[29]. PF_5 was also qualitatively detectable by the FTIR[29] but not quantitatively calibrated. A classical least square (CLS) method was used for the quantification of HF and POF_3 using the spectral bands specified in Table 5. The relative error of the HF prediction is lower than 10 rel-%.

For all measurements, except type G, the measured ppm levels of HF were above the detection level. For POF_3, the maximum concentration was 11 ppm (5-cells) and 19 ppm (10-cells).

When the FTIR measurement stopped, HF levels were, in some of the tests, still somewhat above the detection limit, even though no HRR contribution was measured from the batteries. It is also possible that the HF was temporarily clogged in the sampling system. Some HF might not have been collected in the measurements and the effect of this error is largest for the batteries that give the lowest values. Thus the reported values might underestimate the released gas emissions.

In order to further improve the accuracy of the FTIR measurements, a data offset determination and a subsequent adjustment of the HF values was performed. The improvement was greatest for tests with lower concentrations, closer to the MDL value, e.g. type A with 5 cells with low values during relatively short periods of time. With 10 cells per test, the type A batteries gave higher signal-to-noise levels. The FTIR measurements started around 8 minutes before the burner was started. The calculated average HF ppm noise level was treated as an offset that had both negative and positive values, ranging from extreme values of about −2 to 3.5 ppm. This offset was compensated for by assuming a constant offset value and adding positive or negative offset values to the total HF release value. Note that the reported concentration values in ppm are only valid for the measurements in the smoke duct of our specific test equipment and method. The HF and POF_3 concentration values (in ppm) were used for calculating the corresponding production rates (in mg/s) using the ideal gas law and taking into account the measured ventilation flow rate in the smoke duct.

In the third test period the total amounts of water soluble fluorides were determined using gas-washing bottle technique. This was made in order to validate the results from the FTIR measurements with a separate measurement technique. The water soluble fluorides were collected in the bottles and the amount of HF was calculated by assuming that all fluoride ions present derives from HF. The sample gas was extracted from the center of

the smoke duct using a non-heated 6 mm (o.d.) diameter PTFE sampling tube with a length of about 1.5 m. The sampling was made using two gas-washing bottles connected in series each containing 40 mL of an alkaline buffer solution (20 mM Na_2CO_3/20 mM $NaHCO_3$). The second bottle was used to capture any losses from the first bottle. The sampling flow was 1.0 normal-L/min and the total sampled volume during a test was measured by a calibrated gas volume meter. The sampling flow rate was checked before the start of each test using a *Gilian Gilibrator-2 NIOSH Primary Standard Air Flow Calibrator* gas flow meter. The procedure during a test was to continuously sample during the full test time. When the test was completed, the sampling tube was disconnected from the exhaust duct to allow rinsing of the tube with buffer solution, about 30 mL in the first gas-washing bottle, to collect any fluoride deposited on the inner walls of the tubing, in order to minimize losses in the tube. Since the tube was rinsed, heating of the tube was not necessary (any condensation in tube was collected anyhow). Analysis of fluorine content of the absorption solutions was made using High Performance Ion Chromatography (HPIC). The contents of the two gas-washing bottles were analyzed separately. The bottles were rinsed with distilled water between each test in order to minimize any interference between tests.

Water mist test. In the water mist tests, a custom-made equipment was constructed, including a 12 V automotive pump and water container which was placed on a scale measuring the weight of the water. The scale readings and the on/off manual switching (of the 12 V) was recorded with 1 Hz using *Pico Technology ADC-24* with a custom-made *LabVIEW* program. The water mist was sprayed on or above the batteries using a metal nozzle. In order for precise time synchronization, the on/off 12 V signal was recorded by both data loggers (data logger 1 and data logger 2). A blank test, i.e. using only the propane burner and without batteries, was performed in order to calibrate the setup. The water flow was around 190 g water per min and consisted of deionized water.

References

1. Samsung Note 7: Press Conference Details, Samsung US, Our safety promise, http://www.samsung.com/us/explore/committed-to-quality/?CID=van-brd-brd-0119-10000141, Date of access: 06/04/2017.
2. Prigg, M. Nasa reveals shocking video of secretive military 'RoboSimian' EXPLODING as its batteries catch fire (2016), http://www.dailymail.co.uk/sciencetech/article-3883158/Nasa-reveals-shocking-video-secretive-military-RoboSimian-EXPLODING-batteries-catch-fire.html, Date of access: 06/04/2017.
3. Aircraft Serious Incident Investigation Report, JA804A. Japan Transport Safety Board (2014), Available online: http://www.mlit.go.jp/jtsb/eng-air_report/JA804A.pdf, Date of access: 13/02/2017.
4. Auxiliary Power Unit Battery Fire, Japan Airlines Boeing 787–8, JA829J, Boston, Massachusetts; NTSB/AIR-14/01. National Transportation Safety Board (2014), Available online: http://www.ntsb.gov/investigations/AccidentReports/Reports/AIR1401.pdf, Date of access: 13/02/2017.
5. Chevrolet Volt battery incident overview report, *National Highway Traffic Safety Administration (NHTSA)*, DOT HS 811 573 (2012).
6. Doughty, D. & Roth, E. P. A general discussion of Li ion battery safety. *The Electrochem. Soc. Interface*, **summer 2012**, 37–44 (2012).
7. Larsson, F. & Mellander, B.-E. Abuse by external heating, overcharge and short circuiting of commercial lithium-ion battery cells. *J. of The Electrochem. Soc.* **161**(10), A1611–A1617 (2014).
8. Larsson, F., Andersson, P. & Mellander, B.-E. Are electric vehicles safer than combustion engine vehicles? in *Systems perspectives on* Electromobility (eds. Sandén, B. & Wallgren, P.) 33–44 (Chalmers University of Technology, 2014).
9. Finegan, D. P. *et al*. In-operando high-speed tomography of lithium-ion batteries during thermal runaway. *Nat. Commun.* **6**, 6924 (2015).
10. Larsson, F., Andersson, P. & Mellander, B.-E. Lithium-ion battery aspects on fires in electrified vehicles on the basis of experimental abuse tests. *Batteries* **2**, 9 (2016).
11. Lopez, F. L., Jeevarajan, J. A. & Mukherjee, P. P. Experimental analysis of thermal runaway and propagation in lithium-ion battery modules. *J. of The Electrochem. Soc* **162**(9), A1905–A1915 (2015).
12. Lamb, J., Orendorff, C. J., Steele, L. A. M. & Spangler, S. W. Failure propagation in multi-cell lithium-ion batteries. *J. of Power Sources* **283**, 517–523 (2015).
13. Larsson, F., Anderson, J., Andersson, P. & Mellander, B.-E. Thermal modelling of cell-to-cell fire propagation and cascading thermal runaway failure effects for lithium-ion battery cells and modules using fire walls. *J. of The Electrochem. Soc.* **163**(14), A2854–A2865 (2016).
14. Lebedeva, N. P. & Boon-Brettz, L. Considerations on the chemical toxicity of contemporary Li-ion battery electrolytes and their components. *J. of The Electrochem. Soc.* **163**(6), A821–A830 (2016).
15. Sun, J. *et al*. Toxicity, a serious concern of thermal runaway from commercial Li-ion battery. *Nano Energy* **27**, 313–319 (2016).
16. Nedjalkov, A. *et al*. Toxic gas emissions from damaged lithium ion batteries–analysis and safety enhancement solution. *Batteries* **2**, 5 (2016).
17. Liu, K. *et al*. Electrospun core-shell microfiber separator with thermal-triggered flame-retardant properties for lithium-ion batteries. *Sci. Adv.* **3**, e1601978 (2017).
18. Park, Y.-U. *et al*. Tailoring a fluorophosphate as a novel 4 V cathode for lithium-ion batteries. *Scientific Reports* **2**, 704 (2012).
19. Ortiz, G. F. *et al*. Enhancing the energy density of safer Li-ion batteries by combining high-voltage lithium cobalt fluorophosphate cathodes and nanostructured titania anodes. *Scientific Reports* **6**, 20656 (2016).
20. Yang, H., Zhuang, G. V. & Ross Jr, P. Thermal stability of $LiPF_6$ salt and Li-ion battery electrolytes containing $LiPF_6$. *J. of Power Sources* **161**, 573–579 (2006).
21. Kawamura, T., Okada, S. & Yamaki, J.-i Decomposition reaction of $LiPF_6$-based electrolytes for lithium ion cells. *J. of Power Sources* **156**, 547–554 (2006).
22. Documentation for immediately dangerous to life or health concentrations (IDLHs) for hydrogen fluoride (as F). *The National Institute for Occupational Safety and Health (NOISH)* (1994).
23. Acute exposure guideline levels for selected airborne chemicals: volume 4, subcommittee on acute exposure guideline levels. ISBN: 0-309-53013-X. *Committee on Toxicology, National Research Council* (2004).
24. Middelman, A. Hygiensiska gränsvärden AFS 2015:7, Hygieniska gränsvärden. Arbetsmiljöverkets föreskrifter om hygieniska gränsvärden och allmänna råd om tillämpningen av föreskrifterna. ISBN 978-91-7930-628-1. ISSN 1650-3163. *Swedish Work Environment Authority* (2015).
25. Guéguen, A. *et al*. Decomposition of $LiPF_6$ in high energy lithium-ion batteries studied with online electrochemical mass spectrometry. *J. of The Electrochem. Soc.* **163**(6), A1095–A1100 (2016).

26. Chatelain, M. D. & Adams, T. E. Lithium ion gas sampling of vented cells. *Proceedings of the Power Sources Conference* **42**, 87–89 (2006).
27. Blum, A. F. & Long Jr, R. T. Hazard assessment of lithium ion battery energy storage systems. *Fire Protection Research Foundation* (2016).
28. Larsson, F., Andersson, P., Blomqvist, P., Lorén, A. & Mellander, B.-E. Characteristics of lithium-ion batteries during fire tests. *J. of Power Sources* **271**, 414–420 (2014).
29. Larsson, F., Andersson, P., Blomqvist, P. & Mellander, B.-E. Gas emissions from Lithium-ion battery cells undergoing abuse from external fire in *Conference proceedings of Fires in vehicles* (FIVE) 2016 (eds. Andersson, P. & Sundstrom, B.) 253–256 (SP Technical Research Institute of Sweden, 2016).
30. Ribière, P. *et al*. Investigation on the fire-induced hazards of Li-ion battery cells by fire calorimetry. *Energy Environ. Sci.* **5**, 5271–5280 (2012).
31. Lecocq, A. Scenario-based prediction of Li-ion batteries fire-induced toxicity. *J. of Power Sources* **316**, 197–206 (2016).
32. Lecocq, A., Bertana, M., Truchot, B. & Marlair, G. Comparison of the fire consequences of an electric vehicle and an internal combustion engine vehicle in *Conference proceedings of Fires in vehicles* (FIVE) 2012 (eds. Andersson, P. & Sundstrom, B.) 183–193 (SP Technical Research Institute of Sweden, 2012).
33. Ohsaki, T. *et al*. Overcharge reaction of lithium-ion batteries. *J. of Power Source* **146**, 97–100 (2005).
34. Abraham, D. P. *et al*. Diagnostic examination of thermally abused high-power lithium-ion cells. *J. of Power Sources* **161**, 648–657 (2006).
35. Roth, E. P. Abuse response of 18650 Li-ion cells with different cathodes using EC:EMC/$LiPF_6$ and EC:PC:DMC/$LiPF_6$ electrolytes. *ECS Transactions* **11**(19), 19–41 (2008).
36. Golubkov, A. W. *et al*. Thermal-runaway experiments on consumer Li-ion batteries with metal-oxide and olivin-type cathodes. *RSC Adv.* **4**, 3633–3642 (2014).
37. Golubkov, A. W. *et al*. Thermal runaway of commercial 18650 Li-ion batteries with LFP and NCA cathodes—impact of state of charge and overcharge. *RSC Adv.* **5**, 57171–57186 (2015).
38. Spinner, N. S. *et al*. Physical and chemical analysis of lithium-ion battery cell-to-cell failure events inside custom fire chamber. *J. of Power Sources* **279**, 713–721 (2015).
39. Fu, Y. *et al*. An experimental study on burning behaviors of 18650 lithium ion batteries using a cone calorimeter. *J. of Power Sources* **273**, 216–222 (2015).
40. Huang, P., Wang, Q., Li, K., Ping, P. & Sun, J. The combustion behavior of large scale lithium titanate battery. *Scientific Reports* **5**, 7788 (2015).
41. Ping, P. *et al*. Study of the fire behavior of high-energy lithium-ion batteries with full-scale burning test. *J. of Power Sources* **285**, 80–89 (2015).
42. Roth, E. P. & Orendorff, C. J. How electrolytes influence battery safety. *The Electrochem. Soc. Interface, summer* **2012**, 45–49 (2012).
43. Eshetu, G. G. *et al*. In-depth safety-focused analysis of solvents used in electrolytes for large scale lithium ion batteries. *Phys. Chem. Chem. Phys.* **15**, 9145–9155 (2013).
44. Lamb, J., Orendorff, C. J., Roth, E. P. & Langendorf, J. Studies on the thermal breakdown of common Li-ion battery electrolyte components. *J. of The Electrochem. Soc.* **162**(10), A2131–A2135 (2015).
45. Eshetu, G. G. *et al*. Fire behavior of carbonates-based electrolytes used in Li-ion rechargeable batteries with a focus on the role of the $LiPF_6$ and LiFSI salts. *J. of Power Sources* **269**, 804–811 (2014).
46. Andersson, P., Blomqvist, P., Lorén, A. & Larsson, F. Using Fourier transform infrared spectroscopy to determine toxic gases in fires with lithium-ion batteries. *Fire and Materials* **40**(8), 999–1015 (2016).
47. Lux, S. F. The mechanism of HF formation in $LiPF_6$ based organic carbonate electrolytes. *Electrochem. Comm.* **14**, 47–50 (2012).
48. Lux, S. F., Chevalier, J., Lucas, I. T. & Kostecki, R. HF formation in $LiPF_6$-based organic carbonate electrolytes. *ECS Electrochem. Lett.* **2**(12), A121–A123 (2013).
49. Wilken, S., Treskow, M., Scheers, S., Johansson, P. & Jacobsson, P. Initial stages of thermal decomposition of $LiPF_6$-based lithium ion battery electrolytes by detailed Raman and NMR spectroscopy. *RSC Adv.* **3**, 16359–16364 (2013).
50. Hammami, A., Raymond, N. & Armand, M. Runaway risk of forming toxic compounds. *Nat.* **424**, 635–636 (2013).
51. Campion, C. L. *et al*. Suppression of toxic compounds produced in the decomposition of lithium-ion battery electrolytes. *Electrochem. and Solid-State Lett.* **7**(7), A194–A197 (2004).
52. Liu, X. *et al*. Heat release during thermally-induced failure of a lithium ion battery: impact of cathode composition. *Fire Safety Journal* **85**, 10–22 (2016).
53. Lyon, R. E. & Walters, R. N. Energetics of lithium ion battery failure. *J. of hazardous materials* **318**, 164–172 (2016).
54. EN 13823:2010. Reaction to fire tests for building products–building products excluding floorings exposed to the thermal attack by a single burning item. *European Committee for Standardization* (2010).
55. EN 13501−1:2007 + A1:2009. Fire classification of construction products and building elements - part 1: classification using data from reaction to fire tests. *European Committee for Standardization* (2009).
56. ISO 19702:2006. Toxicity testing of fire effluents–guidance for analysis of gases and vapours in fire effluents using FTIR gas analysis. *International Organization for Standardization* (2006).
57. Andersson, P., Blomqvist, P., Lorén, A. & Larsson, F. Investigation of fire emissions from Li-ion batteries. *SP Technical Research Institute of Sweden*. SP Report 2013:5 (2013).
58. Hollas, J. M. Modern Spectroscopy, 3ed. (John Wiley & Sons, 1996).

Acknowledgements

The Swedish Energy Agency and its FFI-program, and Carl Tryggers Stiftelse för Vetenskaplig Forskning are acknowledged for their financial support. Several persons at RISE Research Institutes of Sweden and Chalmers University of Technology have been involved in this work and are gratefully acknowledged.

Author Contributions

F. Larsson planned the experiments, partially together with P. Andersson and B.-E. Mellander. P. Andersson made the initial data process of the SBI heat release data. P. Blomqvist planned and performed the FTIR and gas-washing bottles measurements and made the initial data processing. F. Larsson prepared the batteries and performed the measurement and data analyses of temperature, cell voltage and water mist, and did the post-measurements and final data processing. Water mist setup was planned and constructed by B.-E. Mellander and F. Larsson. All four authors were involved in the analyses of the data and wrote the paper.

Additional Information

Competing Interests: The authors declare that they have no competing interests.

Publisher's note: Springer Nature remains neutral with regard to jurisdictional claims in published maps and institutional affiliations.

ATTACHMENT 5

CHARACTERIZATION OF LITHIUM-ION BATTERY FIRE EMISSIONS—PART 2

batteries

MDPI

Article

Characterization of Lithium-Ion Battery Fire Emissions—Part 2: Particle Size Distributions and Emission Factors

Matthew Claassen [1,2], Bjoern Bingham [1,3], Judith C. Chow [1], John G. Watson [1], Pengbo Chu [4], Yan Wang [2] and Xiaoliang Wang [1,*]

[1] Division of Atmospheric Sciences, Desert Research Institute, Reno, NV 89512, USA; matt.claassen@dri.edu (M.C.); bjoern.bingham@dri.edu (B.B.); judith.chow@dri.edu (J.C.C.); john.watson@dri.edu (J.G.W.)
[2] Department of Mechanical Engineering, University of Nevada, Reno, NV 89557, USA; yanwang@unr.edu
[3] Atmospheric Sciences, Department of Physics, University of Nevada, Reno, NV 89557, USA
[4] Department of Mining and Metallurgical Engineering, University of Nevada, Reno, NV 89557, USA; pengboc@unr.edu
* Correspondence: xiaoliang.wang@dri.edu; Tel.: +1-775-674-7177

Abstract: The lithium-ion battery (LIB) thermal runaway (TR) emits a wide size range of particles with diverse chemical compositions. When inhaled, these particles can cause serious adverse health effects. This study measured the size distributions of particles with diameters less than 10 µm released throughout the TR-driven combustion of cylindrical lithium iron phosphate (LFP) and pouch-style lithium cobalt oxide (LCO) LIB cells. The chemical composition of fine particles ($PM_{2.5}$) and some acidic gases were also characterized from filter samples. The emission factors of particle number and mass as well as chemical components were calculated. Particle number concentrations were dominated by those smaller than 500 nm with geometric number mean diameters below 130 nm. Mass concentrations were also dominated by smaller particles, with PM_1 particles making up 81–95% of the measured PM_{10} mass. A significant amount of organic and elemental carbon, phosphate, and fluoride was released as $PM_{2.5}$ constituents. The emission factor of gaseous hydrogen fluoride was 10–81 mg/Wh, posing the most immediate danger to human health. The tested LFP cells had higher emission factors of particles and HF than the LCO cells.

Keywords: Li-ion battery; fire; smoke; particulate matter; thermal runaway; ultrafine particles; HF; $PM_{2.5}$; emission factor; particle size distribution

Citation: Claassen, M.; Bingham, B.; Chow, J.C.; Watson, J.G.; Chu, P.; Wang, Y.; Wang, X. Characterization of Lithium-Ion Battery Fire Emissions—Part 2: Particle Size Distributions and Emission Factors. *Batteries* **2024**, *10*, 366. https://doi.org/10.3390/batteries10100366

Academic Editor: Wojciech Mrozik

Received: 24 August 2024
Revised: 17 September 2024
Accepted: 15 October 2024
Published: 16 October 2024

1. Introduction

Lithium-ion batteries (LIB) can generate significant gaseous and particulate emissions when they experience thermal failure, through venting, thermal runaway (TR), fire, and explosion [1,2]. The detailed characterization of particle size distribution (PSD), chemical composition, emission factor, temporal evolution, and thermal stability is important for LIB safety, including understanding the health effects of inhaled smoke particles, proper personal protection, the mechanisms of fire origination and propagation, fire detection and suppression, post-fire cleanup, and material recycling. For example, recent studies of soot particles from LIB fires show higher toxicity to human cells than wood smoke [3,4]. However, as shown in a recent review [2], few studies have examined particle emissions from LIB fires.

Size distribution is an important parameter that describes the transport behavior, atmospheric residence time, and inhalation risk of particles. LIB TR generates a wide range of particle sizes, varying from several nanometers to several millimeters. Most previous studies have focused on larger particles that settled in the combustion chamber after experiments. Zhang et al. [5] collected particles after burning a nickel manganese cobalt (NMC) LIB cell and separated them by sieving into four size fractions. The mass percentages were

44% for 0–0.85 mm, 36% for 0.85–1.70 mm, 9% for 1.70–2.00 mm, and 11% for 2.00–8.00 mm. Laser diffraction particle sizing showed that the volume distribution had a median diameter of 198 μm for the 0–0.85 mm size fraction. Several other studies focusing on larger particles also showed volume distribution median diameters >100 μm [6–8]. Due to their high temperature and large thermal mass, the larger sparking particles may contribute to igniting flammable gases and TR propagation [9]. As they dominate the emitted particle mass, the chemical composition of these larger particles provides useful information about particle origin and TR reactions [5,8,10]. When released into the environment, they may cause air, water, and soil contamination [11–13]. However, these particles represent a low inhalation risk to humans as their large size causes them to settle quickly by gravity and makes them unlikely to be inhaled while suspended in air [14].

Particles with aerodynamic diameters less than 10 μm (PM_{10}), 2.5 μm ($PM_{2.5}$), and even smaller (e.g., ultrafine particles with diameters <100 nm [$PM_{0.1}$]) can remain suspended in air for longer than larger particles. When inhaled, they will deposit at different locations in the human respiratory track depending on the particle size, causing respiratory, cardiovascular, and other diseases [15]. Very few studies have measured PM_{10} size distributions from LIB fires. Premnath et al. [16] used an Engine Exhaust Particle Sizer (EEPS) [17,18] to measure particle number concentrations in the size range of 5.6–560 nm in real time from lithium iron phosphate (LFP) and NMC cells undergoing TR. The geometric number mean diameters (GNMD) of the PSDs [19] ranged from 54 to 69 nm with either monomodal or bimodal distributions. The emission rate varied from 1.6×10^{15} to 2.1×10^{17} particles/hour, 5–6 orders of magnitude higher than modern heavy-duty diesel engines. While the tests evaluated the effects of the TR triggering mechanism (nail penetration vs. overcharging) and LIB chemistry (LFP vs. NMC), the number of tests were small, and the influence of the cell's state of charge (SOC) was not examined. Goupil et al. [20] measured PSDs from an NMC cell fire using a scanning mobility particle sizer (SMPS; 17.5–532.8 nm) and an optical particle spectrometer (250 nm–32 μm). The number distributions were bimodal, with one peak below 50 nm and one centered around 125 nm, while the mass distribution had a peak around 10 μm. The slow SMPS scan time (76 s) may cause inaccuracy in the PSD, and the conversion from optical to aerodynamic diameter is affected by the particle's optical properties, morphology, and density [21,22]. Several other studies have estimated PSDs from image analysis [2,11]. However, this method is prone to multiple artifacts, such as particle loss during collection and sample preparation, a compromise between field of view and size resolution, and potential overlaps between particles [23].

Emission factors (EFs) are commonly used in air quality management to estimate pollutant emissions based on emission activities [24]. Because the total emission amount depends on LIB SOCs and the number of LIBs burned, the proper activity metric for estimating LIB fire emissions is the total energy capacity of the LIB cells burned [25]. Therefore, the particle number EFs are expressed in particles/Wh (watt–hours), and the size-segregated PM mass and $PM_{2.5}$ constituent EFs are expressed in mg/Wh. EFs in these units are easier to use for estimating the total emissions than the emission rates in particles/hour reported by Premnath et al. [16]. To our knowledge, no studies have reported EFs of LIB fire particle chemical constituents.

In companion with the particle chemical characteristics presented by Claassen et al. [26], the objectives of this paper are to: (1) characterize the size distribution of particles in the diameter range of 6 nm–10 μm; (2) quantify the EFs of particle number, particle mass, and $PM_{2.5}$ constituents emitted from LIB combustion; and (3) evaluate the dependence of PSDs and EFs on cell type and SOC.

2. Materials and Methods

The experiments and data analysis have been described in the companion paper [26] and only a brief description is provided here. Two commonly used LIB types were tested: a cylindrical, 18650-style, LFP cell and a pouch-style lithium cobalt oxide (LCO) cell [27,28]. Each cell type was tested at five SOC levels with three to six tests per SOC. The cells used

for these tests were purchased shortly before the experimental campaign and were received at proper storage voltages. It was found that the LFP cells only vented at 0% and 30% SOCs, flamed at 50% and 75% SOCs, and had either venting or flaming at 100% SOCs. In contrast, LCO tests flamed at all SOCs [26]. While these two cell types will be referred to by their cell chemistry (LFP vs. LCO), they also differ in form-factor and casing, both of which can affect emissions. However, this study did not attempt to isolate the effects of these factors. The LIB combustion tests were conducted inside an ~8 m^3 burn chamber [29]. The exhaust flow rate (Q) was set to ~3300 L/min, as determined by thermal anemometer measurements in the exhaust duct [30]. Before each test, the chosen LIB cell was charged to the desired SOC by a programable charger. The cell was then placed in a ceramic crucible and heated to failure by an electric hot plate. A type K thermocouple was used to measure external cell and flame temperatures.

A sample of LIB combustion emissions was extracted from the chamber exhaust vent and directed to a suite of particle analyzers and the filter sampling system. Real-time particle mass concentrations were measured by two DustTrak DRX (TSI Inc., Shoreview, MN, USA) aerosol monitors in five size fractions (i.e., PM_1, $PM_{2.5}$, PM_4, PM_{10}, and PM_{15}) [21,22]. The DustTraks were placed before and after sample line dilution to determine the dilution factors.

Finer resolution PSDs in the range of 6 nm–10 µm were measured every second by an electrical low-pressure impactor (ELPI+; Dekati Ltd., Kangasala, Finland) [31–34] which was placed on a diluted sample line to prevent impactor overloading. In an ELPI+, particles are first introduced into a unipolar diffusion charger to achieve a stable charge distribution, and then are collected on 13 stages of electrically conducting cascade impactors and a final filter, depending on their aerodynamic diameters. The electrical charges carried by the deposited particles are measured as current by sensitive electrometers. An inversion algorithm is used to convert the 14-channel electric current data to particle number distributions with up to 500 bins. In this study, the particle number distributions were converted to mass distributions by assuming spherical particle shape and a density of 1 g/cm^3. The high-resolution data were integrated over the size fractions of <0.1 µm ($PM_{0.1}$), 0.1–1 µm ($PM_{0.1–1}$), 1–2.5 µm ($PM_{1–2.5}$), and 2.5–10 µm ($PM_{2.5–10}$). There are multiple potential artifacts (e.g., deposition of smaller particles at upper stages, size-dependent particle density, and image current) that could lead to errors in the mass concentration calculation [35]. Therefore, the ELPI $PM_{2.5}$ mass was normalized by gravimetric $PM_{2.5}$ mass to account for these artifacts.

Two filter channels were used to collect $PM_{2.5}$ and acidic gases for analysis of mass by gravimetry, ions and acidic gases by ion chromatography (IC), organic and elemental carbon (OC and EC) by thermal/optical analysis, and elements by x-ray fluorescence (XRF) and inductively coupled plasma mass spectrometry (ICP-MS) [24,36]. The backup potassium hydroxide (KOH)-impregnated cellulose-fiber filters behind the Teflon-membrane front filters were analyzed for acidic gases, including hydrogen fluoride (HF), hydrochloric acid (HCl), nitric acid (HNO_3), and sulfuric acid (H_2SO_4) as their corresponding ions (i.e., F^-, Cl^-, NO_3^-, and SO_4^{2-}) by IC [37,38].

Emission factors (EF_i in particles/Wh for particle number and mg/Wh for mass) were calculated for each species i by Equation (1):

$$EF_i = C_i \times Q \times \Delta t / E \quad (1)$$

where C_i (in particles/m^3 for number and mg/m^3 for mass) is the mean stack concentration for species i, Q (in m^3/s) is the mean stack exhaust flow rate, Δt (in s) is the sampling duration, and E (in Wh) is the nominal LIB cell energy capacity.

3. Results

3.1. Particle Size Distributions

Figure 1 shows the heat maps of PSD evolution for the representative tests for each cell type and SOC. The y-axis represents particle aerodynamic diameter (D_p), and the coloring

represents particle number concentration normalized by the size bin width (dlog (D_p)). While most particles had diameters below 500 nm, significant variations in PSD evolution were seen. Low SOC (0 and 30%) LFP tests in this study, which had no flaming combustion, emitted high concentrations of particles over a wide size range, but concentrations never exceeded 10^7 particles/cm^3. These emissions occurred for a long period of time, with maximum concentrations above 10^5 particles/cm^3 for over 30 min for both low SOCs.

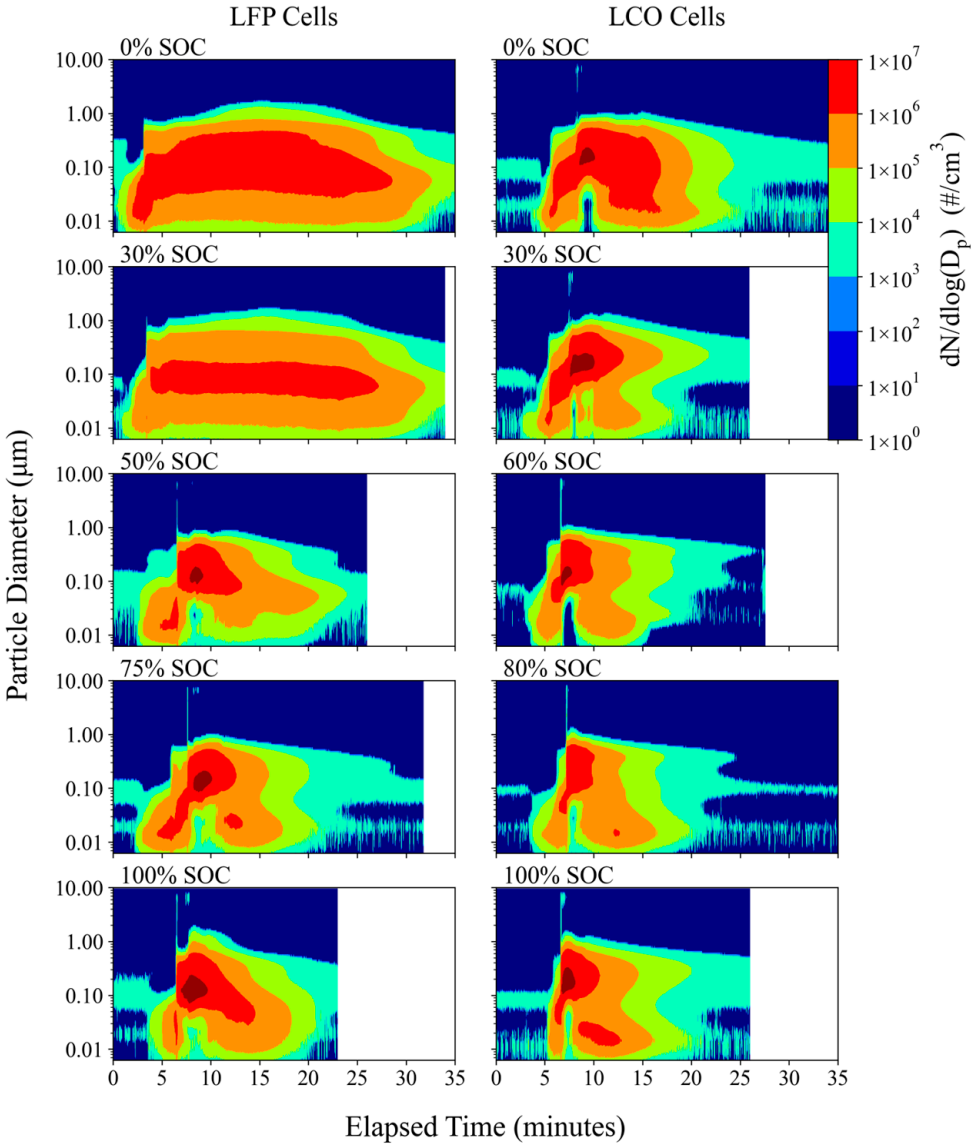

Figure 1. Particle number distribution heatmaps for representative LFP and LCO tests at each SOC.

Particle emissions for other LFP SOCs and LCO tests reached peak concentrations above 10^7 particles/cm^3, but concentrations above 10^5 particles/cm^3 only lasted for 10–18 min. A PSD discontinuity is seen in Figure 1 for these tests, occurring between five and ten minutes of elapsed time and representing abrupt concentration increases and particle size changes. This event coincided with visual and temperature-based TR indicators, suggesting it was caused by the onset of TR. A short 5–10 s long emission of coarse particles (up to 10 µm) can be seen to occur simultaneously, likely corresponding to the ejection of spark particles. Maximum particle concentrations occurred just after TR began. This is where most of the particle mass was emitted as particle sizes peaked here as well, with a notable decrease in particles below 50 nm in diameter. After this, peak

concentrations and particle sizes decreased gradually, often forming a bimodal pattern of nanoparticles (<100 nm) and larger particles between 100 nm and 1 µm.

Figures 2 and 3 show individual PSD "snapshots" for a 0% SOC LFP test and a 60% SOC LCO test, each at four time intervals. The 0% SOC LFP test only vented, without flaming combustion, while the 60% LCO test flamed vigorously. A detailed discussion of the observed combustion behavior for all tests can be found in [26]. The intervals include background concentrations (t_1), when the test cell is outgassing (t_2), after TR (t_3), and after combustion is complete and the test cell is smoldering (t_4). These time intervals were selected to represent similar combustion stages despite the differences in combustion duration between tests. The GNMDs and geometric number standard deviations (GNSD) were calculated to characterize the PSD at each time interval [19].

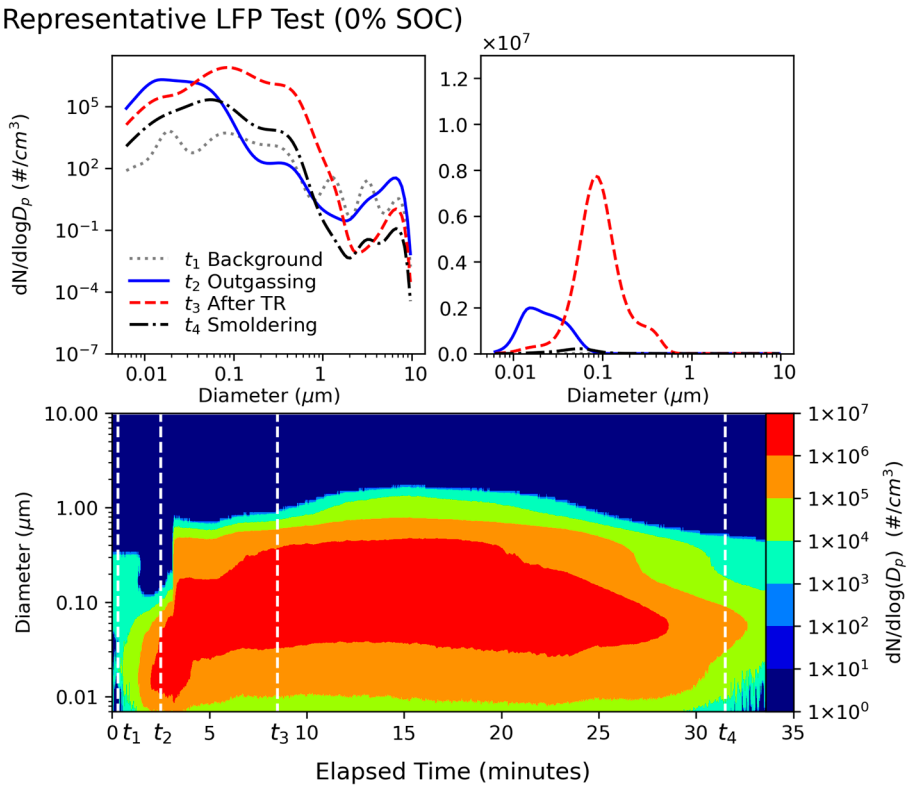

Figure 2. Particle number distribution snapshots (**left**: log scale and **right**: linear scale) and heatmap (**bottom**) for a representative 0% SOC LFP test. GNMDs for $t_{1–4}$ are 59 nm, 22 nm, 91 nm, and 49 nm, respectively.

The 0% SOC LFP "venting" test and the 60% SOC LCO "flaming" test had similar peak outgassing (t_2) concentrations at ~2×10^6 particles/cm^3 but the particle diameters were smaller for the venting test, with a GNMD of 22 nm and a GNSD of 1.7. The flaming outgassing concentrations peaked at 59 nm with a GNSD of 1.9. While different cell types are compared here, the intent is to contrast the PSD differences due to the varied combustion behavior of the tests, not to infer differences due to the cell type itself. Concentrations after TR (t_3) peaked at four and six times the outgassing concentration for the venting and flaming tests, respectively, with the flaming test PSD being generally larger-sized and narrower. GNMDs at this time were 91 nm and 195 nm for the venting and flaming tests, with GNSDs of 1.9 and 1.6, respectively.

Figure 4a,b show the evolution of PM_1, $PM_{2.5}$, and PM_{10} for the tests shown in Figures 2 and 3, respectively. PM_1 accounted for most of the emission mass. Large spikes of PM_{10} were observed at the onset of TR, corresponding to the emission of coarse particles ($PM_{2.5–10}$), as was discussed for Figure 1. Interestingly, small spikes of coarse particles also occurred just before TR and before $PM_{2.5}$ emissions began. This behavior may be

useful for early TR detection by LIB pack monitoring systems. The venting test (Figure 4a) shows $PM_{2.5}$ mass concentrations rising above PM_1 starting when emissions peaked around 15 min of elapsed time and lasting until combustion ended. This behavior occurred for all venting-only tests (LFP tests with 0% and 30% SOCs as well as half of the 100% SOC tests [26]). For tests where flaming occurred, PM_1 dominated PM mass emissions outside of TR onset.

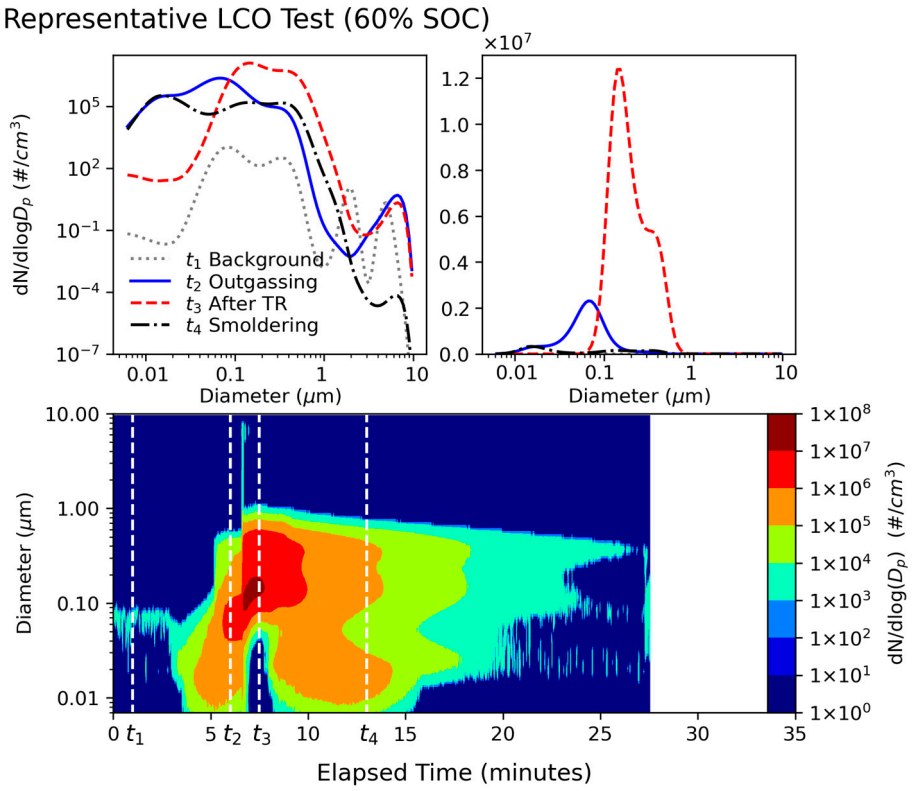

Figure 3. Particle number distribution snapshots (**left**: log scale and **right**: linear scale) and heatmap (**bottom**) for a representative 60% SOC LCO test. GNMDs for $t_{1–4}$ are 117 nm, 59 nm, 195 nm, and 52 nm, respectively.

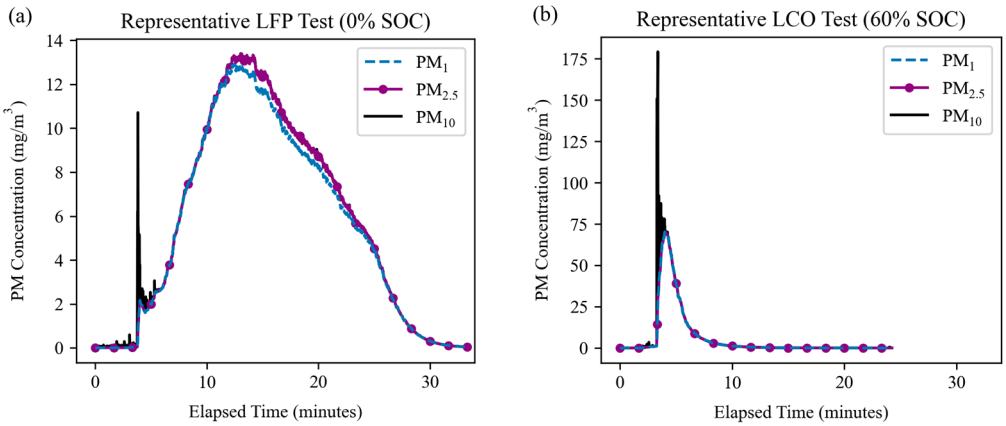

Figure 4. Mass concentrations of PM_1, $PM_{2.5}$, and PM_{10} for the representative tests: (**a**) LFP at 0% SOC and (**b**) LCO at 60% SOC (same as those in Figures 2 and 3). The coarse particles ($PM_{2.5–10}$) are released predominantly during TR.

Figure 5 shows the average number-based (a and b) and mass-based (c and d) PSDs for each SOC and cell type. The number distributions show a dominant mode centered around 70–140 nm, with additional modes centered around 20 nm and 300 nm. These

distributions are similar to those reported by Goupil et al. [20]. For LFP tests, particles were smaller and were released in lower concentrations at low SOCs, increasing in size and concentration at mid-SOCs. Tests with 100% SOC fell in the middle due to having disparate combustion behavior. This is consistent with the combustion behavior of LFP tests: they only vented at 0% and 30% SOCs, intensely flamed at 50% and 75% SOCs, and had more variable combustion at 100% SOCs [26]. Particle sizes also increased with SOC for LCO tests, but there was no consistent dependence of concentrations on SOC, likely because flaming combustion was observed at all SOCs. The mass distributions show that LFP tests with 0% and 30% SOCs only have one mode centered around 460 nm, with elevated concentrations between 1 and 2.5 µm. All other tests had bimodal distributions, with one fine-particle mode centered around 400 nm and a coarse-particle mode centered around 8 µm. This indicates that the coarse particles were generated from flaming rather than cell venting. The coarse particle mode mass increased with SOC for both cell types, being insignificant for low SOC LFP tests. The fine particle mode mass also increased with SOC for LFP tests as the PSD shifted to larger particle sizes. A coarse mode centered around 10 µm was also observed by Goupil et al. [20].

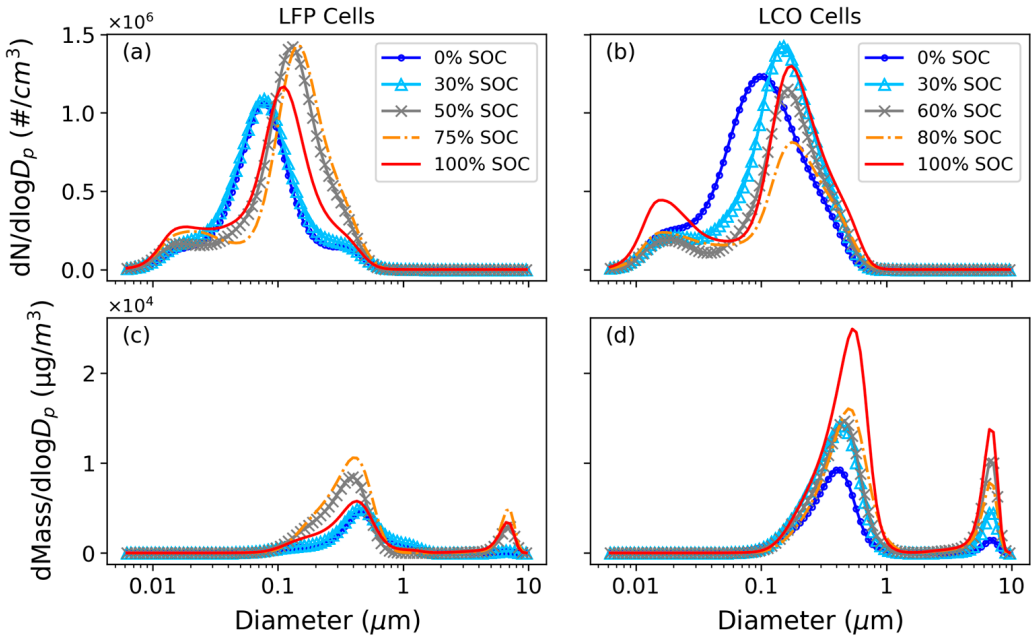

Figure 5. Particle number (top panels) and mass (bottom panels) distributions for LFP (**a**,**c**) and LCO (**b**,**d**) tests. An outlier was removed from some SOC groups to better show the prevailing trends.

Table 1 shows the GNMD and geometric mass mean diameters (GMMD) [19] for each cell type and SOC. The GNMD varied from 74 to 114 nm for LFP tests and 90 to 130 nm for LCO tests, showing that particles from LCO tests tended to be larger. GMMDs were larger than GNMDs due to mass being proportional to the cube of particle diameter. Interestingly, GNMDs peaked at mid-range SOCs while GMMDs increased with SOC, peaking at 100%. This increase at high SOCs, along with the previously discussed emission of large particles at TR, confirms that $PM_{2.5–10}$ is generated by the energetic combustion and ejection of material that occurs in a highly charged LIB cell during TR. Premnath et al. [16] found that GNMD and GMMD ranges were 54–69 nm and 97–204 nm for LFP and NMC cells, respectively, at 100% SOCs. These diameters are smaller than those in Table 1, especially for GMMD, which is likely caused by the lower upper size limit of the EEPS (560 nm) [17,18] than the ELPI+ (10 µm).

Table 1. Average and range (in parentheses) of geometric number mean diameters (GNMD) and geometric mass mean diameters (GMMD) for each SOC and cell type.

Cell Type	SOC (%)	GNMD (nm)	GMMD (nm)
LFP	0	74 (72–77)	415 (409–424)
	30	74 (72–77)	426 (403–453)
	50	110 (109–111)	425 (415–435)
	75	114 (106–129)	479 (434–530)
	100	84 (71–93)	568 (536–611)
LCO	0	90 (78–102)	387 (371–405)
	30	120 (111–137)	474 (470–477)
	60	130 (128–132)	663 (553–751)
	80	118 (109–128)	673 (651–704)
	100	116 (96–129)	668 (602–778)

3.2. Emission Factors (EFs)

EFs for particle number, mass, $PM_{2.5}$ constituents, and acidic gases are listed in Tables S1–S5. The following sections describe EFs for particle numbers, mass, carbon, PO_4^{3-}, selected metals and ions, and acidic gases, as well as the relationship between EF and combustion temperature.

3.2.1. EFs for Particle Number and Mass

Figure 6a shows particle number EFs by cell SOC for each size fraction. The EFs for ultrafine particles ($PM_{0.1}$) ranged between 1.5×10^{13} and 3.6×10^{13} particles/Wh for LFP tests and 3.2×10^{12} and 9.6×10^{12} particles/Wh for LCO tests (Table S1). Total particle numbers decreased with SOC, and LFP tests released several times more particles than LCO tests. $PM_{0.1}$ and $PM_{0.1–1}$ together accounted for >99.9% of PM_{10} numbers, at 42–84% and 16–58% of PM_{10}, respectively. Particles larger than 1 µm had negligible contributions to particle number. $PM_{0.1}$ tended to make up a higher proportion of PM_{10} when particle emissions were high. On the other hand, Figure 6b shows $PM_{0.1}$ made up a much smaller proportion of the PM_{10} mass due to having very small particle volumes, at 1–8%, while $PM_{0.1–1}$ dominated the PM_{10} mass at 77–89% due to their high concentrations. PM_1 particles made up 81–95% of the measured PM_{10} mass, as also shown in Figure 4. Larger particles made up significant portions of PM_{10} mass despite their low number concentrations, with $PM_{1–2.5}$ and $PM_{2.5–10}$ accounting for up to 4% and 18% of PM_{10} mass, respectively. $PM_{1–2.5}$ EFs were high for low SOC LFP tests and venting-only 100% SOC LFP tests while all other tests had higher $PM_{2.5–10}$ EFs instead.

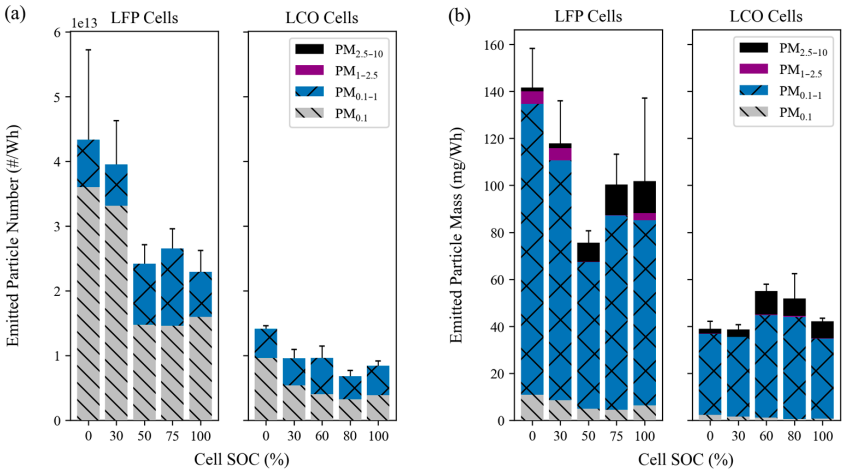

Figure 6. Emission factors for (**a**) particle number and (**b**) particle mass by size fraction for LFP and LCO tests. Error bars represent the total PM_{10} standard error (including all smaller particle sizes) and are symmetric.

3.2.2. EFs for $PM_{2.5}$, OC, EC, PO_4^{3-}, and Toxic Metals

EFs for $PM_{2.5}$, OC, EC, and PO_4^{3-} are shown in Figure 7a. EFs for $PM_{2.5}$ mass were between 35 and 140 mg/Wh. This equates to the emission of 1.4–5.6 g of $PM_{2.5}$ from the combustion of a standard laptop-sized LIB (40 Wh), or 2.1–8.4 kg of $PM_{2.5}$ from the combustion of an electric vehicle battery pack (60 kWh) if all cells are burned in a similar way as those in this study.

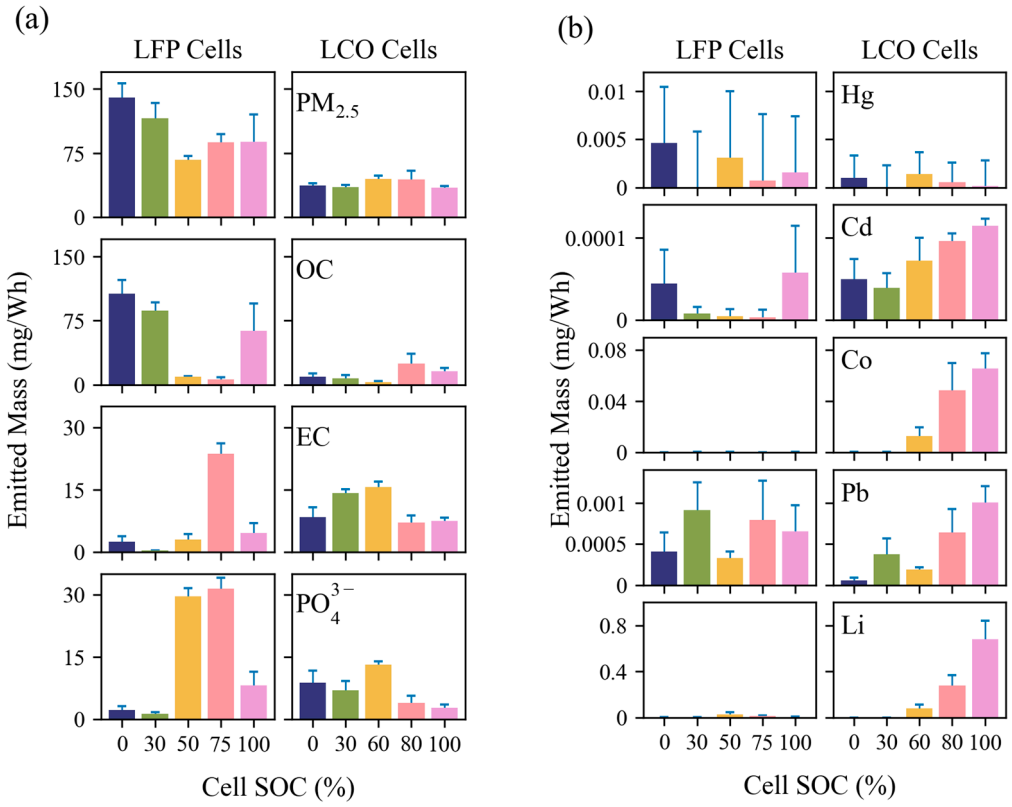

Figure 7. Emission factors for (**a**) $PM_{2.5}$ mass, OC, EC, and PO_4^{3-} and (**b**) selected metals. The error bars represent the larger of the propagated analytical uncertainty or the standard error within each SOC and are symmetric.

LFP tests had $PM_{2.5}$ EFs of 67–140 mg/Wh, with the least mass emitted at 50% SOC and increased variability at 100% SOC. OC EFs were 6–9 mg/Wh for 50–75% SOC and increased to 63–106 mg/Wh otherwise. OC variabilities at 100% SOC were similarly high to $PM_{2.5}$. Low OC emissions at mid-range SOCs corresponded to high EC emissions for 75% SOC only, where EC EFs spiked from <5 mg/Wh for all other SOCs to 24 mg/Wh. This resulted in total carbon EFs dropping from 109 mg/Wh (0% SOC) to 12 mg/Wh (50% SOC), before increasing back to 68 mg/Wh (100% SOC). PO_4^{3-} emissions were also significant for mid-range SOCs, at approximately 30 mg/Wh, but only 1–8 mg/Wh otherwise.

LCO tests had more consistent $PM_{2.5}$ mass EFs of 35–45 mg/Wh, lower than LFP tests by 1.5–3.8 times. EFs for OC, EC, and PO_4^{3-} had much less dependence on SOC for LCO tests than LFP tests. OC EFs were 3–24 mg/Wh and peaked at 75% SOC, where LFP OC was lowest. EC EFs were 7–16 mg/Wh, higher than those of LFP tests except for at 75%/80% SOC. PO_4^{3-} EFs were 3–13 mg/Wh with a similar SOC dependance to EC.

Figure 7b shows EFs for four hazardous air pollutant metals [39] and Li. Variability within SOCs was high but several features are notable. LCO tests had Cd, Co, Pb, and Li emissions that increase with SOC, reaching $(10 \pm 1) \times 10^{-5}$ mg/Wh for Cd, 0.07 ± 0.01 mg/Wh for Co, $(10 \pm 2) \times 10^{-4}$ mg/Wh for Pb, and 0.7 ± 0.2 mg/Wh for Li, all at 100% SOC. All of these elements were near detection limits at low SOCs except for Cd. Only Pb was consistently present for LFP tests at between $(30 \pm 8) \times 10^{-5}$ mg/Wh

and $(9 \pm 3) \times 10^{-4}$ mg/Wh, with no dependence on SOC. Hg and Cd were detected sporadically. EFs for major compositions and elements are summarized in Tables S2 and S5, respectively.

3.2.3. EFs for Anions and Acidic Gases

EFs for acidic gases HF, HCl, HNO_3, and H_2SO_4 and their corresponding particulate anions are shown in Figure 8. These acidic gases are toxic and corrosive and can cause adverse effects on human health and material integrity if not neutralized after emission.

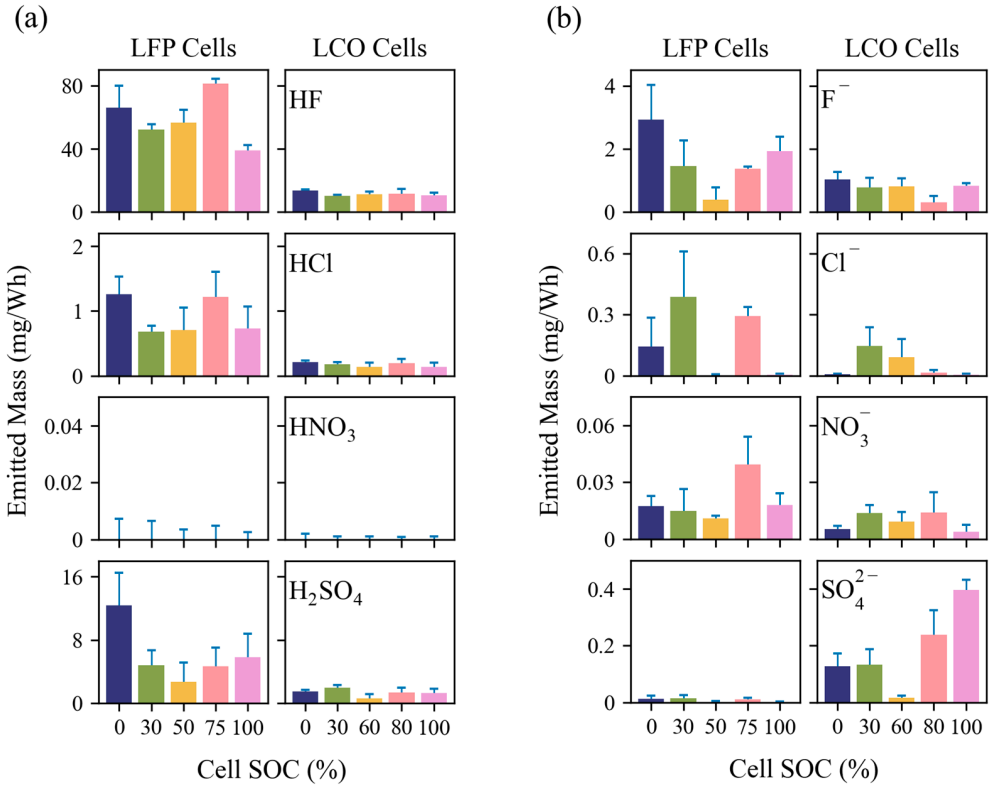

Figure 8. Emission factors for (**a**) selected acidic gases and (**b**) corresponding particulate anions. The error bars represent the larger of the propagated analytical uncertainty or the standard error within each SOC and are symmetric.

Gaseous EFs were higher than that of particulate emissions (by cell type) for all compounds shown except for NO_3^-, where HNO_3 emission was not detected. Gaseous HF and particulate F^- had the highest EFs for all LIB types and SOCs. Gaseous HF EFs ranged from 39 to 81 mg/Wh for LFP tests and 10 to 14 mg/Wh for LCO tests. Neither cell type showed a relationship between SOC and HF emissions. Particulate F^- EFs ranged from 0.4 to 3 mg/Wh for LFP tests and 0.3 to 1 mg/Wh for LCO tests. Particulate F^- had a distinct minimum at 50% SOC for LFP tests, corresponding to the minimum $PM_{2.5}$ EF (Figure 7a). Gaseous H_2SO_4 was the second most emitted acidic compound, with much higher gaseous emissions than particulate. Gaseous EFs were 3–12 mg/Wh for LFP tests and 0.6–2 mg/Wh for LCO tests. Unlike gaseous H_2SO_4 and all other acidic emissions shown, particulate SO_4^{2-} emissions were much higher for LCO tests than LFP tests, where only trace concentrations were detected. LCO tests had EFs of 0.1–0.4 mg/Wh for most SOCs, but only trace amounts for 60% SOC. Both gaseous and particulate emissions were low for 50/60% SOC, but this was more pronounced for LFP tests. Particle SO_4^{2-} emissions for LCO tests increased with SOC with the exception of 60% SOC. Gaseous HCl was consistently detected, averaging 0.9 mg/Wh for LFP tests and 0.2 mg/Wh for LCO tests. Particulate Cl^- was present sporadically for both cell types with EFs of up to 0.4 mg/Wh.

Only particulate NO_3^- was detected at between 0.005 and 0.04 mg/Wh, with higher emissions from LFP tests.

Table 2 compares the gaseous EFs of HF and HCl with the values reported in the literature. LFP HF emissions in this study (39–81 mg/Wh) compared well with the literature values which range at 12–350 mg/Wh. Emissions from LCO tests (10–14 mg/Wh) were lower than the 30–40 mg/Wh found in the literature, but this may be due to the limited number of studies [25,40]. Other cell types were reported to release a comparable 1–200 mg/Wh of HF. HCl emissions were reported by Diaz et al. [40] at 8–125 mg/Wh for LFP and LCO cells, significantly higher than those measured in this study (0.1–1.3 mg/Wh). No published EF values for HNO_3 or H_2SO_4 were found. Acidic gas and particulate ion EFs for all cell types and SOCs are listed in Tables S3 and S4, respectively.

Table 2. Comparison of gaseous emissions of HF and HCl to the literature sources, grouped by cell chemistry. EFs for HNO_3 and H_2SO_4 were not found in the literature.

Source	Cell Type	HF (mg/Wh)	HCl (mg/Wh)
This study	LFP	39–81	0.7–1.3
[40]	LFP	350	125
[25]	LFP	12–24	
[41]	LFP	40–125	
This study	LCO	10–14	0.14–0.21
[40]	LCO	30	8
[25]	LCO	30–40	
[42]	Unknown	20–200	
[43]	LMO	40–70	
[44]	NMC/LFP	23–36	
[45]	NMC	1–10	
[46]	NMC	4.2	

3.2.4. Relationship between Emission Factors and Combustion Temperatures

Figure 9 shows the relationship between the EF and the maximum measured combustion temperature for LFP tests. Cell SOC is also labeled by symbol coloring to show groupings. With the exception of two outlier tests (Tests C1 and C8 in Figure 9a,b), EFs for $PM_{2.5}$ and OC were found to decrease with increasing combustion temperature. This is expected as higher temperatures indicate more complete combustion that will release more gaseous CO_2 instead of carbonaceous particulate. In contrast, PO_4^{3-} increased with combustion temperatures, indicating more efficient conversion of P-containing electrolyte and cathode materials to particle emissions. Low EC emissions were found at lower combustion temperatures as expected; however, EC was not necessarily higher at high temperatures. Figure 9c shows that the 50% SOC tests had temperatures >600 °C but the EC emissions were comparable to those of low temperature tests. Particulate F^- and gaseous HF (Figure 9e,h) had the opposite trend, with F^- decreasing (for SOCs > 30%) and HF increasing with increasing temperature. This is possibly due to more HF remaining in the gas phase at higher temperatures rather than condensing to form particles. Li^+ emissions were hardly detected below 600 °C and increased rapidly thereafter, indicating a potential exponential relationship. More tests with temperatures reaching >700 °C are needed to explore this. Figure 9g shows that the part of $PM_{2.5}$ mass with unidentified composition increased with temperature, a correlation that could help determine what additional components (e.g., unmeasured phosphorous compounds) [26] need to be analyzed for.

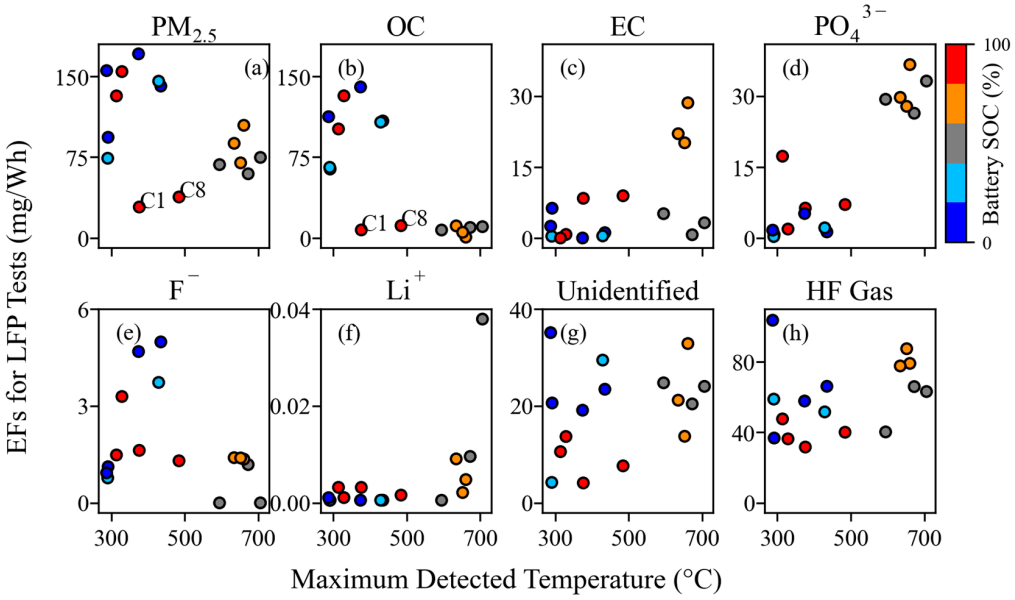

Figure 9. Relationship between EFs and maximum detected combustion temperature for LFP tests. LCO tests showed little correlation, possibly due to poor temperature measurement, and are not shown.

3.3. Cell Mass Losses

Each cell was weighed before and after combustion to determine the cell mass that was lost. LFP cells lost 2.2–2.4 g/Wh during combustion for all except 50% SOC, which lost noticeably less at 1.8–2 g/Wh. LCO cells lost roughly half the mass per Wh of cell capacity at 0.95–1.2 g/Wh. As shown in Table S6, this equates to a loss of ~20% of the cell mass for both cell types. However, only approximately 0.6–1.2% of the total cell mass, or 3–6% of the lost cell mass, was emitted as $PM_{2.5}$ that reached the filter assemblies. The proportion of lost cell mass that was emitted as $PM_{2.5}$ was highest for low SOC LFP tests, where 5–6% was converted to $PM_{2.5}$. All other SOC groups averaged 3–4%. By subtraction, this means that 94–97% of the lost mass, or roughly 16–22% of total cell mass, was emitted as either settleable PM or as gas emissions. As shown in Table S6, cell mass losses from previous studies range from 15% to 60%, with settleable particle mass accounting for 5–50% of the original cell mass, depending on the cell chemistry, casing, and SOCs [5,6,10,47]. Even though $PM_{2.5}$ only accounted for a small fraction of the total PM mass emitted from LIB fires, it accounts for most of the particle numbers that can be inhaled by humans and presents great health risks.

4. Discussion and Conclusions

This study conducted a detailed characterization of the size distribution of particles with diameter less than 10 μm emitted from LIB fires and determined EFs for size-segregated particle number, particle mass, and $PM_{2.5}$ chemical constituents. The analysis covered two cell types at a range of SOCs. While emissions may vary significantly depending on the specific cell types or LIB pack sizes, the cells tested represent two common cell chemistries and form-factors, in terms of both cell construction and energy capacity, that are used widely in modern LIB applications. As such, the findings offer valuable insights into the characteristics of emission from LIB combustion. The key conclusions are as follows:

(1) LIB fires emit high concentrations of fine and ultrafine particles. The particle number distributions showed a dominant mode centered around 100 nm, with additional modes centered around 20 nm and 300 nm. The particle mass distributions showed that the venting-only LFP tests in this study with 0% and 30% SOCs had one mode centered around 460 nm, while all other tests had bimodal distributions, with one fine particle mode centered around 400 nm and a coarse particle mode centered

around 8 μm. $PM_{0.1}$ and $PM_{0.1–1}$ together accounted for >99.9% of PM_{10} numbers, while $PM_{0.1–1}$ dominated the PM_{10} mass at 77–89%. Super-micron particles have non-negligible mass contributions, with $PM_{1–2.5}$ and $PM_{2.5–10}$ accounting for up to 4% and 18% of PM_{10} mass, respectively. $PM_{1–2.5}$ was emitted during cell venting, after TR and when flaming did not occur, while $PM_{2.5–10}$ was emitted just before and during TR onset for all tests.

(2) Venting-only combustion (LFP tests at 0% SOC, 30% SOC, and some at 100% SOC) showed smooth evolution of PSDs, while the onset of TR caused a discontinuity in particle size distribution by increasing both mode diameter and concentration and releasing coarse mode particles (1–10 μm). Particles from LCO tests in this study (GNMD 90–130 nm; GMMD 387–673 nm) were generally larger than those from LFP tests (GNMD 74–114 nm; GMMD 415–568 nm). The GMMD increased with SOC.

(3) LFP tests had higher EFs for particle number and mass than LCO tests. The EFs for ultrafine particles ($PM_{0.1}$) ranged from 1.5×10^{13} to 3.6×10^{13} particles/Wh for LFP and 3.2×10^{12} to 9.6×10^{12} particles/Wh for LCO tests. LFP tests had $PM_{2.5}$ EFs between 67 and 140 mg/Wh with more variability at different SOCs, whereas LCO tests had lower and more consistent $PM_{2.5}$ mass EFs between 35 and 45 mg/Wh. Even though $PM_{2.5}$ only accounted for 0.25–1.5% of the total cell mass and a small fraction of total PM mass emitted from LIB fires, it accounts for the most particle numbers that can be inhaled by humans and presents great health risks.

(4) LIB fires emit acidic gases, such as HF, HCl, and H_2SO_4. Gaseous HF ranged from 39 to 81 mg/Wh for LFP tests and 10 to 14 mg/Wh for LCO tests. These toxic and corrosive gases may represent great hazards to people and properties.

(5) Emissions are highly dependent on cell type, SOC, and combustion temperatures. The emitted $PM_{2.5}$ mass can depend on cell SOC by a factor of two, while the emitted OC, EC, and PO_4^{3-} can differ by a factor of 10 or more. PO_4^{3-} increased with combustion temperature, particularly when it reached >500 °C. Toxic metal emissions increased with SOC, but only for LCO tests, with no trend for LFP tests. Acidic gas emissions depended primarily on cell type, indicating that cell design is crucial to lowering emissions of HF and other corrosive compounds. The emission dependence on LIB cell properties should be considered when evaluating the overall hazard that each LIB pack presents. For example, while LFP cells are known to be more thermally stable, results from this study show that they may release more HF and can generate higher particulate concentrations than LCO cells.

The emissions documented here have implications for health and safety as well as environmental contamination. Considering that modern LIB packs can contain hundreds to millions of Wh of energy capacity, the effects of significant emissions of volatile organics, ultrafine and fine particles, hazardous metals, and acidic compounds must be taken into consideration when responding to and cleaning up after LIB fires.

LIB fires are becoming more common as LIB use expands. The combustion process can occur quickly and without warning, limiting the effectiveness of fire suppression. Therefore, a detailed understanding of the resulting emissions is imperative to allow for effective fire response and cleanup. This paper has detailed the expected fine particulate emissions in a way that allows extrapolation to any size LIB pack if the burned LIB energy capacity is known. This resource will allow first responders, LIB manufacturers, and responsible authorities to plan for and respond to LIB fires.

Supplementary Materials: The following supporting information can be downloaded at: https://www.mdpi.com/article/10.3390/batteries10100366/s1, Table S1. EFs for four size fractions in particles/Wh and mg/Wh for particle number and particle mass, respectively; Table S2. EFs in mg/Wh for $PM_{2.5}$ chemical constituents; Table S3. EFs in mg/Wh for acidic gases for all cell types and SOCs; Table S4. EFs in mg/Wh for particulate anions and cations for all cell types and SOCs; Table S5. EFs in mg/Wh for elements for all cell types and SOCs; Table S6. A comparison of cell mass loss rates to the literature values [5,6,10,47].

Author Contributions: Conceptualization, X.W.; Methodology, M.C. and X.W.; Software, M.C.; Validation, M.C. and X.W.; Formal Analysis, M.C.; Investigation, M.C., B.B., and X.W.; Resources, X.W.; Data Curation, M.C.; Writing—Original Draft Preparation, M.C. and X.W.; Writing—Review and Editing, X.W., J.C.C., J.G.W., P.C., and Y.W.; Visualization, M.C.; Supervision, X.W. and Y.W.; Project Administration, X.W.; Funding Acquisition, X.W. All authors have read and agreed to the published version of the manuscript.

Funding: This research was funded by the U.S. National Aeronautics and Space Administration's Established Program to Stimulate Competitive Research, CAN Grant No. 80NSSC19M0152, and Nevada Space Grant No. 80NSSC20M0043 22–24.

Data Availability Statement: The raw data supporting the conclusions of this article will be made available by the authors on request. The calculated emission factors for all measured species are included in the Supplementary Materials.

Acknowledgments: The authors thank Hans Moosmüller for the use of the burn chamber where experiments were performed and DRI personnel for support and filter analysis.

Conflicts of Interest: The authors declare no conflicts of interest.

Abbreviations

Δt	sampling duration
C	concentration
Cd	cadmium
Cl^-	chloride
Co	cobalt
D_p	particle diameter
E	battery cell energy capacity
EC	elemental carbon
EEPS	engine exhaust particle sizer
EF	emission factor
ELPI	electrical low-pressure impactor
F^-	fluoride
GMMD	geometric mass mean diameter: mean diameter of a particle mass distribution in logarithmic scale
GNMD	geometric number mean diameter: mean diameter of a particle number distribution in logarithmic scale
GNSD	geometric number standard deviation: standard deviation of a particle number distribution in logarithmic scale
HCl	hydrochloric acid
Hg	mercury
HF	hydrofluoric acid
HNO_3	nitric acid
H_2SO_4	sulfuric acid
IC	ion chromatography
ICP-MS	inductively coupled plasma mass spectrometry
KOH	potassium hydroxide
LCO	lithium cobalt oxide
Li	lithium
Li^+	lithium ion
LIB	lithium-ion battery
LFP	lithium iron phosphate
NMC	nickel manganese cobalt
NO_3^-	nitrate
OC	organic carbon
P	phosphorus
Pb	lead
PM	particulate matter
PM_x	particles with aerodynamic diameters $\leq$x μm

PO_4^{3-}	phosphate
PSD	particle size distribution
Q	flow rate
SMPS	scanning mobility particle sizer
SO_4^{2-}	sulfate
SOC	state of charge
TR	thermal runaway
Wh	watt hours
XRF	X-ray fluorescence

References

1. Bugryniec, P.J.; Resendiz, E.G.; Nwophoke, S.M.; Khanna, S.; James, C.; Brown, S.F. Review of gas emissions from lithium-ion battery thermal runaway failure—Considering toxic and flammable compounds. *J. Energy Storage* **2024**, *87*, 111288. [CrossRef]
2. Li, W.; Xue, Y.; Feng, X.; Rao, S.; Zhang, T.; Gao, Z.; Guo, Y.; Zhou, H.; Zhao, H.; Song, Z.; et al. Characteristics of particle emissions from lithium-ion batteries during thermal runaway: A review. *J. Energy Storage* **2024**, *78*, 109980. [CrossRef]
3. Xu, Y.; Wang, Y.; Chen, X.; Pang, K.; Deng, B.; Han, Z.; Shao, J.; Qian, K.; Chen, D. Thermal runaway and soot production of lithium-ion batteries: Implications for safety and environmental concerns. *Appl. Therm. Eng.* **2024**, *248*, 123193. [CrossRef]
4. Xu, Y.; Wang, Y.; Chen, D. Soot formation and its hazards in battery thermal runaway. *J. Aerosol Sci.* **2024**, *181*, 106420. [CrossRef]
5. Zhang, Y.; Wang, H.; Li, W.; Li, C.; Ouyang, M. Size distribution and elemental composition of vent particles from abused prismatic Ni-rich automotive lithium-ion batteries. *J. Energy Storage* **2019**, *26*, 100991. [CrossRef]
6. Zhang, Y.; Wang, H.; Li, W.; Li, C. Quantitative identification of emissions from abused prismatic Ni-rich lithium-ion batteries. *eTransportation* **2019**, *2*, 100031. [CrossRef]
7. Wang, H.; Zhang, Y.; Li, W.; Li, C.; Ouyang, M. Particles released by abused prismatic Ni-rich automotive lithium-ion batteries. *WSEAS Trans. Syst. Control* **2020**, *15*, 30–38. [CrossRef]
8. Wang, H.; Wang, Q.; Jin, C.; Xu, C.; Zhao, Y.; Li, Y.; Zhong, C.; Feng, X. Detailed characterization of particle emissions due to thermal failure of batteries with different cathodes. *J. Hazard. Mater.* **2023**, *458*, 131646. [CrossRef]
9. Wang, G.; Kong, D.; Ping, P.; Wen, J.; He, X.; Zhao, H.; He, X.; Peng, R.; Zhang, Y.; Dai, X. Revealing particle venting of lithium-ion batteries during thermal runaway: A multi-scale model toward multiphase process. *eTransportation* **2023**, *16*, 100237. [CrossRef]
10. Essl, C.; Golubkov, A.W.; Gasser, E.; Nachtnebel, M.; Zankel, A.; Ewert, E.; Fuchs, A. Comprehensive Hazard Analysis of Failing Automotive Lithium-Ion Batteries in Overtemperature Experiments. *Batteries* **2020**, *6*, 30. [CrossRef]
11. Yang, Y.; Fang, D.; Maleki, A.; Kohzadi, S.; Liu, Y.; Chen, Y.; Liu, R.; Gao, G.; Zhi, J. Characterization of Thermal-Runaway Particles from Lithium Nickel Manganese Cobalt Oxide Batteries and Their Biotoxicity Analysis. *ACS Appl. Energy Mater.* **2021**, *4*, 10713–10720. [CrossRef]
12. Held, M.; Tuchschmid, M.; Zennegg, M.; Figi, R.; Schreiner, C.; Mellert, L.D.; Welte, U.; Kompatscher, M.; Hermann, M.; Nachef, L. Thermal runaway and fire of electric vehicle lithium-ion battery and contamination of infrastructure facility. *Renew. Sustain. Energy Rev.* **2022**, *165*, 112474. [CrossRef]
13. Bordes, A.; Papin, A.; Marlair, G.; Claude, T.; El-Masri, A.; Durussel, T.; Bertrand, J.-P.; Truchot, B.; Lecocq, A. Assessment of Run-Off Waters Resulting from Lithium-Ion Battery Fire-Fighting Operations. *Batteries* **2024**, *10*, 118. [CrossRef]
14. ICRP. Human Respiratory Tract Model for Radiological Protection. ICRP Publication 66. Ann. ICRP 24 (1-3). 1994. Available online: https://www.icrp.org/publication.asp?id=icrp%20publication%2066 (accessed on 2 July 2024).
15. Thangavel, P.; Park, D.; Lee, Y.C. Recent Insights into Particulate Matter (PM(2.5))-Mediated Toxicity in Humans: An Overview. *Int. J. Env. Res. Public Health* **2022**, *19*, 7511. [CrossRef] [PubMed]
16. Premnath, V.; Wang, Y.; Wright, N.; Khalek, I.; Uribe, S. Detailed characterization of particle emissions from battery fires. *Aerosol Sci. Technol.* **2022**, *56*, 337–354. [CrossRef]
17. Wang, X.L.; Grose, M.A.; Avenido, A.; Stolzenburg, M.R.; Caldow, R.; Osmondson, B.L.; Chow, J.C.; Watson, J.G. Improvement of Engine Exhaust Particle Sizer (EEPS) size distribution measurement—I. Algorithm and applications to compact-shape particles. *J. Aerosol Sci.* **2016**, *92*, 95–108. [CrossRef]
18. Wang, X.L.; Grose, M.A.; Caldow, R.; Osmondson, B.L.; Swanson, J.J.; Chow, J.C.; Watson, J.G.; Kittelson, D.B.; Li, Y.; Xue, J.; et al. Improvement of Engine Exhaust Particle Sizer (EEPS) size distribution measurement—II. Engine exhaust particles. *J. Aerosol Sci.* **2016**, *92*, 83–94. [CrossRef]
19. Hinds, W.C. *Aerosol Technology, Properties, Behavior, and Measurement of Airborne Particles*, 2nd ed.; Wiley: Los Angeles, CA, USA, 1999.
20. Goupil, V.; Gaya, C.; Boisard, A.; Robert, E. Effect of the heating rate on the degassing and combustion of cylindrical Li-Ion cells. *Fire Saf. J.* **2022**, *133*, 103648. [CrossRef]
21. Wang, X.L.; Chancellor, G.; Evenstad, J.; Farnsworth, J.E.; Hase, A.; Olson, G.M.; Sreenath, A.; Agarwal, J.K. A Novel Optical Instrument for Estimating Size Segregated Aerosol Mass Concentration in Real Time. *Aerosol Sci. Technol.* **2009**, *43*, 939–950. [CrossRef]

22. Wang, X.L.; Zhou, H.; Arnott, W.P.; Meyer, M.E.; Taylor, S.; Firouzkouhi, H.; Moosmüller, H.; Chow, J.C.; Watson, J.G. Evaluation of gas and particle sensors for detecting spacecraft-relevant fire emissions. *Fire Saf. J.* **2020**, *113*, 102977. [CrossRef]
23. Lee, J.; He, S.; Song, G.; Hogan, C.J. Size distribution monitoring for chemical mechanical polishing slurries: An intercomparison of electron microscopy, dynamic light scattering, and differential mobility analysis. *Powder Technol.* **2022**, *396*, 395–405. [CrossRef]
24. Wang, X.L.; Firouzkouhi, H.; Chow, J.C.; Watson, J.G.; Carter, W.; De Vos, A.S. Characterization of gas and particle emissions from open burning of household solid waste from South Africa. *Atmos. Chem. Phys.* **2023**, *23*, 8921–8937. [CrossRef]
25. Larsson, F.; Andersson, P.; Blomqvist, P.; Mellander, B.-E. Toxic fluoride gas emissions from lithium-ion battery fires. *Sci. Rep.* **2017**, *7*, 10018. [CrossRef] [PubMed]
26. Claassen, M.; Bingham, B.; Chow, J.C.; Watson, J.G.; Wang, Y.; Wang, X. Characterization of Lithium-Ion Battery Fire Emissions—Part 1: Chemical Composition of Fine Particles (PM2. 5). *Batteries* **2024**, *10*, 301. [CrossRef]
27. Lithiumwerks. APR18650M1B Nanophosphate® Technology Data Sheet. Austin, Texas. 2023. Available online: https://lithiumwerks.com/products/lithium-ion-18650-cells/ (accessed on 2 July 2024).
28. AA Portable Power Corp. Model 544792 Polymer Lithium-Ion Battery Data Sheet. Available online: https://www.batteryspace.com/prod-specs/3175.pdf (accessed on 2 July 2024).
29. Tian, J.; Chow, J.C.; Cao, J.; Han, Y.; Ni, H.; Chen, L.-W.A.; Wang, X.; Huang, R.; Moosmu, H.; Watson, J.G. A biomass combustion chamber: Design, evaluation, and a case study of wheat straw combustion emission tests. *Aerosol Air Qual. Res.* **2015**, *15*, 2104–2114. [CrossRef]
30. U.S. EPA. Method 1—Sample and Velocity Traverses for Stationary Sources. Code of Federal Regulations, Title 40, Part 60, Appendix A-1. Available online: https://www.ecfr.gov/current/title-40/chapter-I/subchapter-C/part-60/appendix-Appendix%20A-1%20to%20Part%2060 (accessed on 6 August 2024).
31. Järvinen, A.; Aitomaa, M.; Rostedt, A.; Keskinen, J.; Yli-Ojanperä, J. Calibration of the new electrical low pressure impactor (ELPI+). *J. Aerosol Sci.* **2014**, *69*, 150–159. [CrossRef]
32. Saari, S.; Arffman, A.; Harra, J.; Rönkkö, T.; Keskinen, J. Performance evaluation of the HR-ELPI+ inversion. *Aerosol Sci. Technol.* **2018**, *52*, 1037–1047. [CrossRef]
33. Marjamäki, M.; Keskinen, J.; Chen, D.-R.; Pui, D.Y.H. Performance Evaluation of the Electrical Low-Pressure Impactor (ELPI). *J. Aerosol Sci.* **2000**, *31*, 249–261. [CrossRef]
34. Keskinen, J.; Pietarinen, K.; Lehtimäki, M. Electrical low pressure impactor. *J. Aerosol Sci.* **1992**, *23*, 353–360. [CrossRef]
35. Maricq, M.M.; Podsiadlik, D.H.; Chase, R.E. Size Distributions of Motor Vehicle Exhaust PM: A Comparison Between ELPI and SMPS Measurements. *Aerosol Sci. Technol.* **2000**, *33*, 239–260. [CrossRef]
36. Wang, X.; Firouzkouhi, H.; Chow, J.C.; Watson, J.G.; Ho, S.S.H.; Carter, W.; De Vos, A.S. Chemically speciated air pollutant emissions from open burning of household solid waste from South Africa. *Atmos. Chem. Phys.* **2023**, *23*, 15375–15393. [CrossRef]
37. Eldering, A.; Solomon, P.A.; Salmon, L.G.; Fall, T.; Cass, G.R. Hydrochloric acid: A regional perspective on concentrations and formation in the atmosphere of Southern California. *Atmos. Environ. Part A Gen. Top.* **1991**, *25*, 2091–2102. [CrossRef]
38. Sturges, W.T.; Harrison, R.M. The use of nylon filters to collect HCl: Efficiencies, interferences and ambient concentrations. *Atmos. Environ. (1967)* **1989**, *23*, 1987–1996. [CrossRef]
39. U.S. EPA. *Initial List of Hazardous Air Pollutants with Modifications*; Air Toxics Assessment Group, U.S. Environmental Protection Agency: Research Triangle Park, NC, USA, 2020. Available online: https://www.epa.gov/haps/initial-list-hazardous-air-pollutants-modifications (accessed on 6 August 2024).
40. Diaz, F.; Wang, Y.; Weyhe, R.; Friedrich, B. Gas generation measurement and evaluation during mechanical processing and thermal treatment of spent Li-ion batteries. *Waste Manag.* **2019**, *84*, 102–111. [CrossRef]
41. Andersson, P.; Blomqvist, P.; Lorén, A.; Larsson, F. *Investigation of Fire Emissions from Li-Ion Batteries*; SP Technical Research Institute of Sweden: Borås, Sweden, 2013.
42. Larsson, F. *Lithium-Ion Battery Safety-Assessment by Abuse Testing, Fluoride Gas Emissions and Fire Propagation*; Chalmers Tekniska Hogskola: Göteborg, Sweden, 2017.
43. Ribière, P.; Grugeon, S.; Morcrette, M.; Boyanov, S.; Laruelle, S.; Marlair, G. Investigation on the fire-induced hazards of Li-ion battery cells by fire calorimetry. *Energy Environ. Sci.* **2012**, *5*, 5271–5280. [CrossRef]
44. Sturk, D.; Rosell, L.; Blomqvist, P.; Ahlberg Tidblad, A. Analysis of li-ion battery gases vented in an inert atmosphere thermal test chamber. *Batteries* **2019**, *5*, 61. [CrossRef]
45. Bordes, A.; Marlair, G.; Zantman, A.; Herreyre, S.; Papin, A.; Desprez, P.; Lecocq, A. New insight on the risk profile pertaining to lithium-ion batteries under thermal runaway as affected by system modularity and subsequent oxidation regime. *J. Energy Storage* **2022**, *52*, 104790. [CrossRef]
46. Willstrand, O.; Pushp, M.; Andersson, P.; Brandell, D. Impact of different Li-ion cell test conditions on thermal runaway characteristics and gas release measurements. *J. Energy Storage* **2023**, *68*, 107785. [CrossRef]
47. Koch, S.; Fill, A.; Birke, K.P. Comprehensive gas analysis on large scale automotive lithium-ion cells in thermal runaway. *J. Power Sources* **2018**, *398*, 106–112. [CrossRef]